ME 400

Project and Thesis

Electro-Thermo-Mechanical Response of a Thin Conductive Layer of Metal Matrix Composite Reinforced by Graphite Fibers

Submitted for the partial fulfillment of the requirements for the award of the degree of

Bachelor of Science
In
Mechanical Engineering

Submitted By

Md. Niazul Islam Nishat (1510138)

Kazi Tahsin Mahmood (1510148)

Under the Supervision of

Dr. S. Reaz Ahmed

Department of Mechanical Engineering

Bangladesh University of Engineering and Technology

Zahir Raihan Road, Dhaka-1000

Department of Mechanical Engineering
Bangladesh University of Engineering and Technology

Declaration

This thesis is submitted to the Department of Mechanical Engineering, Bangladesh University of Engineering and Technology, Dhaka for the Partial fulfillment of the requirement of the award of degree of Bachelor in Science in Mechanical Engineering. This certifies that the work presented in this section is an outcome of investigation performed by the authors under the supervision of Dr. Sheikh Reaz Ahmed, Professor, Department of Mechanical Engineering.

Author

Md. Niazul Islam Nishat

Kazi Tahsin Mahmood

Signature of Supervisor

Dr. S. Reaz Ahmed

Professor, Department of Mechanical Engineering

ACKNOWLEDGEMENT

We would like to thank Dr. S. Reaz Ahmed for his constant support and motivation. Without his help we would not have accomplished the work. We would like to thank cordially for his instruction and dedication. The thesis is based on the previous work of our supervisor and with his support the thesis was completed.

We would like to thank Pranta Rahman Sarkar and Adib Rahman for supporting us in the understanding of the simulation of the metal line.

We would like to thank Bangladesh University of Engineering and Technology for providing us the necessary equipment needed for undertaking the thesis.

MOTIVATION

The thesis is based on the electrical usage of different structural materials and the sustainability in both heating and the mechanical stability. There are previous works done on the mechanical stability of structural orthotropic materials. But the heat generated due to the DC field current in the metal line in different air flow arrangements are relatively new research approach. Various kinds of PCB traces are used for electrical components. So, we took an approach to observe the stress migration in the trace MMC line due to the electrical current in the system. The thesis is based on the finite difference approach of the electrical and elastic model of the MMC line through entire system. We tried to determine the failure behavior of different materials at different condition.

NOMENCLATURE

k	Thermal Conductivity (W/m.K)
h	Heat Convection Coefficient ($W/m^2.K$)
T	Temperature (K)
ρ	Electrical Resistivity ($\mu\Omega.cm$)
A	Area (m^2)
L	Length (m)
W	Width (m)
I	Current (A)
R	Resistance (Ω)
J	Current Density (A/m^2)
ϕ	Electric Potential
G(x,y)	Heat Generation (J)
Re	Reynolds Number
Nu	Nusselt Number
v	Air Velocity (m/s)
ν	Kinematic Viscosity (m^2/s)
E	Young's Modulus (GPa)
μ	Poisson's Ratio
α	Coefficient of Thermal Expansion (0°C)
G	Shear Modulus (GPa)
σ	Normal Stress (MPa)
τ	Shear Stress (MPa)
ϵ	Normal Strain
γ	Shear Strain
V	Volume Fraction
ψ	Displacement Potential Function
C	Stiffness Matrix
u	Displacement (m)

SUBSCRIPTS

x, 1	Axial Direction
y, 2	Lateral Direction
xy, 1-2	Shear
L	Global
f	Fiber
m	Matrix
max	Maximum

ABSTRACT

The paper was undertaken to analyze the electro thermo mechanical behavior of orthotropic material for metal line of PCB under DC electric field. The behavior was considered of Metal-Graphite composite consists of different mixture volume. The metal matrix was chosen Aluminium. Composite material parameter is calculated using rule of mixture law assuming up to 30% fiber volume content of graphite in the metal matrix. Governing equations describing electromagnetic, thermal and mechanical field in anisotropic materials are analyzed. There are different physical conditions like thermal insulation, natural convection and forced convection is considered to study the thermal behavior change in the composite. The governing equations are of both 2^{nd} order and 4^{th} order which is solved using finite difference method. There are mixed boundary values for both electrical and stress problem are applied in the boundary regions of MMC line. A closed form solution for temperature field is obtained and used for determining the compressive stress developed across the metal line. The change of temperature and compressive stress generation with the different graphite volume has been observed. For the same volume composition, the temperature rises with the increase of current which results in increase of compressive stress. With that, the failure characteristics are studied to determine the sustainability of the composite MMC line. Failure due to melting point temperature and mechanical failure due to stress has been observed.

Contents

List of Figures

List of Tables

Chapter 1

Introduction

1.1 General

In modern technology structural material is prominent due to various kinds of usage in the different sectors. Different types of materials used in these cases. The materials have to undergo different types of procedures in these sectors. In an ongoing age of technology these materials have to perform various types of tasks. One of the sectors the materials are used is in PCB board. The PCB board traces are used for transmitting the electrical signal through current across the components as DC current. Different types of loading are given in these materials. The trace materials have to withstand both electrical and mechanical loading. In a two-dimensional elastic problem with mixed boundary problem there are various approaches that can be taken to solve the problem. DC current is passed through electrical structures. In modern electrical facilities sustainable electrical components are needed for better performance. The structure should sustain both temperature and mechanical change in the system. Electricity on metal thin lines creates high temperature in the structure and the temperature varies with the distance and orientation. Advancement of the DC current creates high temperature in different regions of the metal matrix composite (MMC) line. With the high temperature, stress is created in those regions. For that failure occurs in the specific region. In this specific problem there are two types of failure occurring in the MMC line. For a DC field current the MMC line opposes the current due to internal resistivity. As a matter joule heating is produced across the MMC line. If the heating produced by the system is higher than the melting point than the MMC line fails. A temperature field is produced across the MMC line. Because of the temperature variation across the MMC line thermal stress migration is generated. With the stress migration failure also occurs in different regions of the metal line. So, there are two types of failure that can occur. Failure is an important characteristic for any material as it is related to the durability of the material. Different types of material show different failure characteristics. In this thesis we have studied those failure characteristics of some orthotropic material. This failure characteristics also helps to determine the maximum allowable current across the MMC line and also the maximum allowable load that the material can withstand. Zhupanska and Sieraskowski previously studied the electro-thermo-mechanical coupling of carbon polymer matrix [1]. They have studied the behavior of carbon polymer due to DC electric field. Arani has studied about the electro-thermo mechanical response of FGPM spheres and boron-nitride nanotubes using analytical and ANSYS simulation [2] [3].

The response of a solid body due to the temperature and mechanical load is dependent on the geometry of the body. In our case we have chosen the trace as a simply supported beam structure. The body responses with the loads in different ways. If the geometry is changed the stress migration differs. There are also mixed boundary conditions applied in the MMC line in both electrical field and mechanical load. In our case we are interested in the dis-

placement and the stress generated across the MMC line. The material of the metal line is homogeneous and distributed uniformly along the body.

1.2 Metal Matrix Composite

In the previous studies the electrical current study is emphasized on the isotropic materials. In the beginning of the industrial revolution only the materials of specific and similar properties were used. The use of different types of alloys gives significant improvement of the material properties. With the advancement of the technology composite materials are popular in different structural sectors. Composite materials give huge improvement over the alloy material. Composite materials are also of different types. The material property for an isotropic material is similar across all the orientation. In our approach we tried to study the stress migration due to the DC electric field across the metal line of a composite material. In material science and solid mechanics, orthotropic materials have material properties that differ along three mutually-orthogonal two-fold axes of rotational symmetry at a particular point [4]. The orthotropic material properties are evaluated using metal matrix composite. A metal matrix composite (MMC) is a composite material with at least two constituent parts, one being a metal necessarily, the other material may be a different metal or another material, such as a ceramic or organic compound. When at least three materials are present, it is called a hybrid composite [5]. The metal matrix composites are constituted using different materials and their properties [6] [7] [8]. The properties of the composites are evaluated using mixture law. The evaluation of carbon-based reinforced polymer matrix is used also for the analysis of the electro-thermo-mechanical analysis [9]. The material property for both 0° and 90° fiber are that are used are given in table A6 and table A7.

Different types of material are used for different sectors for their different properties. In recent times structural based materials are used in very high thermal and mechanical load-based work. Metallurgists are using different techniques to find out the best optimum property of the different mixtures of the materials.

1.3 Electrical Modeling

The main objective of our thesis is to study the electric behavior of the MMC line using a DC electric field. In the metal we have passed electricity through one end of the MMC line. The electric current creates an electric potential along the metal line. The electrical conductivity along the MMC line creates an electric potential difference. An electric potential (also called the electric field potential, potential drop or the electrostatic potential) is the amount of work needed to move a unit of charge from a reference point to a specific point inside the field without producing an acceleration [10]. The current density varies along the MMC line

with the change of area. With the change of dimension current density changes.

Previously, Carslaw and Jaeger studied the heat conduction through a wire for current density [11]. Steady heat distribution near the tip of a crack in a homogeneous isotropic conductive plate was analyzed by Saka and Abe [12]. They analyzed the problem under direct electric field with the help of path independent integral. Sasagawa determined the current and temperature distribution near the corner of an angled metal line [13]. They discussed about the intensities of singular current density field and singular heat flux field. Greenwood and Williamson evaluated the electrical conductance in temperature dependent solids [14]. Jang evaluated the same problem using two dissimilar material across an interference [15]. The materials were coupled together and for a steady state electrical and thermal conduction. Wang also presented analytical solutions for the electrical and thermal conduction for a co-linear crack with a constant flux boundary condition at an infinite region [16]. This is accomplished by using a complex function method. Recently, a new approach taken by Saka and Ahmed using a Joule heating residue vector for the steady heat conduction in symmetrical electro-thermal problems [17]. Similarly, a non-linear approach was also taken for the electro-thermal response for a dissimilar material conductive wire with variable thermal conductivity [18]. And with this approach, Saka and Zhao analyzed the 2D electro-thermal problem of dissimilar materials in an angled metal line [19]. In the recent time, Ghosh analyzed the temperature distribution of a thin FGM metal line due to DC electric field [20].

1.4 Thermal Modeling

Due to the electricity, Joule heating is created along the MMC line. The heating results in an increase of temperature across the region of the MMC line. The temperature field changes with the material and surrounding. To study the temperature behavior, we have considered three cases, thermal insulation, natural convection and forced convection. The temperature field shows different behavior due to these conditions. To study the temperature propagation, we have modeled the MMC line using the heat convection equation [21]. In modern technology, heating of metal structures, PCB and electrical circuit boards are common. To cool those down different types of convection are allowed in the metal lines. There are some of the cases where thermal insulation is necessary. So, we have studied the thermal behavior in each of the cases. In force convection, the flow in the metal line changes with the particle movement. If the particle follows a smooth path then the flow is laminar and if the particle creates a vortex and does not follow a smooth path the flow is turbulent. So, to define these characteristics we have to define a non-dimensional parameter called Reynolds number (Re). Again, the heat conduction and convection depend on the heat convection coefficient which defines the heat convection capacity of the fluid. To determine the heat convective coefficient, we have to define another non-dimensional parameter called Nus-

selt number (Nu). To define the fluid and fluid state at different temperatures we have to use the Prandtl number (Pr) [21]. With the joule heating, the temperature in the MMC line increases. We have studied the temperature at a steady state condition generated due to the electric field. Now the increase of current increases temperature. For the failure of the material the temperature has to be increased to the melting point. So, in our thesis we have analyzed the maximum allowable current for a metal line before the melting failure occurs. With this we can determine the current capacity of the metal line.

The temperature distribution along the metal line depends mostly on the material property and material thermal response to different conditions. Thermal distribution varies with the geometry and also with the change of surface area. The orientation of different material properties changes the temperature field across the metal line. Different studies have been conducted to find out the temperature field of different structures. Zhang and Zhou analyzed the heat transfer of both steady state and transient phenomena using element free Galerkin method [22] [23]. Cheng analyzed the temperature field of an anisotropic coating structure by boundary element method [24]. The coating is much thinner in contrast with the conventional boundary element method. The temperature fields are related to the material property and the insulation created within the boundary.

1.5 Stress Modeling

In modern technology, stress and strain of a material is very important for sustainability and longevity. There is plenty of research being developed for the introduction of more reliable material. These materials have to undergo different kinds of load. Due to joule heating the temperature can create thermal stress across the metal line. In the metal line we have also applied external load to determine the mechanical stress produced in the metal line.

In the structural mechanics, precise stress formulation is for building the geometry of the product. Elementary methods were used in solving the stress formulation in an object. But these methods do not give accurate results. And these methods also do not help to determine the local stresses that are built in the edges and also in the cracks. So, to solve the problems exact solutions are used in the stress formulation. But for some simple cases exact solutions can be achieved by mathematical solutions. For non-uniform geometry it is very difficult to make an exact solution of the geometry. Even in the exact mathematical solution of uniform geometry the solution is much more complicated. So, it often creates errors. In case of an easier approach, we use various approximate methods. Approximate methods are more convenient as those give an easier approach solving the multi-dimensional equation. These methods also help to solve the non-uniform geometry products and give better results. But there are some cases where approximate solutions cannot be used. In that case

the best way to solve the problem is to use experimental methods. Different kinds of experimental methods like strain gauge, photo-elastic method, soap film, moiré fringe [25]. These experiments have helped modern design of machine parts and their formulation. It has also helped determine the weak spot of the structure and eliminate crack propagation.

In our thesis we have approached with the approximate solution of the electrical and stress formulation. There are various approximate solutions. Among all of them, the most notable one is the G. B. Airy's displacement parameter approach [25]. The Airy stress function is governed by a fourth order partial differential equation and the stress function is a second order partial differential equation. Solutions were analyzed through various polynomial equations but there are various amounts of errors which decreases the success rate. Conway, Chow, Chapel in their studies has solved the stress function formulation with finite difference technique in plane stress problems which has increased success rate [26] [27] [28]. But the boundary conditions restrained in terms of displacement components can be successfully imposed in stress function. Those difficulties were improved by Durelli [29] and later by Ahmed in their research of different beam structures [30] [31] [32] for solving stress function. Afsar analyzed the thermoelastic field of a rotating FGM circular disk [33]. But the simultaneous evaluation of two functions satisfying two differential equations is extremely difficult especially when the boundary conditions are specified as a mixture of displacements and stresses. As a result, serious attempts had hardly been made in the field of stress analysis using this formulation. There was an analytical solution regarding this process for removing the difficulties in the formulation [34]. In the later Zubaer gave a generalized mathematical formula for solving mixed boundary value elastic problems [35]. The research was suitable for a three-dimensional mixed boundary value problem using finite difference analysis. Ghosh analyzed the stress formulation of a curved beam using the mixed boundary value solution.

In the later studies thermal stress was introduced due to the high effect of temperature in the metal line. Different types of thermal condition then became a point of interest in the study of stress formulation. Malak Naji investigated the thermal stress by determining the transient temperature variation using hyperbolic energy models [36]. In his study he found that the transient thermal stresses that were generated inside the body fluctuates between tensile and compressive stresses, which was not predicted using classical heat models. Demirbas analyzed the thermal stress of one and two dimensional functionally graded materials subjected to in plane heat fluxes [37]. The mathematical formula considers the spatial derivatives of local mechanical and thermal properties. Later, she analyzed the thermal stress using temperature dependent material properties [38]. Xu and Zhou analyzed the thermoelastic property of simply supported beams with variable thickness and subjected to thermomechanical loads [39].

Different studies impacted the analysis of thermo mechanical systems throughout the years. Plenty of studies have been undertaken to make better structural material and structure to undergo various types of loading criteria. Failure to study is a very important perspective in this case as it directly impacts the sustainability of the product.

1.6 Numerical Modeling

The analytical method of solving the differential equations is very tedious as it involves different formulation and derivation. With technological advancement the formulation of these various problems needs to be faster. Analytical methods are slower and time consuming. In numerical analysis the problem becomes easier. Numerical analysis is the study of algorithms that use numerical approximation for the problem of mathematical analysis [40]. Various types of numerical approximation are considered for solving the differential equation. We used a finite difference method to solve the differential equations. The method is also applicable for boundary value problems. To solve the finite difference method, we used the programming language MATLAB. It is a very popular programming language for solving various kinds of computational problems.

Chapter 2

Mathematical Formulation

2.1 General

In our thesis we have considered three different aspects of the MMC line. The MMC line is subjected to DC electric field, a convective air field. These different aspects are solved by using different mathematical equation. When three different aspects are combined there are various kinds of solution is measured at different boundary conditions. The mathematical model works sequentially. The loading of current field creates a temperature field across the MMC line which then migrates to the stress field. We have generated these different fields by using the corresponding governing equations.

2.2 Mixture Law

In materials science, a general rule of mixtures is a weighted mean used to predict various properties of a composite material made up of continuous and unidirectional fibers. It provides a theoretical upper- and lower-bound on properties such as the elastic modulus, mass density, ultimate tensile strength, thermal conductivity, and electrical conductivity[6]. In general there are two models, one for axial loading (Voigt model), and one for transverse loading (Reuss model).

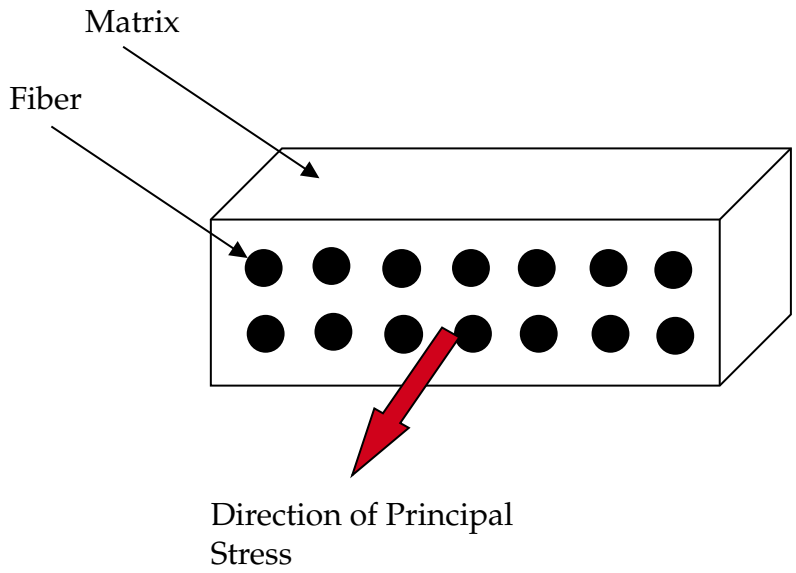

Figure 2.1: Model of idealized transverse isotropic fiber composite structure

2.2.1 Longitudinal Young's Modulus

Assuming that the fibers, matrix, and composite follow Hooke's law and that the fibers and the matrix are isotropic, the stress–strain relationship for each component and the composite is,

$\sigma_c = E_1 \epsilon_c$
$\sigma_f = E_f \epsilon_f$
$\sigma_m = E_m \epsilon_m$

where,

$\epsilon_{c,f,m}$= strains in composite, fiber, and matrix, respectively
$E_{1,f,m}$= elastic modulus of composite, fiber, and matrix, respectively

Thus we get,
$E_1 \epsilon_c A_c = E_f \epsilon_f A_f + E_m \epsilon_m A_m$
The strains in the composite, fiber, and matrix are equal ($\epsilon_c = \epsilon_f = \epsilon_m$); then,
$E_1 = E_f \frac{A_f}{A_c} + E_m \frac{A_m}{A_c}$
from definition of volume fraction,

$$E_1 = E_f V_f + E_m V_m \tag{2.1}$$

2.2.2 Transverse Young's Modulus

Assume now that, the composite is stressed in the transverse direction. The fibers and matrix are again represented by rectangular blocks as shown. The fiber, the matrix, and composite stresses are equal. Thus,
$\sigma_c = \sigma_f = \sigma_m$
Now, the transverse extension in the composite Δ_c is the sum of the transverse extension in the fiber Δ_f, and that is the matrix, Δ_m.

$$\Delta_c = \Delta_f + \Delta_m \tag{2.2}$$

Now, by the definition of normal strain,

$\Delta_c = t_c \epsilon_c$
$\Delta_f = t_f \epsilon_f$
$\Delta_m = t_m \epsilon_m$

where,

$t_{c,f,m}$ = thickness of the composite, fiber and matrix, respectively
$\epsilon_{c,f,m}$ = normal transverse strain in the composite, fiber, and matrix, respectively

By using Hooke's law for the fiber, matrix, and composite and substituting the equation we get,
$\frac{1}{E_2} = \frac{1}{E_f}\frac{t_f}{t_c} + \frac{1}{E_m}\frac{t_m}{t_c}$
Because the thickness fractions are the same as the volume fractions as the other two dimen-

sions are equal for the fiber and the matrix,

$$\frac{1}{E_2} = \frac{V_f}{E_f} + \frac{V_m}{E_m} \tag{2.3}$$

2.2.3 Major Poisson's Ratio

The major Poisson's ratio is defined as the negative of the ratio of the normal strain in the transverse direction to the normal strain in the longitudinal direction, when a normal load is applied in the longitudinal direction. Assume a composite is loaded in the direction parallel to the fibers. The fibers and matrix are again represented by rectangular blocks. The deformations in the transverse direction of the composite (δ_c^T) is the sum of the transverse deformations of the fiber (δ_f^T) and the matrix (δ_m^T) as

$$\delta_c^T = \delta_f^T + \delta_m^T \tag{2.4}$$

Using the definition of normal strains, poisson's ratios for the fiber, matrix, and composite, we get

$$-t_c \mu_{12} \epsilon_c^L = -t_f \mu_{12} \epsilon_f^L - -t_m \mu_{12} \epsilon_m^L$$

where,

$\mu_{12,c,f,m}$= Poisson's ratio of composite, fiber, and matrix, respectively

However, the strains in the composite, fiber, and matrix are assumed to be the equal in the longitudinal direction ($\epsilon_c = \epsilon_f = \epsilon_m$) , which, from Equation

$$\mu_{12} = \mu_f V_f + \mu_m V_m \tag{2.5}$$

2.2.4 In-Plane Shear Modulus

Apply a pure shear stress τ_c to a lamina. The fibers and matrix are represented by rectangular blocks as shown. The resulting shear deformations of the composite δ_c the fiber δ_f, and the matrix δ_m are related by

$$\delta_c = \delta_f + \delta_m \tag{2.6}$$

From the definition of Shear strain,

$$\delta_c = \gamma_c t_c$$
$$\delta_f = \gamma_f t_f$$
$$\delta_m = \gamma_m t_m$$

where,

$\gamma_{c,f,m}$= shearing strains in the composite, fiber, and matrix, respectively

$t_{c,f,m}$= thickness of the composite, fiber, and matrix, respectively

From Hooke's law for the fiber, the matrix, and the composite,

$$\gamma_c = \frac{\tau_c}{G_{12}}$$
$$\gamma_f = \frac{\tau_f}{G_{12}}$$
$$\gamma_m = \frac{\tau_m}{G_{12}}$$

where,

G_{12}= shear modulus of composite, fiber, and matrix, respectively The shear stresses in the composite, fiber and matrix are assumed to be equal ($\tau_c = \tau_f = \tau_m$), and the thickness fraction is equal to the volume fraction we get,

$$\frac{1}{G_{12}} = \frac{V_f}{G_f} + \frac{V_m}{G_m} \tag{2.7}$$

2.2.5 Ultimate Strength of a Unidirectional Lamina

In order to specify the failure criteria, we need to find total five ultimate strength parameters for a unidirectional lamina.

- Longitudinal Tensile Strength $\left(\sigma_1^t\right)_{ult}$
- Longitudinal Compressive Strength $\left(\sigma_1^c\right)_{ult}$
- Transverse Tensile Strength $\left(\sigma_2^t\right)_{ult}$
- Transverse Compressive Strength $\left(\sigma_2^c\right)_{ult}$
- In-Plane Shear Strength $\left(\tau_{12}\right)_{ult}$

We have considered fibers with square array packaging, as shown in figure 2.2. The ratio of the diameter d, to fiber spacing s is *d/s*, varies with geometrical packing.

$$\frac{d}{s} = \left(\frac{4 \times V_f}{\pi}\right)^{1/2} \tag{2.8}$$

This gives a maximum fiber volume fraction of 78.54% as $s \geq d$.

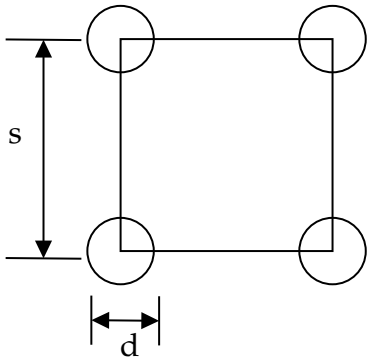

Figure 2.2: Fiber to fiber spacing in square array packaging geometry

Longitudinal Tensile Strength

A simple mechanics of materials approach model is presented.
Assume that

- Fiber and matrix are isotropic, homogeneous, and linearly elastic until failure.
- The failure strain for the matrix is higher than for the fiber, which is the case for polymeric matrix composites.

Now, if

$(\sigma_f)_{ult}$ = ultimate tensile strength of fiber

E_f = Young's modulus of fiber

$(\sigma_m)_{ult}$ = ultimate tensile strength of matrix

E_m = Young's modulus of matrix

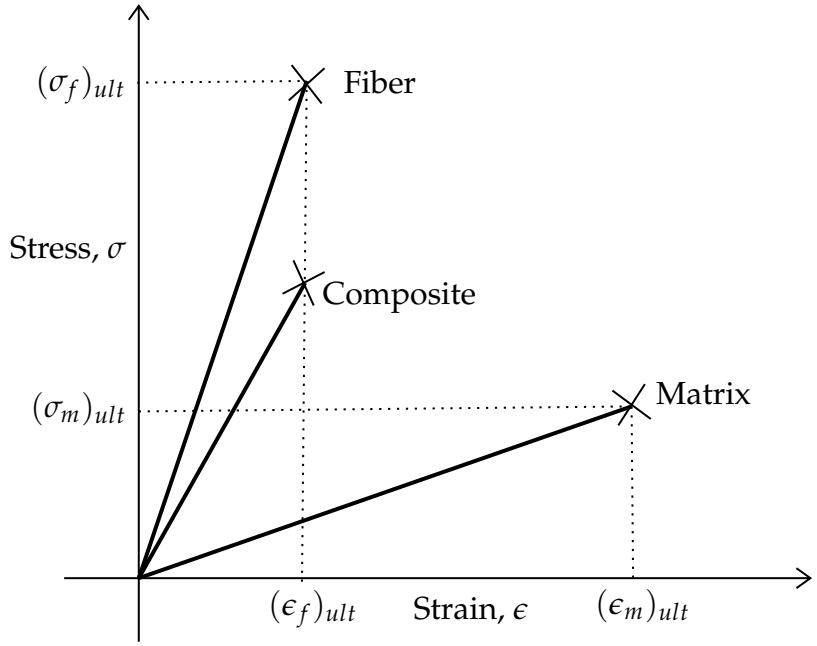

Figure 2.3: Stress–strain curve for a unidirectional composite under uniaxial tensile load along fibers

Then the ultimate failure strain of fiber is,

$$(\epsilon_f)_{ult} = \frac{(\sigma_f)_{ult}}{E_f} \tag{2.9}$$

And the ultimate failure strain of matrix is,

$$(\epsilon_m)_{ult} = \frac{(\sigma_m)_{ult}}{E_m} \tag{2.10}$$

Because the fibers carry most of the load in polymeric matrix composites, it is assumed that, when the fibers fail at the strain of $(\epsilon_f)_{ult}$, the whole composite fails. Thus, the composite tensile strength is given by,

$$\left(\sigma_1^T\right)_{ult} = (\sigma_f)_{ult} V_f + (\epsilon_f)_{ult} E_m V_m \tag{2.11}$$

Longitudinal Compressive Strength

Using maximum strain failure theory, if the transverse strain exceeds the ultimate transverse tensile strain, $(\epsilon_2^T)_{ult}$, the lamina is considered to have failed in the transverse direction. Thus,

$$(\sigma_1^c)_{ult} = \frac{E_1 \left(\epsilon_2^T\right)_{ult}}{\mu_{12}} \tag{2.12}$$

For the value of (ϵ_2^T), we used the mechanics of material formula,

$$\left(\epsilon_2^T\right)_{ult} = \left(\epsilon_m^T\right)_{ult} \left[\frac{d}{s}\left(\frac{E_m}{E_f} - 1\right) + 1\right] \tag{2.13}$$

2.2.6 Electrical Conductivity & Thermal Conductivity

Applying the same rules for the electrical conductivity and thermal conductivity we get,

$$\left(\frac{V_f}{k_f} + \frac{V_m}{k_m}\right)^{-1} \leq k_c \leq V_f k_f \leq V_m k_m \tag{2.14}$$

$$\left(\frac{V_f}{\sigma_f} + \frac{V_m}{\sigma_m}\right)^{-1} \leq \sigma_c \leq V_f \sigma_f \leq V_m \sigma_m \tag{2.15}$$

2.2.7 Fiber Orientation

Generally, a laminate does not consist only of unidirectional laminae because of their low stiffness and strength properties in the transverse direction [6]. Therefore, in most laminates, some laminae are placed at an angle. It is thus necessary to develop the stress–strain relationship for an angle lamina. The coordinate system used for showing an angle lamina is as given in figure 2.4. The axes in the 1–2 coordinate system are called the local axes or the material axes. The direction 1 is parallel to the fibers and the direction 2 is perpendicular to the fibers. In some literature, direction 1 is also called the longitudinal direction L and the direction 2 is called the transverse direction T. The axes in the x–y coordinate system are called the global axes or the off-axes. The angle between the two axes is denoted by an angle θ. The stress–strain relationship in the 1–2 coordinate system has already been established and we are now going to develop the stress–strain equations for the x–y coordinate system.

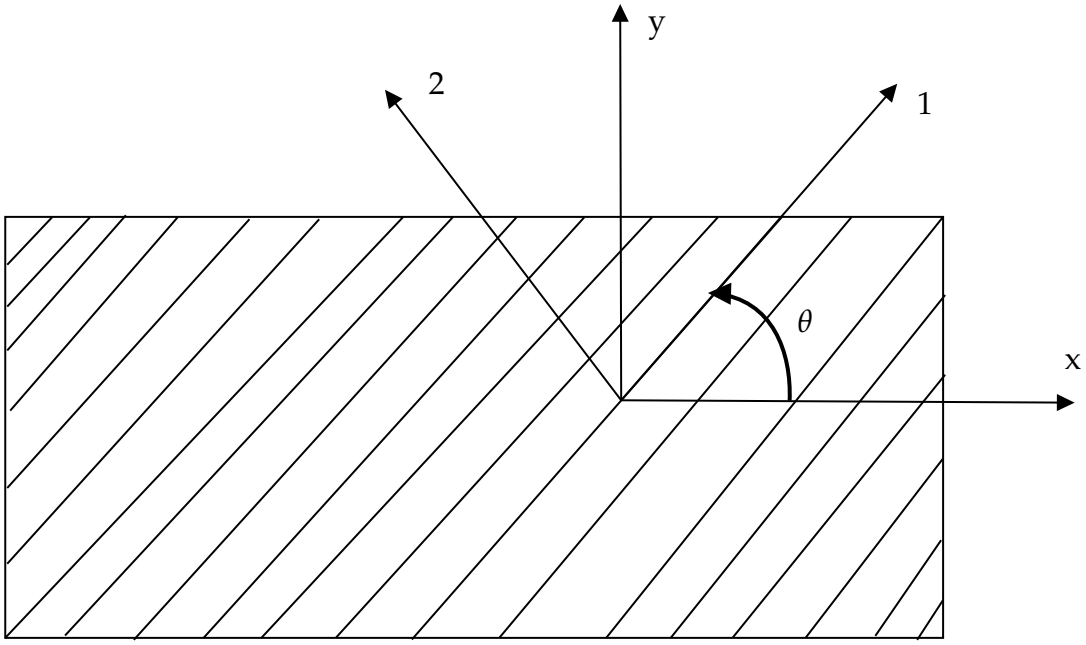

Figure 2.4: Local and Global axes of an angled lamina [6]

The global and local stresses in an angle lamina are related to each other through the angle of the lamina, θ

$$\begin{bmatrix} \sigma_x \\ \sigma_y \\ \tau_{xy} \end{bmatrix} = \Big[T\Big]^{-1} \begin{bmatrix} \sigma_1 \\ \sigma_2 \\ \tau_{12} \end{bmatrix} \tag{2.16}$$

where [T] is called the transformation matrix and is defined as,

$$\Big[T\Big]^{-1} = \begin{bmatrix} c^2 & s^2 & -2sc \\ s^2 & c^2 & 2sc \\ sc & -sc & c^2 - s^2 \end{bmatrix} \tag{2.17}$$

and

$$\Big[T\Big] = \begin{bmatrix} c^2 & s^2 & 2sc \\ s^2 & c^2 & -2sc \\ -sc & sc & c^2 - s^2 \end{bmatrix} \tag{2.18}$$

where,

$$c = cos(\theta)$$
$$s = sin(\theta)$$

With that we can find the corresponding material property for the composite at different fiber angle.

2.3 Governing Equation

There are three kinds of loading is present in the MMC line. So, we have solved the equations of the MMC line individually and used the results simultaneously to study the failure characteristics of the MMC line. The governing equations are partial differential equations meeting the condition of the loading and distribution along the MMC line. The governing equations are also modified to meet the criteria for finite difference method.

2.4 Electrical Governing Equation and Formulation

The DC current field flown across the MMC line creates a potential distribution. This potential distribution also tends to generate electro-thermal heat. Because of the various boundary condition, the heat generation tends to change. We have formulated these equations that are given following sections.

2.4.1 Electric Potential Distribution

In every material there is a property which creates a oppose in the current flow which is known as resistance of the material. It varies to material to material and also in body length and shape. The resistance solely depends on material and shape. The resistance is directly proportional to length and inversely proportional to cross sectional area of the body. Like thick copper wire is more resistive than thin copper wire. For material change the resistivity changes. Resistivity is the fundamental property of the material.

The electrical resistivity is given by

$$\rho = R\frac{A}{L} \tag{2.19}$$

where

ρ= Resistivity (Ωm)
R= Resistance (Ω)
A= Cross Sectional Area (m^2)
L= Length (m)

Electrical Resistivity can also be written as

$$\rho = \frac{E}{J} \tag{2.20}$$

where

E= Magnitude of Current field (V/m)
J= Magnitude of Current density (A/m^2)

Electrical resistivity is also the inverse of the electric admittance σ which can be written as

$$\rho = \frac{1}{\sigma} \tag{2.21}$$

where

σ= Electric Admittance (S)

Electric Potential at any point is defined to be the amount of work required to move a unit charge to the point from far away (infinity). At any point electric field is the negative gradient of the electric potential.

$$E = -\nabla\phi \tag{2.22}$$

where

ϕ= Electric potential (V)

For one dimensional case eq 2.22 becomes

$$E = -\frac{d\phi}{dx} \tag{2.23}$$

In that case eq 2.20 can be written as

$$\frac{d\phi}{dx} = -\rho J \tag{2.24}$$

One dimensional Case

Applying divergence operator in eq 2.24 we get

$$\frac{d^2\phi}{dx^2} = -(J\frac{\partial\rho}{\partial x} + \rho\frac{\partial J}{\partial x}) \tag{2.25}$$

This is the basic governing equation for evaluating electrical problem across a MMC line for one dimension.

In this study the cross sectional area A across the metal is constant.
and J=$\frac{I}{A}$, so J is also constant and ρ depends on the temperature and position of the MMC line.

Now there are various kinds of loading condition in the MMC line. Considering those various cases.

Case 1: When the MMC line has constant geometry and constant property.

$$\frac{d^2\phi}{dx^2} = 0 \tag{2.26}$$

Case 2: When the material has varying geometry with constant property.

$$\frac{d^2\phi}{dx^2} = -\rho\frac{dJ}{dx} \tag{2.27}$$

Case 3: When the MMC line has changing property with constant geometry.

$$\frac{d^2\phi}{dx^2} = -J\frac{d\rho}{dx} \tag{2.28}$$

Case 4: When the geometry and property changes across the MMC line.

$$\frac{d^2\phi}{dx^2} = -(J\frac{\partial\rho}{\partial x} + \rho\frac{\partial J}{\partial x}) \tag{2.29}$$

Two dimensional case

In the two dimensional case, geometry and properties can vary across both direction. The governing equation for two dimensional case becomes.

$$\frac{\partial^2\phi}{\partial x^2} + \frac{\partial^2\phi}{\partial y^2} = -(J\frac{\partial\rho}{\partial x} + \rho\frac{\partial J}{\partial x}) - (J\frac{\partial\rho}{\partial y} + \rho\frac{\partial J}{\partial y}) \tag{2.30}$$

Like the one dimensional case there are various loading conditions. The cases are

Case 1: When the material has constant geometry with constant property.

$$\frac{\partial^2\phi}{\partial x^2} + \frac{\partial^2\phi}{\partial y^2} = 0 \tag{2.31}$$

Case 2: When the material has varying geometry with constant property.

$$\frac{\partial^2\phi}{\partial x^2} + \frac{\partial^2\phi}{\partial y^2} = -\rho\frac{\partial J}{\partial x} \tag{2.32}$$

Case 3: When the MMC line has changing property with constant geometry.

$$\frac{\partial^2\phi}{\partial x^2} + \frac{\partial^2\phi}{\partial y^2} = -J\frac{\partial\rho}{\partial x} \tag{2.33}$$

Case 4: When the geometry and property changes across the MMC line.

$$\frac{\partial^2 \phi}{\partial x^2} + \frac{\partial^2 \phi}{\partial y^2} = -(J\frac{\partial \rho}{\partial x} + \rho\frac{\partial J}{\partial x}) - (J\frac{\partial \rho}{\partial y} + \rho\frac{\partial J}{\partial y}) \tag{2.34}$$

2.4.2 Electrical Boundary Conditions

The boundary conditions for electric potential distribution can be prescribed as electric potential, electric insulation and electric current density. It can be visualized as.

(a) Prescribed Potential

at $x = \frac{L}{2}$ and $y = \frac{W}{2}$, ϕ=0

(b) Prescribed Current Density

1 at x=0, $\frac{d\phi}{dx} = -\rho J$

2 at x=L, $\frac{d\phi}{dx} = \rho J$

3 at y=0, $\frac{d\phi}{dy} = 0$

4 at y=W, $\frac{d\phi}{dy} = 0$

These boundary conditions are sufficient for current which is injected through full cross section of one side and other side is grounded for the outlet of the current, is

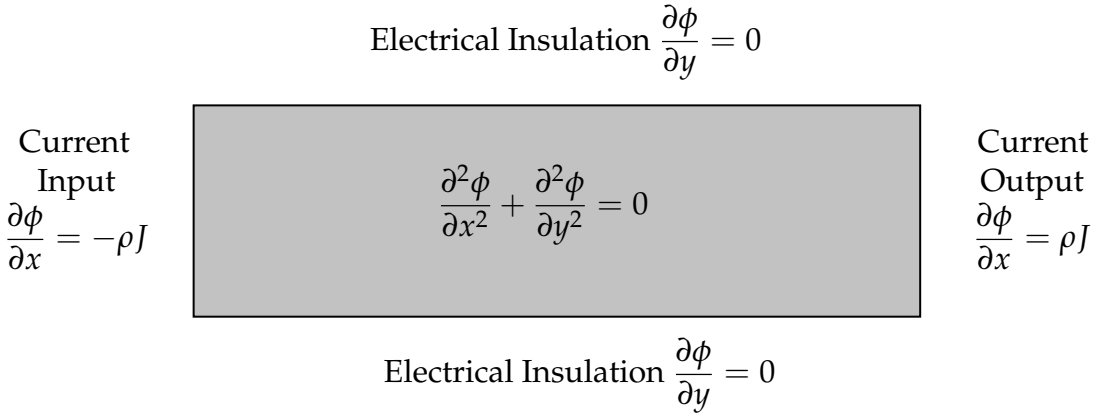

Figure 2.5: Electrical System

2.4.3 Joule Heating

Joule heating is a renowned phenomena founded by James Prescott Joule and was studied by Henry Lenz at the same time. So it is often called Joule-Lenz phenomenon. Joule heating, also known as resistive, resistance, or Ohmic heating, is the process by which the passage of

an electric current through a conductor produces heat. Joule's first law, also known as the Joule–Lenz law [41] states that the power of heating generated by an electrical conductor is proportional to the product of its resistance and the square of the current:

$$H \propto I^2 R \tag{2.35}$$

When an electric field is applied by creating a voltage difference between two points, the electrons attain a drift velocity aligned to the direction of the electric field. However, due to the presence of ionic particles in the path, the electrons get scattered, increasing the kinetic energy of the material and thus raises the temperature. From continuum description, Joule heating can be written as

$$G(x,y) = \frac{1}{A_m \rho} \mid \nabla \phi \mid^2 \tag{2.36}$$

where A_m is the Mechanical Equivalent of heat
In two dimensional case we can write

$$G(x,y) = \frac{1}{A_m \rho}[(\frac{\partial \phi}{\partial x})^2 + (\frac{\partial \phi}{\partial y})^2] \tag{2.37}$$

2.5 Thermal Governing Equation and Formulation

The heat generation produced by the electric potential creates a temperature rise across the MMC line. There are heat conduction and convection present in the MMC line. For that we get a temperature profile in the MMC line. To determine the temperature profile we have to derive the governing equation for the thermal section. We have also applied different types of ambient condition like insulation, natural and forced convection. This creates an effect in the heat transfer convection coefficient. To determine the coefficient we need some of the non dimensional parameter. This parameter changes with different conditions.

2.5.1 Thermal Temperature Distribution

The governing equation of the thermal problem is the partial differentiation equation of 2^{nd} order.The governing equation related to the temperature distribution in a MMC line in the ambient temperature (T_∞) is

$$\frac{1}{A}\frac{\partial}{\partial x}(Ak\frac{\partial T}{\partial x}) + \frac{1}{A}\frac{\partial}{\partial y}(Ak\frac{\partial T}{\partial y}) - \frac{hC}{A}(T - T_\infty) - \epsilon A\sigma(T^4 - T_\infty^4) + G(x,y) = \alpha C_p \frac{\partial T}{\partial t} \tag{2.38}$$

where

A= Cross sectional area (m^2)

k= Thermal conductivity of MMC line (W/m.K)

h= Convective heat transfer coefficient ($W/m^2.K$)
C= Perimeter of the heat transfer surface (m)
α= Thermal diffusivity (m^2/s)
C_p= Specific heat capacity (J/kg.K)
ϵ= Emmisivity factor ($0 \sim 1$)
σ= Stefen-Boltzmann constant= 5.67×10^{-8} ($W.m^{-2}.K^{-4}$)

There are various kinds of conditions that we have considered in our study. At first we have considered that it is a steady state condition so the time dependent temperature variant becomes zero. Heat radiation is not considered as the temperature rise is not that big and radiation is insulated. The thermal conductivity of the material varies at the direction of longitudinal and transverse. So, the conductivity is not constant for the material direction The cross sectional area and thermal conductivity is uniform across the MMC line. So, considering these conditions eq 2.38 becomes

$$k_x \frac{\partial^2 T}{\partial x^2} + k_y \frac{\partial^2 T}{\partial y^2} - \frac{hC}{A}(T - T_\infty) + G(x, y) = 0 \tag{2.39}$$

This is the simplified equation for determining the temperature field across the MMC line. Convective heat transfer coefficient *'h'* depends on the surrounding ambient condition and air properties.

2.5.2 Thermal Conditions

There are three different condition considers in our study. The convection coefficient *'h'* depends on this condition.

1. **Thermal Insulation:** The whole body of the MMC line is insulated so that no heat transfer is allowed. in that case h= 0 $W/m^2.K$.

2. **Natural Convection:** The whole body of the MMC line is subjected to heat transfer with surroundings without any air speed. So, no fan is required for this process. This is called natural convection. It is a phenomena that is generated by differences in fluid density but not through external source. The convective heat transfer coefficient is considered to be h= 10 $W/m^2.K$.

3. **Forced Convection:** The whole body of the metal is subjected to heat transfer with surroundings with a constant air speed. The air is provided with a external fan. The body can heat transfer through one side or two side depending on the air flow condition. This is called forced convection. The heat transfer coefficient depends on various non-dimensional parameters.

2.5.3 Convection Coefficient

Convection and conduction are similar in that both mechanism require the presence of a material medium. But they are different in that convection requires the presence of fluid motion. Heat transfer through a fluid is by convection in the presence of bulk fluid motion and by conduction in the absence of it. So when the fluid flows over a solid surface or inside a channel where the temperature of the fluid and solid surface are different. Heat transfer between fluid and solid surface takes place as a consequence of the motion of fluid relative to the surface, Rate of convection heat transfer is observed to be proportional to the temperature difference and is conveniently expressed by Newton's law of cooling as,

$$Q_{conv} = A_s h(T - T_\infty) \tag{2.40}$$

The transition from laminar to turbulent flow depends on the geometry, surface roughness, flow velocity, surface temperature, and type of fluid, among other things. flow regime depends mainly on the ratio of inertial forces to viscous forces in the fluid. Reynolds number is the ratio of the inertial force to the viscous force of a fluid flow. It is defined as,

$$Re_L = \frac{Inertia\ force}{Viscous\ force} = \frac{VL}{\nu} \tag{2.41}$$

where

Re_L= Reynolds number
V= Velocity of fluid (m/s)
L= Characteristics length (m)
ν= kinematic viscosity (m^2/s)

At large Reynolds numbers, the inertial forces, which are proportional to the fluid density and the square of the fluid velocity, are large relative to the viscous forces, and thus the viscous forces cannot prevent the random and rapid fluctuations of the fluid. At small or moderate Reynolds numbers, however, the viscous forces are large enough to suppress these fluctuations and to keep the fluid "in line." Thus the flow is turbulent in the first case and laminar in the second. The Reynolds number at which the flow becomes turbulent is called the critical Reynolds number. The value of the critical Reynolds number is different for different geometries and flow conditions [21].
For a flat horizontal plate, if $Re_L \leq 5 \times 10^5$ then the flow is considered laminar otherwise the flow is turbulent.
Prandtl, Pr number is a Dimensionless number. It is defined as the ratio of momentum diffusivity and thermal diffusivity. Note that whereas the Reynolds number are subscripted with a length scale variable, the Prandtl number contains no such length scale in its definition and is dependent only on the fluid and the fluid state. As such, the Prandtl number

is often found in property tables alongside other properties such as viscosity and thermal conductivity.
For most gases over a wide range of temperature and pressure, Pr is approximately constant. Therefore, it can be used to determine the thermal conductivity of gases at high temperatures, where it is difficult to measure experimentally due to the formation of convection currents.
The Nusselt number is the ratio of convective to conductive heat transfer across a boundary. The convection and conduction heat flows are parallel to each other and to the surface normal of the boundary surface, and are all perpendicular to the mean fluid flow in the simple case.

$$Nu_L = \frac{Convective\ heat\ transfer}{Conductive\ heat\ transfer} = \frac{hL}{k} \tag{2.42}$$

Nusselt number also depends on the isoflux and isothermal boundary conditions of the MMC line. The correlations are given in table A3.
In the table we can see the changes of different conditions with respect to conditions. In our study we have considered average heat transfer coefficient in isoflux boundary condition.The heat transfer coefficient also varies with these conditions. Average conditions give the average heat transfer coefficient over the MMC line.

2.6 Stress Governing Equation and Formulation

Stress modeling of a MMC line is necessary for understanding the failure characteristics across the body. There are two different kinds of loading is applied. Mechanical and thermal loading creates stress in the MMC line. So, different formulation is required for the analysis if stress. In the early stages G.B. Airy had given a stress function approach using ϕ formulation. But the difficulties involved in trying to solve practical problems using the stress function are pointed out by Durelli [29].

To formulate these problem we have to develop the governing equation in terms of σ_x, σ_y and σ_{xy}. Let us consider a rectangular element under load.

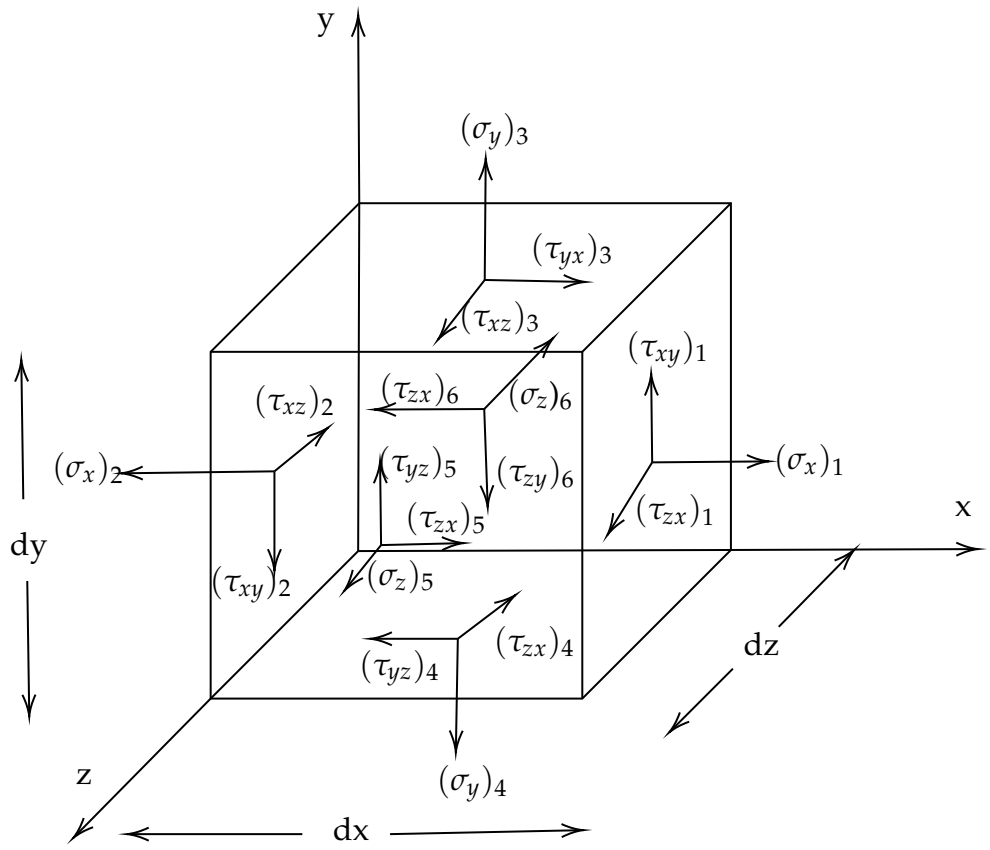

Figure 2.6: A cubical element subjected to loading [6]

In figure 2.6 the volume of the cubical surface becomes ($dx \times dy \times dz$). The force generated in the body is in equilibrium state.
Considering force equilibrium along both axes.

$\overrightarrow{+} \sum F_x = 0$

$(\sigma_x)_1 \Delta y \Delta z$ - $(\sigma_x)_2 \Delta y \Delta z$ + $(\tau_{xy})_3 \Delta x \Delta z$ - $(\tau_{xy})_4 \Delta x \Delta z$ + $(\tau_{zx})_5 \Delta x \Delta y$ - $(\tau_{zx})_6 \Delta x \Delta y$ + $F_x \Delta x \Delta y \Delta z = 0$

$\Rightarrow [(\sigma_x)_1 - (\sigma_x)_2] \Delta y \Delta z + [(\tau_{xy})_3 - (\tau_{xy})_4] \Delta x \Delta z + [(\tau_{zx})_5 - (\tau_{zx})_6] \Delta x \Delta y + F_x \Delta x \Delta y \Delta z = 0$

$\Rightarrow \frac{(\sigma_x)_1 - (\sigma_x)_2}{\Delta x} + \frac{(\tau_{xy})_3 - (\tau_{xy})_4}{\Delta y} + \frac{(\tau_{zx})_5 - (\tau_{zx})_6}{\Delta z} = 0$

Now for limiting cases of the dimensions, i.e. $\Delta x \Rightarrow 0$, $\Delta y arrow 0$, $\Delta z arrow 0$

$$\lim_{\Delta x \to 0} \frac{(\sigma_x)_1 - (\sigma_x)_2}{\Delta x} + \lim_{\Delta y \to 0} \frac{(\tau_{xy})_3 - (\tau_{xy})_4}{\Delta y} + \lim_{\Delta z \to 0} \frac{(\tau_{zx})_5 - (\tau_{zx})_6}{\Delta z} + F_x = 0$$

$$\Rightarrow \frac{\partial \sigma_x}{\partial x} + \frac{\partial \tau_{xy}}{\partial y} + \frac{\partial \tau_{zx}}{\partial z} + F_x = 0 \tag{2.43}$$

Similarly along y and z axis

$$\frac{\partial \sigma_y}{\partial y} + \frac{\partial \tau_{yz}}{\partial x} + \frac{\partial \tau_{yz}}{\partial z} + F_y = 0 \tag{2.44}$$

$$\frac{\partial \sigma_z}{\partial z} + \frac{\partial \tau_{yz}}{\partial y} + \frac{\partial \tau_{zx}}{\partial x} + F_z = 0 \tag{2.45}$$

Three differential equation for general 3-D solids. They are also known as *Navier's Equation of Equilibrium*

2.6.1 Two Dimensional Elasticity

Two dimensional elasticity approach gives us easy simpler way to analyze 3-D bodies considering them 2-D ones.
There are two simplifying assumptions by which 3-D bodies can be approximated as planar problems and we can apply the above approach, which are,

- Plane stress conditions.
- Plane strain conditions.

Plane stress condition is considered to be a state of stress in which the normal stress σ_{zz} and the shear stresses τ_{xz} and τ_{yz} directed perpendicular to the plane are assumed to be zero (but not the strain). Generally, members that are thin (those with a small z dimension compared to the in-plane x and y dimensions) and whose loads act only in the x-y plane can be considered to be under plane stress. Thus, a state of plane stress exists in a thin object loaded in the plane of its largest dimensions. The non-zero stresses σ_{xx}, σ_{yy}, and τ_{xy} lie in the x-y plane and do not vary in the z direction. A thin beam loaded in its plane and a spur gear tooth are good examples of plane stress problems.

On the other hand plane strain is said to be a state of strain in which the strain normal to the x-y plane ϵ_{zz} and the shear strains γ_{xz} and γ_{yz} are assumed to be zero. The assumptions of the plane strain are realistic for long bodies (saying in the z direction) with constant cross-sectional area subjected to loads that act only in the x or y directions and do not vary in the z direction. The option i.e. the plane stress condition has been followed in the present study. Thus,
$\sigma_{zz} = \tau_{zx} = \tau_{yz} = 0$
With that we get,

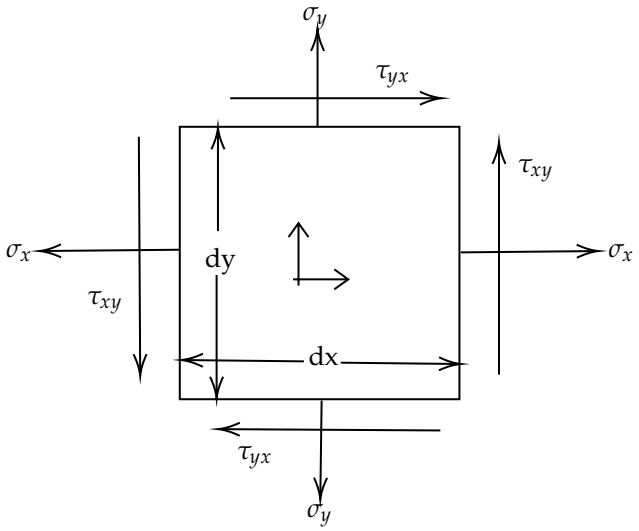

Figure 2.7: A rectangular element subjected to loading

The rectangular element of area ($dx \times dy$) is considered to be both in plane stress and plane strain condition. So, considering plane stress condition, the equilibrium condition for equation 2.43, 2.44 and 2.45 becomes,

$$\frac{\partial \sigma_x}{\partial x} + \frac{\partial \tau_{xy}}{\partial y} + F_x = 0 \tag{2.46}$$

$$\frac{\partial \sigma_y}{\partial y} + \frac{\partial \tau_{yz}}{\partial x} + F_y = 0 \tag{2.47}$$

2.6.2 Solution of Plane Problems of Elasticity

For plane problems there are some additional conditions we use to determine the compatibility equation. The conditions are,

- $\epsilon_x = \dfrac{\partial u}{\partial x} \Rightarrow \dfrac{\partial^2 \epsilon_x}{\partial y^2} = \dfrac{\partial^3 u}{\partial x \partial y^2}$
- $\epsilon_y = \dfrac{\partial v}{\partial y} \Rightarrow \dfrac{\partial^2 \epsilon_y}{\partial x^2} = \dfrac{\partial^3 v}{\partial x^2 \partial y}$
- $\tau_{xy} = \dfrac{\partial u}{\partial y} + \dfrac{\partial v}{\partial x} \Rightarrow \dfrac{\partial^2 \tau_{xy}}{\partial x \partial y} = \dfrac{\partial^3 u}{\partial x \partial y^2} + \dfrac{\partial^3 v}{\partial x^2 \partial y}$

The governing equation due to plane strain condition becomes,

$$\Rightarrow \frac{\partial^2 \epsilon_x}{\partial y^2} + \frac{\partial^2 \epsilon_y}{\partial x^2} = \frac{\partial^2 \gamma_{xy}}{\partial x \partial y}$$

For plane stress problems.

- $\epsilon_x = \dfrac{1}{E}[\sigma_x - \mu \sigma_y]$

- $\epsilon_y = \frac{1}{E}[\sigma_y - \mu\sigma_z]$
- $\gamma_{xy} = \frac{1}{G}\tau_{xy} = \frac{2(1+\mu)}{E}\tau_{xy}$

In this case the plane strain governing equation becomes,

$$\frac{\partial^2}{\partial y^2}[\frac{\sigma_x - \mu\sigma_y}{E}] + \frac{\partial^2}{\partial x^2}[\frac{\sigma_y - \mu\sigma_x}{E}] = \frac{\partial^2}{\partial x \partial y}[\frac{2(1+\mu)}{E}\tau_{xy}]$$

$$\Rightarrow \frac{\partial^2\sigma_x}{\partial y^2} - \mu\frac{\partial^2\sigma_y}{\partial y^2} + \frac{\partial^2\sigma_y}{\partial x^2} - \mu\frac{\partial^2\sigma_x}{\partial x^2} = 2(1+\mu)\frac{\partial^2\tau_{xy}}{\partial x\partial y}$$

$$\Rightarrow \frac{\partial^2\sigma_x}{\partial y^2} + \frac{\partial^2\sigma_y}{\partial x^2} - \mu(\frac{\partial^2\sigma_x}{\partial x^2} + \frac{\partial^2\sigma_y}{\partial y^2}) = 2(1+\mu)\frac{\partial^2\tau_{xy}}{\partial x\partial y}$$

The equilibrium equation of plane stress conditions can be written as,

- $\frac{\partial^2\sigma_x}{\partial x^2} + \frac{\partial^2\tau_{xy}}{\partial x\partial y} = 0$
- $\frac{\partial^2\sigma_y}{\partial y^2} + \frac{\partial^2\tau_{xy}}{\partial x\partial y} = 0$

The governing equation,

$$\frac{\partial^2\sigma_x}{\partial x^2} + \frac{\partial^2\sigma_y}{\partial y^2} = -2\frac{\partial^2\tau_{xy}}{\partial x\partial y}$$

$$\Rightarrow \frac{\partial^2\sigma_x}{\partial y^2} + \frac{\partial^2\sigma_y}{\partial x^2} - \mu(\frac{\partial^2\sigma_x}{\partial x^2} + \frac{\partial^2\sigma_y}{\partial y^2}) = -(1+\mu)(\frac{\partial^2\sigma_x}{\partial x^2} + \frac{\partial^2\sigma_y}{\partial y^2})$$

$$\Rightarrow \frac{\partial^2\sigma_x}{\partial y^2} + \frac{\partial^2\sigma_y}{\partial x^2} + \frac{\partial^2\sigma_x}{\partial x^2} + \frac{\partial^2\sigma_y}{\partial y^2} = 0$$

This leads to the continuity equation of strain components.

$$(\frac{\partial^2}{\partial x^2} + \frac{\partial^2}{\partial y^2})(\sigma_x + \sigma_y) = 0 \tag{2.48}$$

This is the compatibility equation of Elasticity.

2.6.3 Hooke's Law

In simplest approximation solution of the stress and strain relation is taken to be linear and it's called Hooke's law. The general approximation of the Hooke's law with respect to

thermal expansion coefficient of the material is,

$$\begin{Bmatrix} \sigma_{xx} \\ \sigma_{yy} \\ \sigma_{zz} \\ \tau_{yz} \\ \tau_{zx} \\ \tau_{xy} \\ \tau_{yz} \\ \tau_{xz} \\ \tau_{zy} \end{Bmatrix} = \begin{bmatrix} C_{11} & C_{12} & C_{13} & C_{14} & C_{15} & C_{16} & C_{17} & C_{18} & C_{19} \\ C_{21} & C_{22} & C_{23} & C_{24} & C_{25} & C_{26} & C_{27} & C_{28} & C_{29} \\ C_{31} & C_{32} & C_{33} & C_{34} & C_{35} & C_{36} & C_{37} & C_{38} & C_{39} \\ C_{41} & C_{42} & C_{43} & C_{44} & C_{45} & C_{46} & C_{47} & C_{48} & C_{49} \\ C_{51} & C_{52} & C_{53} & C_{54} & C_{55} & C_{56} & C_{57} & C_{58} & C_{59} \\ C_{61} & C_{62} & C_{63} & C_{64} & C_{65} & C_{66} & C_{67} & C_{68} & C_{69} \\ C_{71} & C_{72} & C_{73} & C_{74} & C_{75} & C_{76} & C_{77} & C_{78} & C_{79} \\ C_{81} & C_{82} & C_{83} & C_{84} & C_{85} & C_{86} & C_{87} & C_{88} & C_{89} \\ C_{91} & C_{92} & C_{93} & C_{94} & C_{95} & C_{96} & C_{97} & C_{98} & C_{99} \end{bmatrix} \begin{Bmatrix} \epsilon_{xx} - \alpha_x \Delta T \\ \epsilon_{yy} - \alpha_y \Delta T \\ \epsilon_{zz} - \alpha_z \Delta T \\ \gamma_{yz} \\ \gamma_{zx} \\ \gamma_{xy} \\ \gamma_{zy} \\ \gamma_{xz} \\ \gamma_{yx} \end{Bmatrix} \tag{2.49}$$

Where the 81 coefficients C_{11},$\cdots\cdots\cdots$,C_{99} are called elastic coefficient or stiffness. For the equilibrium condition $\tau_{ij} = \tau_{ji}$ and $\gamma_{ij} = \gamma_{ji}$, equation 2.49 becomes,

$$\begin{Bmatrix} \sigma_{xx} \\ \sigma_{yy} \\ \sigma_{zz} \\ \tau_{yz} \\ \tau_{zx} \\ \tau_{yx} \end{Bmatrix} = \begin{bmatrix} C_{11} & C_{12} & C_{13} & C_{14} & C_{15} & C_{16} \\ C_{21} & C_{22} & C_{23} & C_{24} & C_{25} & C_{26} \\ C_{31} & C_{32} & C_{33} & C_{34} & C_{35} & C_{36} \\ C_{41} & C_{42} & C_{43} & C_{44} & C_{45} & C_{46} \\ C_{51} & C_{52} & C_{53} & C_{54} & C_{55} & C_{56} \\ C_{61} & C_{62} & C_{63} & C_{64} & C_{65} & C_{66} \end{bmatrix} \begin{Bmatrix} \epsilon_{xx} - \alpha_x \Delta T \\ \epsilon_{yy} - \alpha_y \Delta T \\ \epsilon_{zz} - \alpha_z \Delta T \\ \gamma_{yz} \\ \gamma_{zx} \\ \gamma_{xy} \end{Bmatrix} \tag{2.50}$$

From the consideration of strain energy density, it can be written as $C_{ij} = C_{ji}$, Thus the 36 stiffness matrix comes down to 21 and the stiffness matrix becomes,

$$\left[C_{ij}\right] = \begin{bmatrix} C_{11} & C_{12} & C_{13} & C_{14} & C_{15} & C_{16} \\ C_{21} & C_{22} & C_{23} & C_{24} & C_{25} & C_{26} \\ C_{31} & C_{32} & C_{33} & C_{34} & C_{35} & C_{36} \\ C_{14} & C_{24} & C_{34} & C_{44} & C_{45} & C_{46} \\ C_{15} & C_{25} & C_{35} & C_{45} & C_{55} & C_{56} \\ C_{16} & C_{26} & C_{36} & C_{46} & C_{56} & C_{66} \end{bmatrix} \tag{2.51}$$

Materials having symmetry with respect to one plane is referred to as non-clinic material. For such cases of material, transformation of the axes can be done and found that $C_{14} = C_{15} = C_{24} = C_{25} = C_{34} = C_{35} = C_{44} = C_{46} = C_{56} = C_{66} = 0$, then the number of stiffness

matrix becomes 13 and equation 2.51 becomes,

$$\left[C_{ij}\right] = \begin{bmatrix} C_{11} & C_{12} & C_{13} & 0 & 0 & C_{16} \\ C_{21} & C_{22} & C_{23} & 0 & 0 & C_{26} \\ C_{31} & C_{32} & C_{33} & 0 & 0 & C_{36} \\ 0 & 0 & 0 & C_{44} & C_{45} & 0 \\ 0 & 0 & 0 & C_{45} & C_{55} & 0 \\ C_{16} & C_{26} & C_{36} & 0 & 0 & 0 \end{bmatrix} \tag{2.52}$$

Again an orthotropic material has at least two orthogonal planes of symmetry, where material properties are independent of direction within each plane. Normally the reference system of coordinates is selected along the principal plane of an orthogonal material include a single lamina of continuous fibre composite arranged in a rectangular array, a wooden bar and rolled steel. For such cases of material symmetry. Examples: $C_{16} = C_{26} = C_{36} = C_{45} = 0$ and then this type of materials require 9 independent variables as elastic constants in their stiffness matrix as follows.

$$\left[C_{ij}\right]_{orthotropic} = \begin{bmatrix} C_{11} & C_{12} & C_{13} & 0 & 0 & 0 \\ C_{21} & C_{22} & C_{23} & 0 & 0 & 0 \\ C_{31} & C_{32} & C_{33} & 0 & 0 & 0 \\ 0 & 0 & 0 & C_{44} & 0 & 0 \\ 0 & 0 & 0 & 0 & C_{55} & 0 \\ 0 & 0 & 0 & 0 & 0 & C_{66} \end{bmatrix} \tag{2.53}$$

Most metallic alloys and thermoset polymers are considered isotropic material, where by definition the mechanical properties are independent of direction. In this case there are infinite planes of symmetry. Such materials have only two independent variables i.e. elastic in constants in their stiffness matrix as,

$$\left[C_{ij}\right]_{isotropic} = \begin{bmatrix} C_{11} & C_{12} & C_{12} & 0 & 0 & 0 \\ C_{12} & C_{11} & C_{12} & 0 & 0 & 0 \\ C_{12} & C_{12} & C_{11} & 0 & 0 & 0 \\ 0 & 0 & 0 & \frac{C_{11}-C_{12}}{2} & 0 & 0 \\ 0 & 0 & 0 & 0 & \frac{C_{11}-C_{12}}{2} & 0 \\ 0 & 0 & 0 & 0 & 0 & \frac{C_{11}-C_{12}}{2} \end{bmatrix} \tag{2.54}$$

The summarised form of independent elastic constants for general anisotropic, anisotropic with symmetric stress and strain components or with energy consideration, orthotropic and isotropic materials can be thus presented in table 2.1 as follows.

Table 2.1: Elastic Components

Serial	Material	Condition	No of Constant
1	Anisotropic	General form	81
2	Anisotropic	Equilibrium condition	36
3	Anisotropic	Stain energy consideration	21
4	Monoclinic	Symmetric to a plane	13
5	Orthotropic	Having Mutually Perpendicular Plane of Symmetry	9
6	Isotropic	Same Elastic Properties in all Directions (having Infinite Perpendicular Plane of Symmetry)	2

As we are working on the orthotropic material, we need to reduce equation 2.50 to two dimensional form. For two dimensional case of orthotropic material, stiffness matrix given in equation 2.50 can be reduced to

$$\begin{Bmatrix} \sigma_{xx} \\ \sigma_{yy} \\ \tau_{xy} \end{Bmatrix} = \begin{bmatrix} \overline{Q}_{11} & \overline{Q}_{12} & \overline{Q}_{16} \\ \overline{Q}_{21} & \overline{Q}_{22} & \overline{Q}_{26} \\ \overline{Q}_{16} & \overline{Q}_{26} & \overline{Q}_{66} \end{bmatrix} \begin{Bmatrix} \epsilon_{xx} - \alpha_x \Delta T \\ \epsilon_{yy} - \alpha_y \Delta T \\ \gamma_{xy} \end{Bmatrix} \tag{2.55}$$

where,

$$\overline{Q}_{11} = Q_{11}cos^4\theta + 2(Q_{12} + Q_{66})sin^2\theta cos^2\theta + Q_{22}sin^4\theta$$

$$\overline{Q}_{12} = Q_{12}(sin^4\theta + cos^4\theta + (Q_{11} + Q_{22} - 4Q_{66})sin^2\theta cos^2\theta$$

$$\overline{Q}_{22} = Q_{11}sin^4\theta + 2(Q_{12} + 2Q_{66})sin^2\theta cos^2\theta + Q_{22}cos^4\theta$$

$$\overline{Q}_{16} = (Q_{11} - Q_{12} - 2Q_{66})sin\theta cos^3\theta + (Q_{12} - Q_{22} + 2Q_{66})sin^3\theta cos\theta$$

$$\overline{Q}_{26} = (Q_{11} - Q_{12} - 2Q_{66})sin^3\theta cos\theta + (Q_{12} - Q_{22} + 2Q_{66})sin\theta cos^3\theta$$

$$\overline{Q}_{66} = (Q_{11} + Q_{22} - 2Q_{12} - 2Q_{66})sin^2\theta cos^2\theta + Q_{66}(sin^4\theta + cos^4\theta)$$

and,

$$Q_{11} = \frac{E_{11}}{1-\mu_{12}\mu_{21}} = \frac{E_{11}^2}{E_{11}-\mu_{12}^2 E_{22}}$$

$$Q_{22} = \frac{E_{22}}{1-\mu_{12}\mu_{21}} = \frac{E_{11}E_{22}}{E_{11}-\mu_{12}^2 E_{22}}$$

$$Q_{12} = Q_{21} = \frac{\mu_{12}E_{22}}{1-\mu_{12}\mu_{21}} = \frac{\mu_{21}E_{11}}{1-\mu_{12}\mu_{21}} = \frac{\mu_{12}E_{11}E_{22}}{E_{11}-\mu_{12}^2 E_{22}}$$

$$Q_{66} = G_{12}, \qquad Q_{16} = Q_{26} = 0$$

In the above displacement formulation, the stresses are expressed in terms of the displacement components for their determination. The three stress–displacement relations for the

plane problems of orthotropic materials, obtained from equation 2.55 are as follows,

$$\sigma_x = \overline{Q}_{11}\frac{\partial u_x}{\partial x} + \overline{Q}_{12}\frac{\partial u_y}{\partial y} - (\overline{Q}_{11}\alpha_x + \overline{Q}_{12}\alpha_y)\Delta T \tag{2.56a}$$

$$\sigma_y = \overline{Q}_{12}\frac{\partial u_x}{\partial x} + \overline{Q}_{22}\frac{\partial u_y}{\partial y} - (\overline{Q}_{12}\alpha_x + \overline{Q}_{22}\alpha_y)\Delta T \tag{2.56b}$$

$$\tau_{xy} = \overline{Q}_{66}(\frac{\partial u_x}{\partial y} + \frac{\partial u_y}{\partial x}) \tag{2.56c}$$

Now substituting this equations in equation 2.46 we can get

$$\frac{\partial}{\partial x}[\overline{Q}_{11}\frac{\partial u_x}{\partial x} + \overline{Q}_{12}\frac{\partial u_y}{\partial y} - (\overline{Q}_{11}\alpha_x + \overline{Q}_{12}\alpha_y)\Delta T] + \frac{\partial}{\partial y}[\overline{Q}_{66}(\frac{\partial u_x}{\partial y} + \frac{\partial u_y}{\partial x})] = 0$$

$$\Rightarrow \overline{Q}_{11}\frac{\partial^2 u_x}{\partial x^2} + \overline{Q}_{12}\frac{\partial^2 u_y}{\partial x \partial y} - (\overline{Q}_{11}\alpha_x + \overline{Q}_{12}\alpha_y)\frac{\partial T}{\partial x} + \overline{Q}_{66}(\frac{\partial^2 u_x}{\partial y^2} + \frac{\partial^2 u_y}{\partial x \partial y}) = 0$$

$$\Rightarrow \overline{Q}_{11}\frac{\partial^2 u_x}{\partial x^2} + (\overline{Q}_{12} + \overline{Q}_{66})\frac{\partial^2 u_y}{\partial x \partial y} + \overline{Q}_{66}\frac{\partial^2 u_x}{\partial y^2} - (\overline{Q}_{11}\alpha_x + \overline{Q}_{12}\alpha_y)\frac{\partial T}{\partial x} = 0 \tag{2.57}$$

and also from equation 2.47 we get

$$\frac{\partial}{\partial y}[\overline{Q}_{12}\frac{\partial u_x}{\partial x} + \overline{Q}_{22}\frac{\partial u_y}{\partial y}) - (\overline{Q}_{12}\alpha_x + \overline{Q}_{22}\alpha_y)\Delta T] + \frac{\partial}{\partial x}[\overline{Q}_{66}(\frac{\partial u_x}{\partial y} + \frac{\partial u_y}{\partial x})] = 0$$

$$\Rightarrow \overline{Q}_{12}\frac{\partial^2 u_x}{\partial x \partial y} + \overline{Q}_{22}\frac{\partial^2 u_y}{\partial y^2} - (\overline{Q}_{12}\alpha_x + \overline{Q}_{22}\alpha_y)\frac{\partial T}{\partial y} + \overline{Q}_{66}(\frac{\partial^2 u_x}{\partial x \partial y} + \frac{\partial^2 u_y}{\partial y^2}) = 0$$

$$\Rightarrow \overline{Q}_{22}\frac{\partial^2 u_y}{\partial y^2} + (\overline{Q}_{12} + \overline{Q}_{66})\frac{\partial^2 u_x}{\partial x \partial y} + \overline{Q}_{66}\frac{\partial^2 u_y}{\partial x^2} - (\overline{Q}_{12}\alpha_x + \overline{Q}_{22}\alpha_y)\frac{\partial T}{\partial y} = 0 \tag{2.58}$$

2.7 Displacement Potential Function

Now, we have to solve the equations to determine different components across the MMC line. As the difficulty of solving multi variable solution is high, a single variable ψ is introduced to deduce the equations to a single variable. The variable satisfies the stress equations and the corresponding boundary conditions. It is called displacement potential function and defined with ψ of space variable x and y. The components are expressed as follows,

$$u_x = \alpha_1\frac{\partial^2 \psi}{\partial x^2} + \alpha_2\frac{\partial^2 \psi}{\partial x \partial y} + \alpha_3\frac{\partial^2 \psi}{\partial y^2} \tag{2.59a}$$

$$u_y = \alpha_4\frac{\partial^2 \psi}{\partial x^2} + \alpha_5\frac{\partial^2 \psi}{\partial x \partial y} + \alpha_6\frac{\partial^2 \psi}{\partial y^2} \tag{2.59b}$$

Substituting the equation 2.59 in equation 2.57 we get,

$$\overline{Q}_{11}\frac{\partial^2}{\partial x^2}[\alpha_1\frac{\partial^2\psi}{\partial x^2}+\alpha_2\frac{\partial^2\psi}{\partial x\partial y}+\alpha_3\frac{\partial^2\psi}{\partial y^2}]+(\overline{Q}_{12}+\overline{Q}_{66})\frac{\partial^2}{\partial x\partial y}[\alpha_4\frac{\partial^2\psi}{\partial x^2}+\alpha_5\frac{\partial^2\psi}{\partial x\partial y}+\alpha_6\frac{\partial^2\psi}{\partial y^2}]$$
$$+\overline{Q}_{66}\frac{\partial^2}{\partial y^2}[\alpha_1\frac{\partial^2\psi}{\partial x^2}+\alpha_2\frac{\partial^2\psi}{\partial x\partial y}+\alpha_3\frac{\partial^2\psi}{\partial y^2}]-(\overline{Q}_{11}\alpha_x+\overline{Q}_{12}\alpha_y)\frac{\partial T}{\partial x}=0$$
$$\Rightarrow \overline{Q}_{11}[\alpha_1\frac{\partial^4\psi}{\partial x^4}+\alpha_2\frac{\partial^4\psi}{\partial x^3\partial y}+\alpha_3\frac{\partial^4\psi}{\partial x^2\partial y^2}]+(\overline{Q}_{12}+\overline{Q}_{66})[\alpha_4\frac{\partial^4\psi}{\partial x^3\partial y}+\alpha_5\frac{\partial^4\psi}{\partial x^2\partial y^2}+\alpha_6\frac{\partial^4\psi}{\partial x\partial y^3}]$$
$$+\overline{Q}_{66}[\alpha_1\frac{\partial^4\psi}{\partial x^2\partial y^2}+\alpha_2\frac{\partial^4\psi}{\partial x\partial y^3}+\alpha_3\frac{\partial^4\psi}{\partial y^4}]-(\overline{Q}_{11}\alpha_x+\overline{Q}_{12}\alpha_y)\frac{\partial T}{\partial x}=0$$

$$\Rightarrow \alpha_1\overline{Q}_{11}\frac{\partial^4\psi}{\partial x^4}+\alpha_2\overline{Q}_{11}+\alpha_4(\overline{Q}_{12}+\overline{Q}_{66})\frac{\partial^4\psi}{\partial x^3\partial y}+\alpha_3\overline{Q}_{11}+\alpha_5(\overline{Q}_{12}+\overline{Q}_{66})+\alpha_1\overline{Q}_{66}\frac{\partial^4\psi}{\partial x^2\partial y^2}$$
$$+\alpha_6(\overline{Q}_{12}+\overline{Q}_{66})+\alpha_2\overline{Q}_{66}\frac{\partial^4\psi}{\partial x\partial y^3}+\alpha_3\overline{Q}_{66}\frac{\partial^4\psi}{\partial y^4}-(\overline{Q}_{11}\alpha_x+\overline{Q}_{12}\alpha_y)\frac{\partial T}{\partial x}=0 \quad (2.60)$$

Again substituting equation 2.59 in equation 2.58 we get,

$$\overline{Q}_{22}\frac{\partial^2}{\partial y^2}[\alpha_4\frac{\partial^2\psi}{\partial x^2}+\alpha_5\frac{\partial^2\psi}{\partial x\partial y}+\alpha_6\frac{\partial^2\psi}{\partial y^2}]+(\overline{Q}_{12}+\overline{Q}_{66})\frac{\partial^2}{\partial x\partial y}[\alpha_1\frac{\partial^2\psi}{\partial x^2}+\alpha_2\frac{\partial^2\psi}{\partial x\partial y}+\alpha_3\frac{\partial^2\psi}{\partial y^2}]$$
$$+\overline{Q}_{66}\frac{\partial^2}{\partial x^2}[\alpha_4\frac{\partial^2\psi}{\partial x^2}+\alpha_5\frac{\partial^2\psi}{\partial x\partial y}+\alpha_6\frac{\partial^2\psi}{\partial y^2}]-(\overline{Q}_{12}\alpha_x+\overline{Q}_{22}\alpha_y)\frac{\partial T}{\partial y}=0$$
$$\Rightarrow \overline{Q}_{22}[\alpha_4\frac{\partial^4\psi}{\partial x^2\partial y^2}+\alpha_5\frac{\partial^4\psi}{\partial x\partial y^3}+\alpha_6\frac{\partial^4\psi}{\partial y^4}]+(\overline{Q}_{12}+\overline{Q}_{66})[\alpha_1\frac{\partial^4\psi}{\partial x^3\partial y}+\alpha_2\frac{\partial^4\psi}{\partial x^2\partial y^2}+\alpha_3\frac{\partial^4\psi}{\partial x\partial y^3}]$$
$$+\overline{Q}_{66}[\alpha_4\frac{\partial^4\psi}{\partial x^4}+\alpha_5\frac{\partial^4\psi}{\partial x^3\partial y}+\alpha_6\frac{\partial^4\psi}{\partial x^2\partial y^2}]-(\overline{Q}_{12}\alpha_x+\overline{Q}_{22}\alpha_y)\frac{\partial T}{\partial y}=0$$

$$\Rightarrow \alpha_4\overline{Q}_{66}\frac{\partial^4\psi}{\partial x^4}+\alpha_1(\overline{Q}_{12}+\overline{Q}_{66})+\alpha_5\overline{Q}_{66}\frac{\partial^4\psi}{\partial x^3\partial y}+\alpha_4\overline{Q}_{22}+\alpha_2(\overline{Q}_{12}+\overline{Q}_{66})+\alpha_6\overline{Q}_{66}\frac{\partial^4\psi}{\partial x^2\partial y^2}$$
$$+\alpha_5\overline{Q}_{22}+\alpha_3(\overline{Q}_{12}+\overline{Q}_{66})\frac{\partial^4\psi}{\partial x\partial y^3}+\alpha_6\overline{Q}_{22}\frac{\partial^4\psi}{\partial y^4}-(\overline{Q}_{12}\alpha_x+\overline{Q}_{22}\alpha_y)\frac{\partial T}{\partial y}=0 \quad (2.61)$$

2.7.1 Temperature Variation only in x-direction

Now, let's consider the temperature varies in x-direction so we can write, $\frac{dT}{dy}=0$. So, from equation 2.61 we get,

$$\Rightarrow \alpha_4\overline{Q}_{66}\frac{\partial^4\psi}{\partial x^4}+\alpha_1(\overline{Q}_{12}+\overline{Q}_{66})+\alpha_5\overline{Q}_{66}\frac{\partial^4\psi}{\partial x^3\partial y}+\alpha_4\overline{Q}_{22}+\alpha_2(\overline{Q}_{12}+\overline{Q}_{66})+\alpha_6\overline{Q}_{66}\frac{\partial^4\psi}{\partial x^2\partial y^2}$$
$$+\alpha_5\overline{Q}_{22}+\alpha_3(\overline{Q}_{12}+\overline{Q}_{66})\frac{\partial^4\psi}{\partial x\partial y^3}+\alpha_6\overline{Q}_{22}\frac{\partial^4\psi}{\partial y^4}=0$$

Equating the equation on both side we get,

- $\alpha_4=0$
- $\alpha_1(\overline{Q}_{12}+\overline{Q}_{66})+\alpha_5\overline{Q}_{66}=0\Rightarrow\alpha_1=-\frac{\overline{Q}_{66}}{\overline{Q}_{12}+\overline{Q}_{66}}$

- $\alpha_4\overline{Q}_{22} + \alpha_2(\overline{Q}_{12} + \overline{Q}_{66}) + \alpha_6\overline{Q}_{66} = 0 \Rightarrow \alpha_2 = 0$
- $\alpha_5\overline{Q}_{22} + \alpha_3(\overline{Q}_{12} + \overline{Q}_{66}) = 0 \Rightarrow \alpha_3 = -\dfrac{\overline{Q}_{22}}{\overline{Q}_{12} + \overline{Q}_{66}}$
- $\alpha_6 = 0$
- $\alpha_5 = 1$

Now from equation 2.60,

$$\{-\frac{\overline{Q}_{66}.\overline{Q}_{11}}{\overline{Q}_{12} + \overline{Q}_{66}}\}\frac{\partial^4\psi}{\partial x^4} + \{-\frac{\overline{Q}_{11}.\overline{Q}_{22}}{\overline{Q}_{12} + \overline{Q}_{66}} + (\overline{Q}_{12} + \overline{Q}_{66}) - \frac{\overline{Q}_{66}.\overline{Q}_{66}}{\overline{Q}_{12} + \overline{Q}_{66}}\}\frac{\partial^4\psi}{\partial x^2\partial y^2} - \{\frac{\overline{Q}_{22}.\overline{Q}_{66}}{\overline{Q}_{12} + \overline{Q}_{66}}\}\frac{\partial^4\psi}{\partial y^4}$$
$$- (\overline{Q}_{11}\alpha_x + \overline{Q}_{12}\alpha_y)\frac{\partial T}{\partial x} = 0$$
$$\Rightarrow \{\frac{\overline{Q}_{66}.\overline{Q}_{11}}{\overline{Q}_{12} + \overline{Q}_{66}}\}\frac{\partial^4\psi}{\partial x^4} + \{\frac{\overline{Q}_{11}.\overline{Q}_{22}}{\overline{Q}_{12} + \overline{Q}_{66}} - (\overline{Q}_{12} + \overline{Q}_{66}) + \frac{\overline{Q}_{66}.\overline{Q}_{66}}{\overline{Q}_{12} + \overline{Q}_{66}}\}\frac{\partial^4\psi}{\partial x^2\partial y^2} + \{\frac{\overline{Q}_{22}.\overline{Q}_{66}}{\overline{Q}_{12} + \overline{Q}_{66}}\}\frac{\partial^4\psi}{\partial y^4}$$
$$+ (\overline{Q}_{11}\alpha_x + \overline{Q}_{12}\alpha_y)\frac{\partial T}{\partial x} = 0$$

$$\Rightarrow \frac{\partial^4\psi}{\partial x^4} + \frac{\overline{Q}_{22}}{\overline{Q}_{66}} - \frac{\overline{Q}_{12}^2}{\overline{Q}_{66}.\overline{Q}_{11}} - \frac{2\overline{Q}_{12}}{\overline{Q}_{11}}\frac{\partial^4\psi}{\partial x^2\partial y^2} + \frac{\overline{Q}_{22}}{\overline{Q}_{11}}\frac{\partial^4\psi}{\partial y^4} + (\frac{\overline{Q}_{12} + \overline{Q}_{66}}{\overline{Q}_{66}.\overline{Q}_{11}})(\overline{Q}_{11}\alpha_x + \overline{Q}_{12}\alpha_y)\frac{\partial T}{\partial x} = 0 \quad (2.62)$$

This is the bi-harmonic equation for the MMC line along x-direction. For that equation 2.59 becomes,

- $u_x = -\dfrac{\overline{Q}_{66}}{\overline{Q}_{12} + \overline{Q}_{66}}\dfrac{\partial^2\psi}{\partial x^2} - \dfrac{\overline{Q}_{22}}{\overline{Q}_{12} + \overline{Q}_{66}}\dfrac{\partial^2\psi}{\partial y^2}$
- $u_y = \dfrac{\partial^2\psi}{\partial x\partial y}$

Now from equation 2.56 σ_x, σ_y and τ_{xy} becomes,

$$\sigma_x = \overline{Q}_{11}\{\frac{\partial}{\partial x} - \frac{\overline{Q}_{66}}{\overline{Q}_{12} + \overline{Q}_{66}}\}\frac{\partial^2\psi}{\partial x^2} - \{\frac{\overline{Q}_{22}}{\overline{Q}_{12} + \overline{Q}_{66}}\}\frac{\partial^2\psi}{\partial y^2} + \overline{Q}_{12}\frac{\partial}{\partial y}(\frac{\partial^2\psi}{\partial x\partial y}) - (\overline{Q}_{11}\alpha_x + \overline{Q}_{12}\alpha_y)\Delta T$$
$$= -\frac{\overline{Q}_{11}.\overline{Q}_{66}}{\overline{Q}_{12} + \overline{Q}_{66}}\frac{\partial^3\psi}{\partial x^3} + \overline{Q}_{12}\frac{\partial^3\psi}{\partial x\partial y^2} - \frac{\overline{Q}_{11}.\overline{Q}_{22}}{\overline{Q}_{12} + \overline{Q}_{66}}\frac{\partial^3\psi}{\partial x\partial y^2} - (\overline{Q}_{11}\alpha_x + \overline{Q}_{12}\alpha_y)\Delta T$$
$$\sigma_x = -\frac{\overline{Q}_{11}.\overline{Q}_{66}}{\overline{Q}_{12} + \overline{Q}_{66}}\frac{\partial^3\psi}{\partial x^3} + (\overline{Q}_{12} - \frac{\overline{Q}_{11}.\overline{Q}_{22}}{\overline{Q}_{12} + \overline{Q}_{66}})\frac{\partial^3\psi}{\partial x\partial y^2} - (\overline{Q}_{11}\alpha_x + \overline{Q}_{12}\alpha_y)\Delta T \quad (2.63)$$

$$\sigma_y = \overline{Q}_{12}\frac{\partial}{\partial x}\{-\frac{\overline{Q}_{66}}{\overline{Q}_{12}+\overline{Q}_{66}}\}\frac{\partial^2\psi}{\partial x^2} - \{\frac{\overline{Q}_{22}}{\overline{Q}_{12}+\overline{Q}_{66}}\}\frac{\partial^2\psi}{\partial y^2} + \overline{Q}_{22}\frac{\partial}{\partial y}(\frac{\partial^2\psi}{\partial x\partial y}) - (\overline{Q}_{12}\alpha_x + \overline{Q}_{22}\alpha_y)\Delta T$$
$$= -\frac{\overline{Q}_{12}.\overline{Q}_{66}}{\overline{Q}_{12}+\overline{Q}_{66}}\frac{\partial^3\psi}{\partial x^3} - \frac{\overline{Q}_{12}.\overline{Q}_{22}}{\overline{Q}_{12}+\overline{Q}_{66}}\frac{\partial^3\psi}{\partial x\partial y^2} + \overline{Q}_{22}\frac{\partial^3\psi}{\partial x\partial y^2} - (\overline{Q}_{12}\alpha_x + \overline{Q}_{22}\alpha_y)\Delta T$$
$$\sigma_y = -\frac{\overline{Q}_{12}.\overline{Q}_{66}}{\overline{Q}_{12}+\overline{Q}_{66}}\frac{\partial^3\psi}{\partial x^3} + (\overline{Q}_{22} - \frac{\overline{Q}_{12}.\overline{Q}_{22}}{\overline{Q}_{12}+\overline{Q}_{66}})\frac{\partial^3\psi}{\partial x\partial y^2} - (\overline{Q}_{12}\alpha_x + \overline{Q}_{22}\alpha_y)\Delta T \tag{2.64}$$

$$\tau_{xy} = \overline{Q}_{66}\frac{\partial}{\partial y}\{-\frac{\overline{Q}_{66}}{\overline{Q}_{12}+\overline{Q}_{66}}\}\frac{\partial^2\psi}{\partial x^2} - \frac{\overline{Q}_{22}}{\overline{Q}_{12}+\overline{Q}_{66}}\frac{\partial^2\psi}{\partial y^2} + \overline{Q}_{66}\frac{\partial}{\partial x}(\frac{\partial^2\psi}{\partial x\partial y})$$
$$= \{\overline{Q}_{66} - \frac{\overline{Q}_{66}}{\overline{Q}_{12}+\overline{Q}_{66}}\}\frac{\partial^3\psi}{\partial x^2\partial y} - \frac{\overline{Q}_{22}}{\overline{Q}_{12}+\overline{Q}_{66}}\frac{\partial^3\psi}{\partial y^3} + \overline{Q}_{66}\frac{\partial}{\partial x}(\frac{\partial^2\psi}{\partial x\partial y})$$
$$\tau_{xy} = (\overline{Q}_{66} - \frac{\overline{Q}_{66}.\overline{Q}_{66}}{\overline{Q}_{12}+\overline{Q}_{66}})\frac{\partial^3\psi}{\partial x^2\partial y} - \frac{\overline{Q}_{22}.\overline{Q}_{66}}{\overline{Q}_{12}+\overline{Q}_{66}}\frac{\partial^3\psi}{\partial y^3} \tag{2.65}$$

2.7.2 Temperature Variation only in y-direction

Now, let's consider the temperature varies in y-direction so we can write, $\frac{dT}{dx} = 0$. So, from equation 2.60 we get,

$$\Rightarrow \alpha_1\overline{Q}_{11}\frac{\partial^4\psi}{\partial x^4} + \alpha_2\overline{Q}_{11} + \alpha_4(\overline{Q}_{12}+\overline{Q}_{66})\frac{\partial^4\psi}{\partial x^3\partial y} + \alpha_3\overline{Q}_{11} + \alpha_5(\overline{Q}_{12}+\overline{Q}_{66}) + \alpha_1\overline{Q}_{66}\frac{\partial^4\psi}{\partial x^2\partial y^2}$$
$$+ \alpha_6(\overline{Q}_{12}+\overline{Q}_{66}) + \alpha_2\overline{Q}_{66}\frac{\partial^4\psi}{\partial x\partial y^3} + \alpha_3\overline{Q}_{66}\frac{\partial^4\psi}{\partial y^4} = 0$$

Equating the equation on both side we get,

- $\alpha_1 = 0$
- $\alpha_2\overline{Q}_{11} + \alpha_4(\overline{Q}_{12}+\overline{Q}_{66}) = 0 \Rightarrow \alpha_4 = -\frac{\overline{Q}_{11}}{\overline{Q}_{12}+\overline{Q}_{66}}$
- $\alpha_3\overline{Q}_{11} + \alpha_5(\overline{Q}_{12}+\overline{Q}_{66}) + \alpha_1\overline{Q}_{66} = 0 \Rightarrow \alpha_5 = 0$
- $\alpha_6(\overline{Q}_{12}+\overline{Q}_{66}) + \alpha_2\overline{Q}_{66} = 0 \Rightarrow \alpha_6 = -\frac{\overline{Q}_{66}}{\overline{Q}_{12}+\overline{Q}_{66}}$
- $\alpha_2 = -\frac{\overline{Q}_{66}.\overline{Q}_{66}}{\overline{Q}_{12}+\overline{Q}_{66}}$
- $\alpha_3 = 0$

Now from equation 2.60,

$$\{-\frac{\overline{Q}_{66}.\overline{Q}_{11}}{\overline{Q}_{12}+\overline{Q}_{66}}\}\frac{\partial^4\psi}{\partial x^4} + \{-\frac{\overline{Q}_{11}.\overline{Q}_{22}}{\overline{Q}_{12}+\overline{Q}_{66}} + (\overline{Q}_{12}+\overline{Q}_{66}) - \frac{\overline{Q}_{66}.\overline{Q}_{66}}{\overline{Q}_{12}+\overline{Q}_{66}}\}\frac{\partial^4\psi}{\partial x^2\partial y^2} + \{-\frac{\overline{Q}_{22}.\overline{Q}_{66}}{\overline{Q}_{12}+\overline{Q}_{66}}\}\frac{\partial^4\psi}{\partial y^4}$$
$$- (\overline{Q}_{12}\alpha_x + \overline{Q}_{22}\alpha_y)\frac{\partial T}{\partial y} = 0$$

$$\Rightarrow \{\frac{\overline{Q}_{66}.\overline{Q}_{11}}{\overline{Q}_{12}+\overline{Q}_{66}}\}\frac{\partial^4\psi}{\partial x^4}+\{\frac{\overline{Q}_{11}.\overline{Q}_{22}}{\overline{Q}_{12}+\overline{Q}_{66}}-(\overline{Q}_{12}+\overline{Q}_{66})+\frac{\overline{Q}_{66}.\overline{Q}_{66}}{\overline{Q}_{12}+\overline{Q}_{66}}\}\frac{\partial^4\psi}{\partial x^2\partial y^2}+\{\frac{\overline{Q}_{22}.\overline{Q}_{66}}{\overline{Q}_{12}+\overline{Q}_{66}}\}\frac{\partial^4\psi}{\partial y^4}$$
$$+(\overline{Q}_{12}\alpha_x+\overline{Q}_{22}\alpha_y)\frac{\partial T}{\partial y}=0$$

$$\Rightarrow \frac{\partial^4\psi}{\partial x^4}+(\frac{\overline{Q}_{22}}{\overline{Q}_{66}}-\frac{\overline{Q}_{12}^2}{\overline{Q}_{66}.\overline{Q}_{11}}-\frac{2\overline{Q}_{12}}{\overline{Q}_{11}})\frac{\partial^4\psi}{\partial x^2\partial y^2}+\frac{\overline{Q}_{22}}{\overline{Q}_{11}}\frac{\partial^4\psi}{\partial y^4}$$
$$+(\frac{\overline{Q}_{12}+\overline{Q}_{66}}{\overline{Q}_{66}.\overline{Q}_{11}})(\overline{Q}_{12}\alpha_x+\overline{Q}_{22}\alpha_y)\frac{\partial T}{\partial y}=0 \quad (2.66)$$

This is the bi-harmonic equation for the MMC line along y-direction. For that equation 2.59 becomes,

- $u_x=\dfrac{\partial^2\psi}{\partial x\partial y}$
- $u_y=-\dfrac{\overline{Q}_{11}}{\overline{Q}_{12}+\overline{Q}_{66}}\dfrac{\partial^2\psi}{\partial y^2}-\dfrac{\overline{Q}_{66}}{\overline{Q}_{12}+\overline{Q}_{66}}\dfrac{\partial^2\psi}{\partial x^2}$

Now from equation 2.56 σ_x, σ_y and τ_{xy} becomes,

$$\sigma_x=\overline{Q}_{11}\frac{\partial}{\partial x}(\frac{\partial^2\psi}{\partial x\partial y})+\overline{Q}_{12}\frac{\partial}{\partial y}\{-\frac{\overline{Q}_{11}}{\overline{Q}_{12}+\overline{Q}_{66}}\frac{\partial^2\psi}{\partial x^2}-\frac{\overline{Q}_{66}}{\overline{Q}_{12}+\overline{Q}_{66}}\frac{\partial^2\psi}{\partial y^2}\}-(\overline{Q}_{11}\alpha_x+\overline{Q}_{12}\alpha_y)\Delta T$$
$$=\overline{Q}_{11}\frac{\partial^3\psi}{\partial x^2\partial y}-\frac{\overline{Q}_{11}.\overline{Q}_{12}}{\overline{Q}_{12}+\overline{Q}_{66}}\frac{\partial^3\psi}{\partial x^2\partial y}-\frac{\overline{Q}_{12}.\overline{Q}_{66}}{\overline{Q}_{12}+\overline{Q}_{66}}\frac{\partial^3\psi}{\partial y^3}-(\overline{Q}_{11}\alpha_x+\overline{Q}_{12}\alpha_y)\Delta T$$
$$\sigma_x=(\overline{Q}_{11}-\frac{\overline{Q}_{11}.\overline{Q}_{66}}{\overline{Q}_{12}+\overline{Q}_{66}})\frac{\partial^3\psi}{\partial x^2\partial y}-\frac{\overline{Q}_{12}.\overline{Q}_{66}}{\overline{Q}_{12}+\overline{Q}_{66}}\frac{\partial^3\psi}{\partial y^3}-(\overline{Q}_{11}\alpha_x+\overline{Q}_{12}\alpha_y)\Delta T \quad (2.67)$$

$$\sigma_y=\overline{Q}_{12}\frac{\partial}{\partial x}(\frac{\partial^2\psi}{\partial x\partial y})+\overline{Q}_{22}\frac{\partial}{\partial y}\{-\frac{\overline{Q}_{11}}{\overline{Q}_{12}+\overline{Q}_{66}}\frac{\partial^2\psi}{\partial x^2}-\frac{\overline{Q}_{66}}{\overline{Q}_{12}+\overline{Q}_{66}}\frac{\partial^2\psi}{\partial y^2}\}-(\overline{Q}_{12}\alpha_x+\overline{Q}_{22}\alpha_y)\Delta T$$
$$=\overline{Q}_{12}\frac{\partial^3\psi}{\partial x^2\partial y}-\frac{\overline{Q}_{11}.\overline{Q}_{22}}{\overline{Q}_{12}+\overline{Q}_{66}}\frac{\partial^3\psi}{\partial x^2\partial y}-\frac{\overline{Q}_{22}.\overline{Q}_{66}}{\overline{Q}_{12}+\overline{Q}_{66}}\frac{\partial^3\psi}{\partial y^3}-(\overline{Q}_{12}\alpha_x+\overline{Q}_{22}\alpha_y)\Delta T$$
$$\sigma_y=(\overline{Q}_{12}-\frac{\overline{Q}_{11}.\overline{Q}_{22}}{\overline{Q}_{12}+\overline{Q}_{66}})\frac{\partial^3\psi}{\partial x^2\partial y}-\frac{\overline{Q}_{22}.\overline{Q}_{66}}{\overline{Q}_{12}+\overline{Q}_{66}}\frac{\partial^3\psi}{\partial y^3}-(\overline{Q}_{12}\alpha_x+\overline{Q}_{22}\alpha_y)\Delta T \quad (2.68)$$

$$\tau_{xy}=\overline{Q}_{66}\frac{\partial}{\partial y}(\frac{\partial^2\psi}{\partial x\partial y})+\overline{Q}_{66}\frac{\partial}{\partial x}\{-\frac{\overline{Q}_{11}}{\overline{Q}_{12}+\overline{Q}_{66}}\frac{\partial^2\psi}{\partial x^2}-\frac{\overline{Q}_{66}}{\overline{Q}_{12}+\overline{Q}_{66}}\frac{\partial^2\psi}{\partial y^2}\}$$
$$=\overline{Q}_{66}\frac{\partial^3\psi}{\partial x\partial y^2}-\frac{\overline{Q}_{11}.\overline{Q}_{66}}{\overline{Q}_{12}+\overline{Q}_{66}}\frac{\partial^3\psi}{\partial x^3}-\frac{\overline{Q}_{66}.\overline{Q}_{66}}{\overline{Q}_{12}+\overline{Q}_{66}}\frac{\partial^3\psi}{\partial x\partial y^2}$$
$$\tau_{xy}=\frac{\overline{Q}_{12}.\overline{Q}_{66}}{\overline{Q}_{12}+\overline{Q}_{66}}\frac{\partial^3\psi}{\partial x\partial y^2}-\frac{\overline{Q}_{11}.\overline{Q}_{66}}{\overline{Q}_{12}+\overline{Q}_{66}}\frac{\partial^3\psi}{\partial x^3} \quad (2.69)$$

2.7.3 Von-Mises Stress

The Von Mises stress is often used in determining whether an isotropic and ductile metal will yield when subjected to a complex loading condition. This is accomplished by calculating the Von-Mises stress and comparing it to the material's yield stress, which constitutes the Von-Mises Yield Criterion.

The general equations for determining Von-Mises stress are,

$$\sigma_1 = \frac{\sigma_x + \sigma_y}{2} + \sqrt{(\frac{\sigma_x - \sigma_y}{2})^2 + \tau_{xy}^2} \tag{2.70a}$$

$$\sigma_2 = \frac{\sigma_x + \sigma_y}{2} - \sqrt{(\frac{\sigma_x - \sigma_y}{2})^2 + \tau_{xy}^2} \tag{2.70b}$$

where, the principal stresses σ_1 and σ_2 are the maximum and minimum normal stresses on the element at the geometric center of the plate.

So, the Von-Mises stress becomes,

$$\sigma_{von-mises} = \sqrt{\sigma_1^2 - \sigma_1\sigma_2 + \sigma_2^2} \tag{2.71}$$

2.7.4 Mechanical Boundary Conditions

In a PCB trace which is rigidly attached to the surface of the board have a specific boundary conditions. As the movement along side the edges is fixed so the displacement along those edges become zero. So, in that case the four edges of the MMC line has same boundary conditions in our thesis. As the governing equation of the stress problem is 4^{th} order, there are two boundary conditions in each edges. The boundary conditions are,

- $u_x = 0$, along four edges
- $u_y = 0$, along four edges

2.8 Failure Theory

The failure theory is based on the total failure theory of Beltrami. Tsai-Wu applied the failure theory in a lamina in plane stress[6]. A lamina is considered to be failed if,

$$H_1\sigma_1 + H_2\sigma_2 + H_6\tau_{12} + H_{11}\sigma_1^2 + H_{22}\sigma_2^2 + H_{66}\tau_{12}^2 + 2H_{12}\sigma_1\sigma_2 < 1 \tag{2.72}$$

is violated. This failure theory is more general than the Tsai-Hill failure theory because it distinguishes between the compressive and tensile strengths of lamina.
The components H_1, H_2, H_6, H_{11}, H_{22}, H_{12} and H_{66} of the failure theory are given as follows,

- $H_1 = \dfrac{1}{(\sigma_1^T)_{ult}} - \dfrac{1}{(\sigma_1^C)_{ult}}$
- $H_2 = \dfrac{1}{(\sigma_2^T)_{ult}} - \dfrac{1}{(\sigma_2^C)_{ult}}$
- $H_6 = 0$
- $H_{11} = \dfrac{1}{(\sigma_1^T)_{ult}(\sigma_1^C)_{ult}}$
- $H_{22} = \dfrac{1}{(\sigma_2^T)_{ult}(\sigma_2^C)_{ult}}$
- $H_{66} = \dfrac{1}{(\tau_{12})_{ult}^2}$
- $H_{12} = -\dfrac{1}{2}\sqrt{\dfrac{1}{(\sigma_1^T)_{ult}(\sigma_1^C)_{ult}(\sigma_2^T)_{ult}(\sigma_2^C)_{ult}}}$, per Mises-Hencky criterion.

Chapter 3

Numerical Formulation

3.1 General

While the derivation of the governing equations for most of the problems is not unduly difficult, their solution by exact methods of analysis is often difficult due to geometric and material complexities. In such cases, numerical methods of analysis provide alternative means of findings solutions. Numerical methods are techniques by which mathematical problems are formulated so that they can be solved with arithmetic operations and always give an approximate solution. Although numerical methods can't give an exact result, it is used extensively by the researchers to save money and time, compromising with the accuracy, especially when analytical methods are not available. The error in this method is consistent across the whole calculation and also can be minimized using higher order of the numerical solution. The more the higher order, the lesser is the error in the approximation. Numerical methods typically transform differential equations governing a continuum to a set of algebraic equations of a discrete model of the continuum that are to be solved using computers. The use of a numerical method and a computer to evaluate the mathematical model of a process and estimate its characteristics is called numerical simulation. There are several reasons why an engineer or a scientist should study a numerical method:

1. Most practical problems involve complicated domains (both geometry and material constitution), loads, and non-linearity that forbid the development of analytical solutions. Therefore, the only alternative is to find approximate solutions using numerical methods.

2. A numerical method, with the advent of a computer, can be used to investigate the effects of various parameters of the system on its response to gain a better understanding of the process/system being analyzed.

3. It is cost effective and saves time and material resources compared to the multitude of physical experiments needed to gain the same level of understanding.

4. Because of the power of numerical methods and electronic computation, it is possible to include all relevant features in a mathematical model of a physical process without worrying about its solution by exact means.

5. Those who are quick to use a computer program rather than think about the problem to be analyzed may find it difficult to interpret or explain the computer-generated results. Even to develop proper input data for the computer program, a good understanding of the underlying theory of the problem as well as the numerical method is required.

3.2 Finite Difference Method

The finite-difference method is one of the oldest numerical methods known for solving PDE's. In finite difference method, the derivatives of an original differential equation are replaced by the finite divided difference formulae for derivatives which are obtained by approximations of Tailor's series. So a differential equation is converted into a set of linear algebraic equation which can be solved by a suitable technique. Since all finite difference formulae are approximation of infinite series of differences, it is necessary that the series should converge or the error caused by the truncation should be sufficiently small to give a reliable result.

In this method, the region of the body under consideration is divided by lines parallel to the co-ordinate axes. And points hence formed at the intersection of these lines are treated as a grid of finite number of discrete points which are called node points as shown in figure 3.1. The continuous problem domain is discretized so that the dependent variables are considered to exist only at discrete nodal points. The finite difference form of governing partial differential equation is applied to all node points except the boundary node points and appropriate boundary conditions are applied to the boundary node points. To apply the boundary conditions at the boundary, a false or imaginary boundary is considered outside of real boundary as shown in figure 3.1. This imaginary boundary is necessary because each boundary point is subjected to a pair of boundary conditions such as u,v or u,σ_x or u,τ_{xy} etc. From these two boundary conditions one is applied to real boundary and other is applied to real boundary by using pivot at corresponding imaginary boundary points. This gives a complete set of simultaneous equations, i.e. number of equations in the set is equal to the number of grid points, which is solved by a suitable numerical technique.

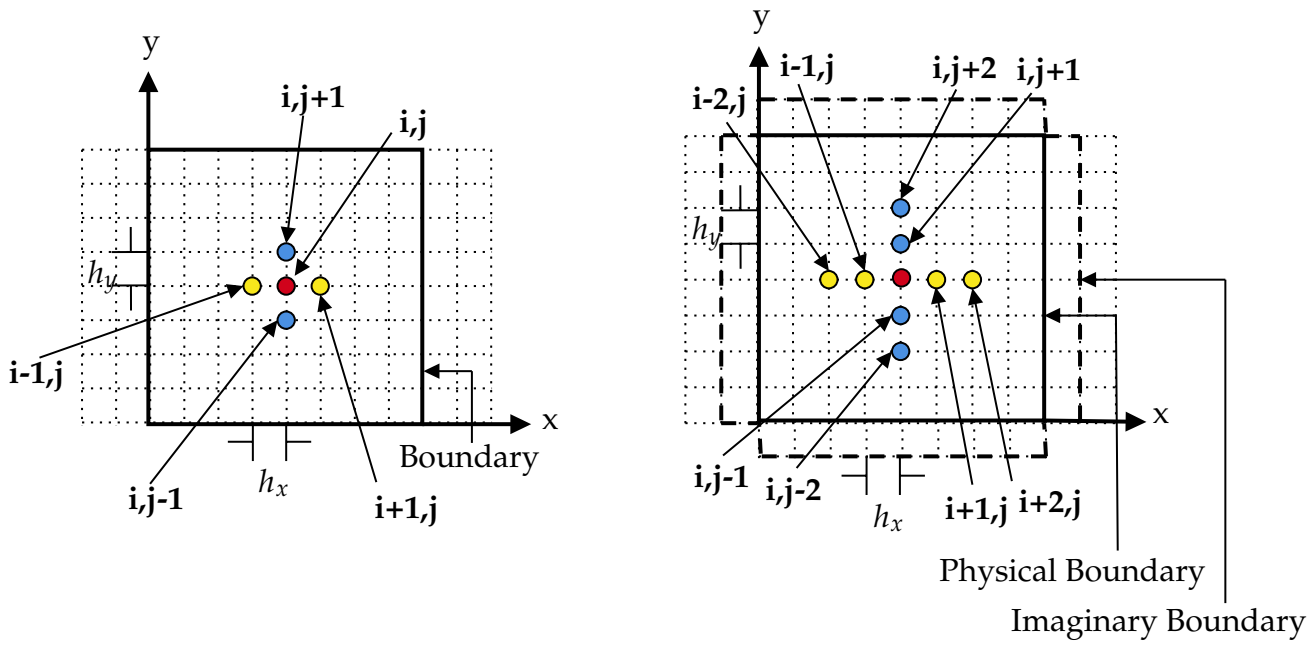

(a) 2^{nd} order scheme

(b) 4^{th} order scheme

Figure 3.1: Discretization of rectangular body into a grid of points

3.2.1 Finite Difference Approximation of the Derivatives

Finite difference formula of the derivatives are truncated from the Taylor's series. If a certain function f(x, y) has continuous partial derivatives of considerably higher order, then according to Taylor's series the value of function at a point (i+1,j) and (i-1,j) can be given by,

$$f(i+1,j) = f(i,j) + h_x f'(i,j) + \frac{h_x^2}{2!} f''(i,j) + \frac{h_x^3}{3!} f'''(i,j) + \cdots\cdots + \frac{h_x^n}{n!} f^n(i,j) + \cdots \tag{3.1a}$$

$$f(i-1,j) = f(i,j) - h_x f'(i,j) + \frac{h_x^2}{2!} f''(i,j) - \frac{h_x^3}{3!} f'''(i,j) + \cdots\cdots + (-1)^n \frac{h_x^n}{n!} f^n(i,j) + \cdots \tag{3.1b}$$

where, $h_x = (x_{i+1,j} - x_{i,j})$

The level of accuracy of each form depends on the number of terms of the Taylor's series that are retained during the derivation of these formulas. There are three different kinds of finite formulation is used in these cases,

1. Forward Finite Difference
2. Backward Finite Difference
3. Central Finite Difference

The finite difference formula for the derivative for second order equation can be obtained for 3 of these kinds. The equations are given below,

Table 3.1: Forward Finite Difference

Formula	Order
$f'(x_i) = \frac{-3f(x_i) + 4f(x_{i+1}) - f(x_{i+2})}{2h}$	$O(h^2)$
$f''(x_i) = \frac{2f(x_i) - 5f(x_{i+1}) + 4f(x_{i+2}) - f(x_{i+3})}{h^2}$	$O(h^2)$
$f'''(x_i) = \frac{-5f(x_i) + 18f(x_{i+1}) - 24f(x_{i+2}) + 14(x_{i+3}) - 3f(x_{i+4})}{2h^3}$	$O(h^2)$
$f''''(x_i) = \frac{3f(x_i) - 14f(x_{i+1}) + 26f(x_{i+2}) - 24(x_{i+3}) + 11f(x_{i+4}) - 2f(x_{i+5})}{h^4}$	$O(h^2)$

Table 3.2: Backward Finite Difference

Formula	Order
$f'(x_i) = \frac{f(x_{i-2}) - 4f(x_{i-1}) + 3f(x_i)}{2h}$	$O(h^2)$
$f''(x_i) = \frac{-f(x_{i-3}) + 4f(x_{i-2}) - 5f(x_{i-1}) + 2f(x_i)}{h^2}$	$O(h^2)$
$f'''(x_i) = \frac{3f(x_{i-4}) - 14f(x_{i-3}) + 24f(x_{i-2}) - 18f(x_{i-1}) + 5f(x_i)}{2h^3}$	$O(h^2)$
$f''''(x_i) = \frac{-2f(x_{i-5}) + 11f(x_{i-4}) - 24f(x_{i-3}) + 26f(x_{i-2}) - 14f(x_{i-1}) + 3f(x_i)}{h^4}$	$O(h^2)$

Table 3.3: Central Finite Difference

Formula	Order
$f'(x_i) = \frac{f(x_{i+1}) - f(x_{i-1})}{2h}$	$O(h^2)$
$f''(x_i) = \frac{f(x_{i-1}) - 2f(x_i) + f(x_{i+1})}{h^2}$	$O(h^2)$
$f'''(x_i) = \frac{-f(x_{i-2}) + 2f(x_{i-1}) - 2f(x_{i+1}) + f(x_{i+2})}{2h^3}$	$O(h^2)$
$f''''(x_i) = \frac{f(x_{i-2}) - 4f(x_{i-1}) + 6f(x_i) - 4f(x_{i+1}) + f(x_{i+2})}{h^4}$	$O(h^2)$

3.2.2 Scheme of Finite Difference Method

The method of finite difference is an approximate technique which yields a direct simplified solution form, in which the differential equations of equilibrium and the boundary condi-

tions are replaced by a set of algebraic equations. The general approach of finite difference solution assumes that the function can be represented in a prescribed range with a sufficient degree of accuracy either by Taylor's series with origin at the successive pivotal points of the range or the polynomial which passes through a certain number of selected pivotal points. The values of the functions at the nodal points are required to satisfy difference equations obtained by replacing the partial derivatives by their difference formulae. All finite difference formulas are approximations to infinite series of differences. Therefore, it is necessary that the series should converge, or that the error, caused by truncation after a certain number of terms should be sufficiently small. In this problem the pivotal points are taken as the regular net points of the domain of dependence of the functions obtained y dividing the domain by lines parallel to the co-ordinate axes.

Different region of the MMC line have to be considered as different finite difference scheme. There are various forms of permutation in the finite difference scheme of solution can be done. If we summarize the possibilities it can be shown,

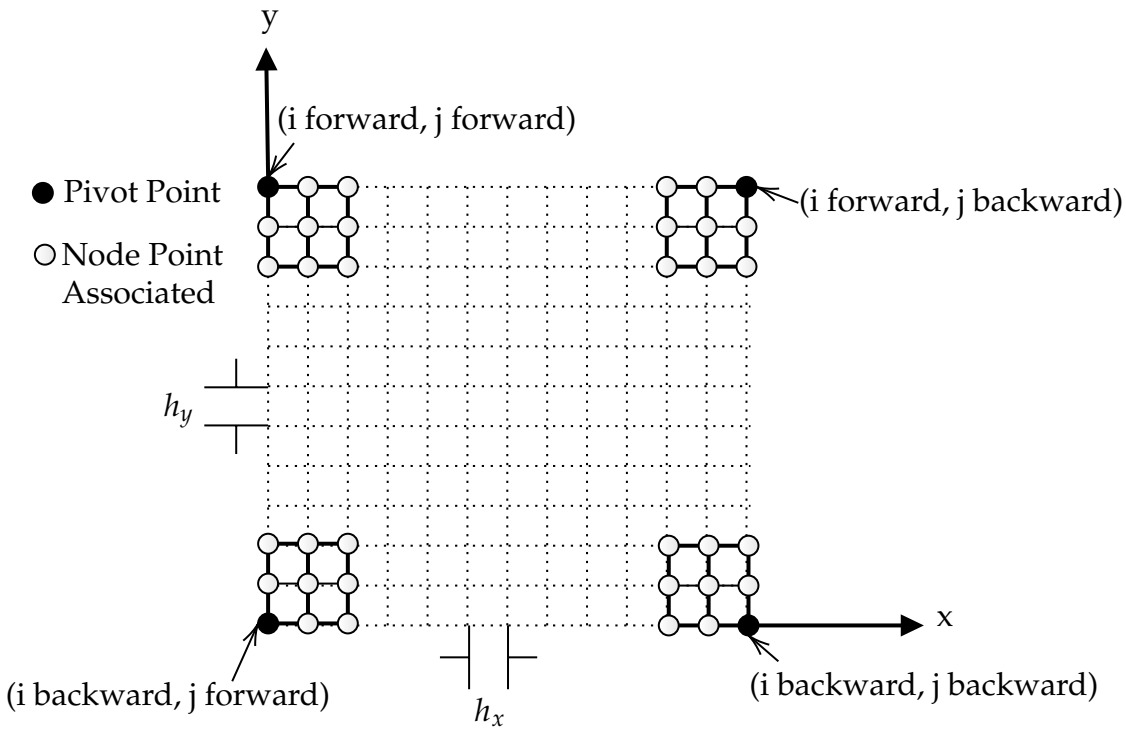

Figure 3.2: Application of Different form of Differential Equation

These different types of forms are required for the solution, if has to apply at different parts of the body. If a rectangular body is considered then application of different forms are shown in figure 3.2. Here it will be worthy to mention that, the shape and the number of the node points of the stencils is same but the values of the coefficients of the associated node points may vary or remain same.

3.3 Numerical Modeling of Electrical Problem

The electrical governing equation and boundary conditions given in equation 2.31 for evaluating the finite difference scheme.

3.3.1 Electrical Governing Equation

The governing equation of the electrical problem is valid in the interior stencils of the MMC line. So, central finite difference method can be used for minimization of the approximation error. The order of the finite difference method is $O(h_x^2, h_y^2)$. The governing equation of 2.31 can be written for finite difference scheme are given below,

$$\frac{(\phi_{i+1,j} - 2\phi_{i,j} + \phi_{i-1,j})}{h_x^2} + \frac{(\phi_{i,j+1} - 2\phi_{i,j} + \phi_{i,j-1})}{h_y^2} = 0 \tag{3.2}$$

The stencils can be described as,

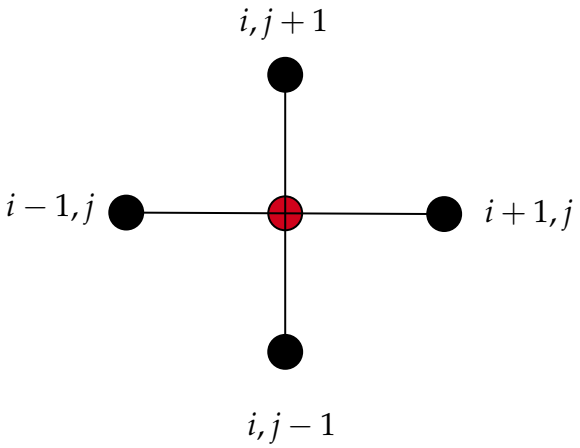

Figure 3.3: Stencils of Electrical Governing Equation

3.3.2 Boundary Conditions of Electrical Problem

To formulate the boundary conditions applied, we have to use both forward and backward finite difference method of $O(h_x^2)$ and $O(h_y^2)$. The stencils can be visualized as,

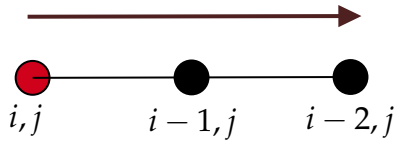

Case A: Forward Finite Difference

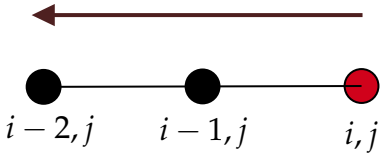

Case B: Backward Finite Difference

Figure 3.4: Boundary Stencils Implementation

With that the finite difference boundary conditions are,

- Left Boundary (Current Input): $\frac{-\phi_{i+2,j} + 4\phi_{i+1.j} - 3\phi_{i,j}}{2h} = -\rho J$
- Right Boundary (Current Output): $\frac{\phi_{i-2,j} - 4\phi_{i-1.j} + 3\phi_{i,j}}{2h} = \rho J$
- Top Boundary (Insulation): $\frac{\phi_{i,j-2} - 4\phi_{i,j-1} + 3\phi_{i,j}}{2h} = 0$
- Bottom Boundary (Insulation): $\frac{-\phi_{i,j+2} + 4\phi_{i,j+1} - 3\phi_{i,j}}{2h} = 0$

3.3.3 Heat Generation Governing Equation

The heat generation in the MMC line due to DC current field is given by the equation 2.37 can be written as a central finite difference scheme,

$$G(x,y) = \frac{1}{A_m \rho}\left[\left(\frac{\phi_{i+1,j} - \phi_{i-1,j}}{2h_x}\right)^2 + \left(\frac{\phi_{i,j+1} - \phi_{i,j-1}}{2h_y}\right)^2\right] \tag{3.3}$$

3.4 Numerical Modeling of Thermal Problem

The thermal governing equation corresponding to equation 2.39 is formulated in central finite difference scheme and given by,

$$k_x \frac{T_{i+1,j} - 2T_{i,j} + T_{i-1,j}}{h_x^2} + k_y \frac{T_{i,j+1} - 2T_{i,j} + T_{i,j-1}}{h_y^2} - \frac{hC}{A}(T_{i,j} - T_\infty) + G_{i,j} = 0$$
$$\Rightarrow \frac{k_x}{h_x^2} T_{i+1,j} + \frac{k_x}{h_x^2} T_{i-1,j} + \frac{k_y}{h_y^2} T_{i,j+1} + \frac{k_y}{h_y^2} T_{i,j-1} - \left(\frac{2k_x}{h_x^2} + \frac{2k_y}{h_y^2} + \frac{hC}{A} \right) T_{i,j} = -G_{i,j} - \frac{hC}{A} T_\infty \tag{3.4}$$

The boundary conditions is the temperature kept at the boundary. In our case the boundaries are kept at ambient temperature.

3.5 Numerical Modeling of Stress Problem

The finite difference scheme of the stress problem is different from the others in the boundary values as there are two different conditions for each boundary. So, we have to consider an imaginary boundary to apply the boundary conditions on the MMC line. Both the physical and imaginary boundary are discretized using forward and backward finite difference method. The governing equations for the interior stencils apply same method as there are only the equations are considered. All the equations of the interior stencils are discretized using forward difference method.

3.5.1 Stress Governing Equation

We have evaluated the governing equations for the stress problem in the previous chapter. Now, the finite different scheme of those equations are discussed in this chapter. At first we will derive the interior stencils governing equation with central finite difference method. There are two bi-harmonic equations for change of temperature along x and y direction.

3.5.2 Stress Governing Equation along x direction

The governing equations are given in equation 2.62. If we discretized the equation using central finite difference method, it stands for,

$$\frac{\psi_{i-2,j}-4\psi_{i-1,j}+6\psi_{i,j}-4\psi_{i+1,j}+\psi_{i+2,j}}{h_x^4}+\{\frac{\overline{Q}_{22}}{\overline{Q}_{66}}-\frac{\overline{Q}_{12}^2}{\overline{Q}_{66}.\overline{Q}_{11}}-\frac{2\overline{Q}_{12}}{\overline{Q}_{11}}\}[\frac{1}{h_x^2}\{2\psi_{i-1,j}-5\psi_{i,j}$$
$$+4\psi_{i+1,j}-\psi_{i+2,j}-4\psi_{i,j}+10\psi_{i+1,j}-8\psi_{i+2,j}+2\psi_{i+3,j}+2\psi_{i+1,j}-5\psi_{i+2,j}+4\psi_{i+3,j}-\psi_{i+4,j}\}$$
$$+\frac{1}{h_x^2h_y^2}\{\psi_{i-1,j-1}-2\psi_{i-1,j}+\psi_{i-1,j+1}-2\psi_{i,j-1}+4\psi_{i,j}-2\psi_{i,j+1}+\psi_{i+1,j-1}-2\psi_{i+1,j}+\psi_{i+1,j+1}\}$$
$$+\frac{1}{h_y^2}\{2\psi_{i,j-1}-5\psi_{i,j}+4\psi_{i,j+1}-\psi_{i,j+2}-4\psi_{i,j}+10\psi_{i,j+1}-8\psi_{i,j+2}+2\psi_{i,j+3}+2\psi_{i,j+1}-5\psi_{i,j+2}$$
$$+4\psi_{i,j+3}-\psi_{i,j+4}\}]+\frac{\overline{Q}_{22}}{\overline{Q}_{11}}\{\frac{\psi_{i,j-2}-4\psi_{i,j-1}+6\psi_{i,j}-4\psi_{i,j+1}+\psi_{i,j+2}}{h_y^4}\}$$
$$+(\frac{\overline{Q}_{12}+\overline{Q}_{66}}{\overline{Q}_{66}.\overline{Q}_{11}})(\overline{Q}_{11}\alpha_x+\overline{Q}_{12}\alpha_y)\frac{T_{i+1,j}-T_{i-1,j}}{2h_x}=0 \quad (3.5)$$

Now to determine the components equation 2.63, 2.64, 2.65 becomes,

$$u_x=-\frac{\overline{Q}_{66}}{\overline{Q}_{12}+\overline{Q}_{66}}\left\{\frac{\psi_{i-1,j}-2\psi_{i,j}+\psi_{i+1,j}}{h_x^2}\right\}-\frac{\overline{Q}_{11}}{\overline{Q}_{12}+\overline{Q}_{66}}\left\{\frac{\psi_{i,j-1}-2\psi_{i,j}+\psi_{i,j+1}}{h_y^2}\right\} \quad (3.6)$$

$$u_y=\frac{1}{4h_xh_y}[\psi_{i+1,j+1}-\psi_{i+1,j}+\psi_{i,j+1}-2\psi_{i,j}-\psi_{i-1,j}-\psi_{i-1,j}-\psi_{i,j-1}+\psi_{i-1,j-1}] \quad (3.7)$$

$$\sigma_x=-\frac{\overline{Q}_{11}.\overline{Q}_{66}}{\overline{Q}_{12}+\overline{Q}_{66}}\{\frac{-\psi_{i-2,j}+2\psi_{i-1,j}-2\psi_{i+1,j}+\psi_{i+2,j}}{2h_x^3}\}+(\overline{Q}_{12}-\frac{\overline{Q}_{11}.\overline{Q}_{22}}{\overline{Q}_{12}+\overline{Q}_{66}})[\frac{1}{2h_x^2h_y}\{-3\psi_{i,j-1}$$
$$+4\psi_{i+1,j-1}-\psi_{i+2,j-1}+6\psi_{i,j}-8\psi_{i+1,j}+2\psi_{i+2,j}-3\psi_{i,j+1}+4\psi_{i+1,j+1}-\psi_{i+2,j+1}\}]$$
$$-(\overline{Q}_{11}\alpha_x+\overline{Q}_{12}\alpha_y)(T_{i+1,j}-T_{i-1,j}) \quad (3.8)$$

$$\sigma_y=-\frac{\overline{Q}_{12}.\overline{Q}_{66}}{\overline{Q}_{12}+\overline{Q}_{66}}\{\frac{-\psi_{i-2,j}+2\psi_{i-1,j}-2\psi_{i+1,j}+\psi_{i+2,j}}{2h_x^3}\}+(\overline{Q}_{12}-\frac{\overline{Q}_{12}.\overline{Q}_{22}}{\overline{Q}_{12}+\overline{Q}_{66}})[\frac{1}{2h_x^2h_y}\{-3\psi_{i,j-1}$$
$$+4\psi_{i+1,j-1}-\psi_{i+2,j-1}+6\psi_{i,j}-8\psi_{i+1,j}+2\psi_{i+2,j}-3\psi_{i,j+1}+4\psi_{i+1,j+1}-\psi_{i+2,j+1}\}]$$
$$-(\overline{Q}_{12}\alpha_x+\overline{Q}_{22}\alpha_y)(T_{i+1,j}-T_{i-1,j}) \quad (3.9)$$

$$\tau_{xy} = (\overline{Q}_{66} - \frac{\overline{Q}_{66}.\overline{Q}_{66}}{\overline{Q}_{12}+\overline{Q}_{66}})[\frac{1}{2h_x^2h_y}\{-3\psi_{i-1,j} + 4\psi_{i-1,j+1} - \psi_{i-1,j+2} + 6\psi_{i,j} - 8\psi_{i,j+1} + 2\psi_{i,j+2}$$
$$- 3\psi_{i+1,j} + 4\psi_{i+1,j+1} - \psi_{i+1,j+2}\}] - \frac{\overline{Q}_{22}.\overline{Q}_{66}}{\overline{Q}_{12}+\overline{Q}_{66}}\{\frac{-\psi_{i,j-2} + 2\psi_{i,j-1} - 2\psi_{i,j+1} + \psi_{i,j+2}}{2h_y^3}\} \quad (3.10)$$

3.5.3 Stress Governing Equation along y direction

The governing equations are given in equation 2.66. If we discretized the equation using central finite difference method, it stands for,

$$\frac{\psi_{i-2,j} - 4\psi_{i-1,j} + 6\psi_{i,j} - 4\psi_{i+1,j} + \psi_{i+2,j}}{h_x^4} + \{\frac{\overline{Q}_{22}}{\overline{Q}_{66}} - \frac{\overline{Q}_{12}^2}{\overline{Q}_{66}.\overline{Q}_{11}} - \frac{2\overline{Q}_{12}}{\overline{Q}_{11}}\}[\frac{1}{h_x^2}\{2\psi_{i-1,j} - 5\psi_{i,j}$$
$$+ 4\psi_{i+1,j} - \psi_{i+2,j} - 4\psi_{i,j} + 10\psi_{i+1,j} - 8\psi_{i+2,j} + 2\psi_{i+3,j} + 2\psi_{i+1,j} - 5\psi_{i+2,j} + 4\psi_{i+3,j} - \psi_{i+4,j}\}$$
$$+ \frac{1}{h_x^2h_y^2}\{\psi_{i-1,j-1} - 2\psi_{i-1,j} + \psi_{i-1,j+1} - 2\psi_{i,j-1} + 4\psi_{i,j} - 2\psi_{i,j+1} + \psi_{i+1,j-1} - 2\psi_{i+1,j} + \psi_{i+1,j+1}\}$$
$$+ \frac{1}{h_y^2}\{2\psi_{i,j-1} - 5\psi_{i,j} + 4\psi_{i,j+1} - \psi_{i,j+2} - 4\psi_{i,j} + 10\psi_{i,j+1} - 8\psi_{i,j+2} + 2\psi_{i,j+3} + 2\psi_{i,j+1} - 5\psi_{i,j+2}$$
$$+ 4\psi_{i,j+3} - \psi_{i,j+4}\}] + \frac{\overline{Q}_{22}}{\overline{Q}_{11}}\{\frac{\psi_{i,j-2} - 4\psi_{i,j-1} + 6\psi_{i,j} - 4\psi_{i,j+1} + \psi_{i,j+2}}{h_y^4}\}$$
$$+ (\frac{\overline{Q}_{12}+\overline{Q}_{66}}{\overline{Q}_{66}.\overline{Q}_{11}})(\overline{Q}_{12}\alpha_x + \overline{Q}_{22}\alpha_y)\frac{T_{i,j+1} - T_{i,j-1}}{2h_y} = 0 \quad (3.11)$$

Now to determine the components equation 2.67, 2.68, 2.69 becomes,

$$u_x = \frac{1}{4h_xh_y}[\psi_{i+1,j+1} - \psi_{i+1,j} + \psi_{i,j+1} - 2\psi_{i,j} - \psi_{i-1,j} - \psi_{i-1,j} - \psi_{i,j-1} + \psi_{i-1,j-1}] \quad (3.12)$$

$$u_y = -\frac{\overline{Q}_{11}}{\overline{Q}_{12}+\overline{Q}_{66}}\left\{\frac{\psi_{i,j-1} - 2\psi_{i,j} + \psi_{i,j+1}}{h_y^2}\right\} - \frac{\overline{Q}_{66}}{\overline{Q}_{12}+\overline{Q}_{66}}\left\{\frac{\psi_{i-1,j} - 2\psi_{i,j} + \psi_{i+1,j}}{h_x^2}\right\} \quad (3.13)$$

$$\sigma_x = (\overline{Q}_{11} - \frac{\overline{Q}_{11}.\overline{Q}_{66}}{\overline{Q}_{12}+\overline{Q}_{66}})[\frac{1}{2h_x^2h_y}\{-3\psi_{i-1,j} + 4\psi_{i-1,j+1} - \psi_{i-1,j+2} + 6\psi_{i,j} - 8\psi_{i,j+1} + 2\psi_{i,j+2}$$
$$- 3\psi_{i+1,j} + 4\psi_{i+1,j+1} - \psi_{i+1,j+2}\}] + \frac{\overline{Q}_{12}.\overline{Q}_{66}}{\overline{Q}_{12}+\overline{Q}_{66}}\{\frac{-\psi_{i,j-2} + 2\psi_{i,j-1} - 2\psi_{i,j+1} + \psi_{i,j+2}}{2h_y^3}\}$$
$$- (\overline{Q}_{12}\alpha_x + \overline{Q}_{22}\alpha_y)(T_{i,j+1} - T_{i,j-1}) \quad (3.14)$$

$$\sigma_y = (\overline{Q}_{12} - \frac{\overline{Q}_{11}.\overline{Q}_{66}}{\overline{Q}_{12}+\overline{Q}_{66}})[\frac{1}{2h_x^2 h_y}\{-3\psi_{i-1,j} + 4\psi_{i-1,j+1} - \psi_{i-1,j+2} + 6\psi_{i,j} - 8\psi_{i,j+1} + 2\psi_{i,j+2} - 3\psi_{i+1,j} + 4\psi_{i+1,j+1} - \psi_{i+1,j+2}\}] + \frac{\overline{Q}_{22}.\overline{Q}_{66}}{\overline{Q}_{12}+\overline{Q}_{66}}\{\frac{-\psi_{i,j-2} + 2\psi_{i,j-1} - 2\psi_{i,j+1} + \psi_{i,j+2}}{2h_y^3}\} - (\overline{Q}_{12}\alpha_x + \overline{Q}_{22}\alpha_y)(T_{i,j+1} - T_{i,j-1}) \quad (3.15)$$

$$\tau_{xy} = \frac{\overline{Q}_{12}.\overline{Q}_{66}}{\overline{Q}_{12}+\overline{Q}_{66}}[\frac{1}{2h_x h_y^2}\{-3\psi_{i,j-1} + 4\psi_{i+1,j-1} - \psi_{i+2,j-1} + 6\psi_{i,j} - 8\psi_{i+1,j} + 2\psi_{i+2,j} - 3\psi_{i,j+1} + 4\psi_{i+1,j+1} - \psi_{i+2,j+1}\}] - \frac{\overline{Q}_{11}.\overline{Q}_{66}}{\overline{Q}_{12}+\overline{Q}_{66}}\{\frac{-\psi_{i-2,j} + 2\psi_{i-1,j} - 2\psi_{i+1,j} + \psi_{i+2,j}}{2h_x^3}\} \quad (3.16)$$

3.5.4 Boundary Conditions of Stress Problem

As shown in figure 3.5 each boundary node points experiences two boundary conditions. If both the two boundary conditions are applied at each boundary node points then the system of linear equations will have a greater number of algebraic equations than the number of points. Therefore, to yield a unique solution from the system of linear equations will be very difficult.

This problem can be solved if only one boundary condition is applied in each boundary node points. It can be accomplished by applying one boundary condition in a particular node point and the other boundary condition in the next neighboring node point and so on. But in that case, solving procedure of the problem becomes difficult in terms of applying governing equation because central difference form of governing equation cannot be applied at domain nodal points that are situated just next to the physical boundary.

To overcome this problem a boundary near the physical boundary is assumed to exist, which is named as the imaginary boundary. If only the top boundary is considered then it can be shown by figure 3.5.

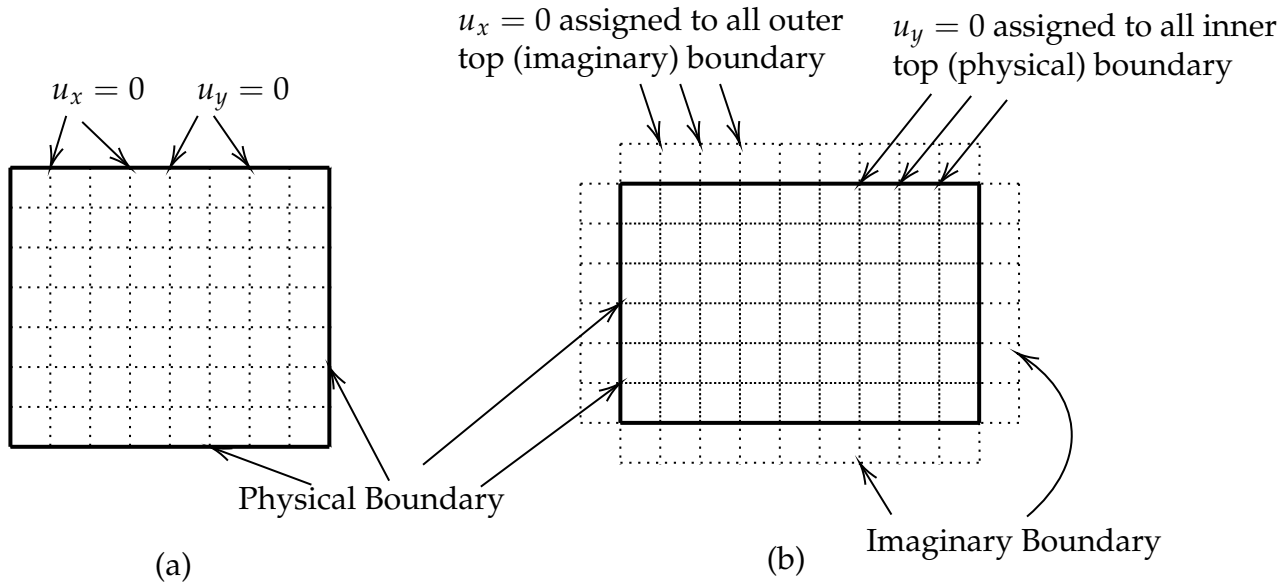

Figure 3.5: Boundary Condition Management (a) without (b) with Imaginary Boundary

The boundary conditions applied in this study have been discretized using both forward and backward finite difference scheme.

Boundary Conditions along x-direction

Forward Finite Difference

$$u_x = -\frac{\overline{Q}_{66}}{\overline{Q}_{12}+\overline{Q}_{66}}\frac{\psi_{i,j}-2\psi_{i+1,j}+\psi_{i+2,j}}{h_x^2} - \frac{\overline{Q}_{22}}{\overline{Q}_{12}+\overline{Q}_{66}}\frac{\psi_{i,j}-2\psi_{i,j+1}+\psi_{i,j+2}}{h_y^2} \tag{3.17}$$

$$u_y = \frac{1}{4h_xh_y}[\psi_{i+2,j+2}-4\psi_{i+2,j+1}+3\psi_{i+2,j}-4\psi_{i+1,j+2}+16\psi_{i+1,j+1} - 12\psi_{i+1,j}+3\psi_{i,j+2}-12\psi_{i,j+1}+9\psi_{i,j}] \tag{3.18}$$

Backward Finite Difference

$$u_x = -\frac{\overline{Q}_{66}}{\overline{Q}_{12}+\overline{Q}_{66}}\frac{\psi_{i,j}-2\psi_{i-1,j}+\psi_{i-2,j}}{h_x^2} - \frac{\overline{Q}_{22}}{\overline{Q}_{12}+\overline{Q}_{66}}\frac{\psi_{i,j}-2\psi_{i,j-1}+\psi_{i,j-2}}{h_y^2} \tag{3.19}$$

$$u_y = \frac{1}{4h_xh_y}[\psi_{i-2,j-2}-4\psi_{i-2,j-1}+3\psi_{i-2,j}-4\psi_{i-1,j-2}+16\psi_{i-1,j-1} - 12\psi_{i-1,j}+3\psi_{i,j-2}-12\psi_{i,j-1}+9\psi_{i,j}] \tag{3.20}$$

Boundary Conditions along y-direction

Forward Finite Difference

$$u_x = \frac{1}{4h_x h_y}[\psi_{i+2,j+2} - 4\psi_{i+2,j+1} + 3\psi_{i+2,j} - 4\psi_{i+1,j+2} + 16\psi_{i+1,j+1} - 12\psi_{i+1,j} + 3\psi_{i,j+2} - 12\psi_{i,j+1} + 9\psi_{i,j}] \quad (3.21)$$

$$u_y = \frac{\overline{Q}_{11}}{\overline{Q}_{12} + \overline{Q}_{66}} \frac{\psi_{i,j} - 2\psi_{i,j+1} + \psi_{i,j+2}}{h_y^2} - \frac{\overline{Q}_{66}}{\overline{Q}_{12} + \overline{Q}_{66}} \frac{\psi_{i,j} - 2\psi_{i+1,j} + \psi_{i+2,j}}{h_x^2} \quad (3.22)$$

Backward Finite Difference

$$u_x = \frac{1}{4h_x h_y}[\psi_{i-2,j-2} - 4\psi_{i-2,j-1} + 3\psi_{i-2,j} - 4\psi_{i-1,j-2} + 16\psi_{i-1,j-1} - 12\psi_{i-1,j} + 3\psi_{i,j-2} - 12\psi_{i,j-1} + 9\psi_{i,j}] \quad (3.23)$$

$$u_y = \frac{\overline{Q}_{11}}{\overline{Q}_{12} + \overline{Q}_{66}} \frac{\psi_{i,j} - 2\psi_{i,j-1} + \psi_{i,j-2}}{h_y^2} - \frac{\overline{Q}_{66}}{\overline{Q}_{12} + \overline{Q}_{66}} \frac{\psi_{i,j} - 2\psi_{i-1,j} + \psi_{i-2,j}}{h_x^2} \quad (3.24)$$

Chapter 4

Electro-Thermo-Mechanical Analysis

4.1 General

We have analyzed the response of graphite reinforced metal under the influence of a DC current field. To understand the failure criteria, we have to analyze some of the parameters under different loading condition. Aluminium has some distinctive material properties given in table A4. Graphite also has some material properties which are given in table A5. Also the material properties vary with the change of graphite volume mixture. To define these material properties we have used the mixture law and the properties are given in table A6.

For this process, we have first analyzed the electrical and thermal response for the metal line. Different parameters (Electric Potential, Heat Generation) and temperature distribution field along the MMC line. With the progression of the DC current field, the temperature rise is variant across the MMC line. This means the temperature changes with respect to length and area. For failure criteria we have to identify the node and region of the maximum temperature as this is the region where the failure will occur first.

For the analysis of stress mechanics, different components (σ_x, σ_y, τ_{xy}) are determined using ψ-formulation. Then we have calculated the Von-Mises stress for the yield criterion.

We have discussed all these parameters in the later section.

4.2 Distribution of Electric Potential, Temperature and Von-Mises Stress

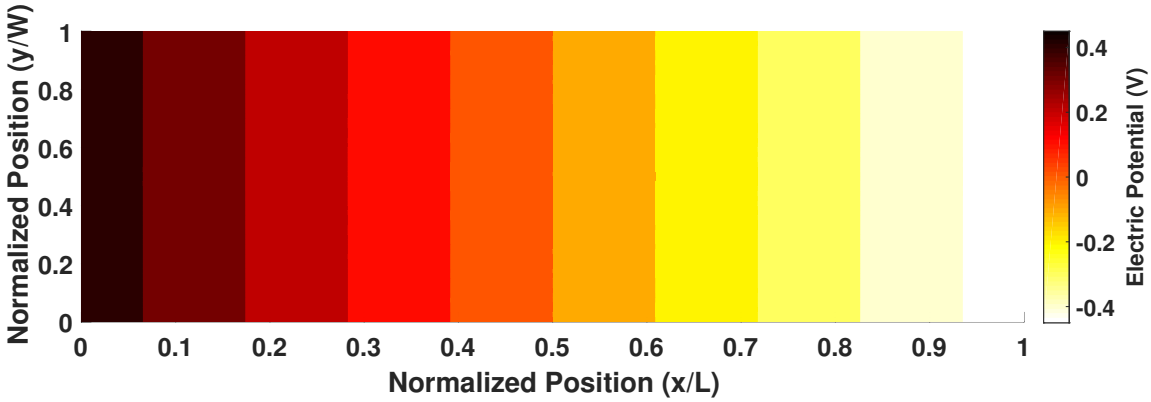

(a) Electric Potential distribution along the MMC line

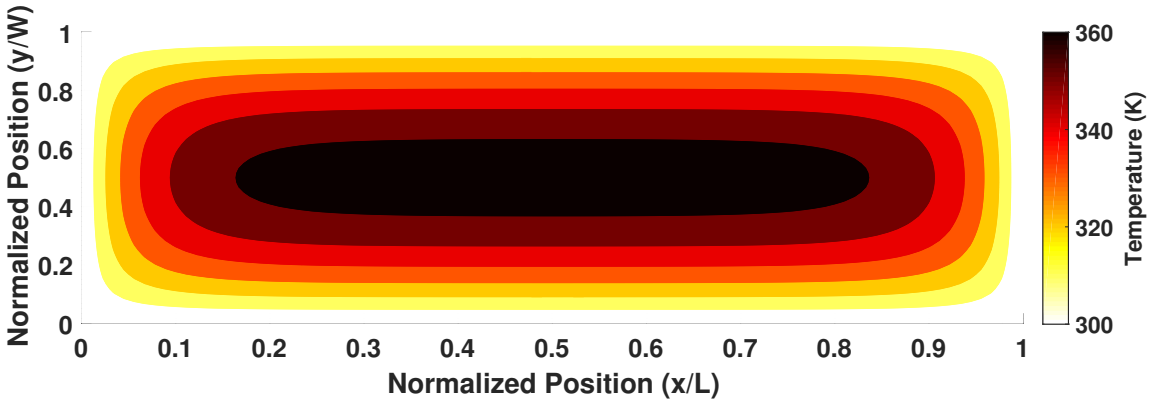

(b) Temperature distribution along the MMC line

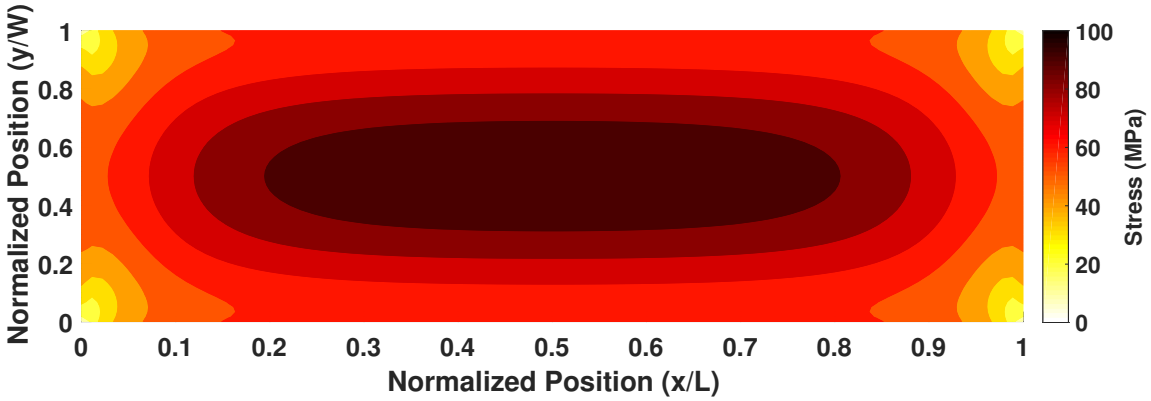

(c) Von-Mises stress distribution along the MMC line

Figure 4.1: Electric Potential, Temperature and Von-Mises Stress distribution along the MMC line (10A current, 15% Graphite, Natural Convection)

In figure 4.1, we can see the different parameter distribution field across the MMC line. The distribution field is generated due to the increase in current density applied at the boundary. To see the change of this parameters, all the properties and thermal conditions are kept

same. Different conditions are also applied to observe the changes along the MMC line.

In figure 4.1a, we can see the change of potential distribution along the MMC line. As the left boundary x/L=0 is the input region of the current, the electric potential generated in that region is higher. The potential decreases with the increase of the length. At the middle point where x/L=0.5, the potential reaches to 0. With the increase of the length where x/L=1, the potential reaches at it's lower value. For different current density, the maximum and minimum electric potential along with the internals changes, but the trend of the decrease of the potential remains same. At the width of the MMC line, the electric potential remains same along y/W=0 to y/W=1. This is because the length across the current is flowing remains same along the width. For different current density, the maximum and minimum electric potential along with the internals changes, but the trend of the decrease of the potential remains same.

In figure 4.1b, we can observe the trend of the temperature distribution along the MMC line. With the electricity, heat generation occurs along the MMC line. Electric potential creates a gradient of heat generation. The maximum heat generation generates at the center of the MMC line. Heat generation plays an important role for increasing temperature. The temperature increases with the increase of the both length and width. When the electricity passes through the MMC line, thermal conductivity of the composites dissipates the heat along the MMC line. As the boundary are kept at ambient condition, the increase of the temperature tends to go into the center. The dissipation of the heat is towards the center of the line. At x/L=0.5 and y/W=0.5, most of the heat accumulates. So, the maximum temperature occurs at the center of the MMC line.

4.3 Potential and Temperature Field

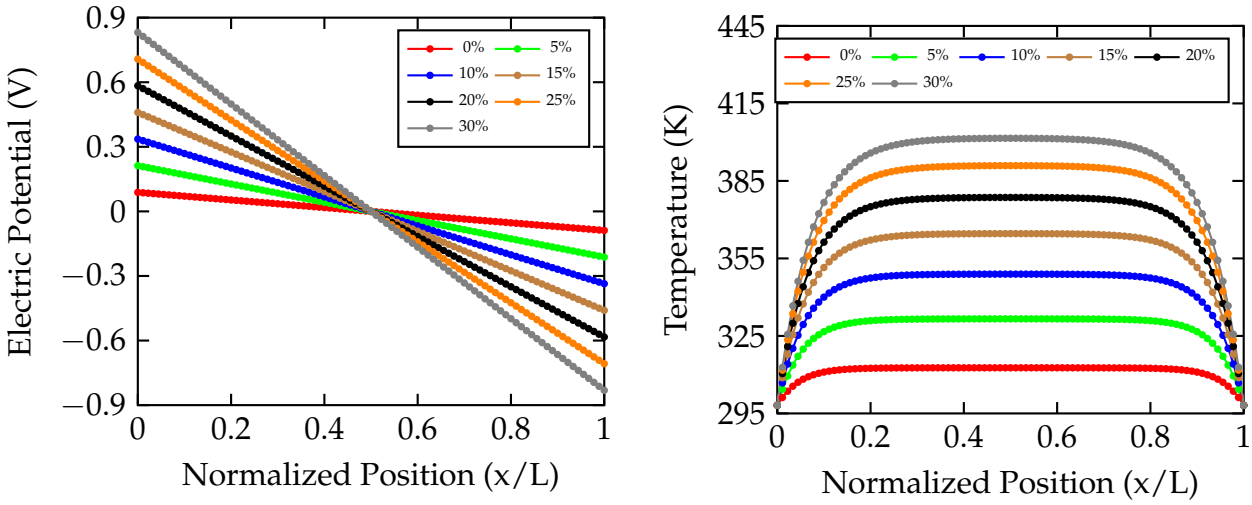

(a) Potential distribution

(b) Temperature distribution

Figure 4.2: Electric Potential and Temperature distribution along the middle of the metal line for different Graphite content (10A Current, Natural Convection)

We have determined the electric potential and temperature across the length of the MMC line at the middle of the width. Figure 4.2 represents the change of the electric potential and temperature along the length of the MMC line.

The maximum electric potential can be found at the input region of current. Figure 4.2a shows that the same. Along the length the potential decreases and at middle of the MMC line it becomes zero. At the end of the line where output of current region occurs it becomes lower. We can see that the graphite percentage changes the potential field. This is due to the fact that with the increase of graphite content, electric resistivity increases. This in term increases the electric potential generated.

The temperature increases with the length as the heat dissipates in the middle. Because the electric potential becomes zero at the middle. So, because of the high heat generation in the middle the temperature increases. Figure 4.2b shows that the high temperature at the middle. With the length the temperature increases. The temperature at the boundary where x/L=0 and x/L=1 are kept at the ambient temperature. The temperature field also depends on the graphite content. With the increase of graphite content electric resistivity and thermal conductivity increases. So high heat generation occurs. In that case, the temperature increases with the increase of graphite content.

4.4 Stress and Temperature Increase

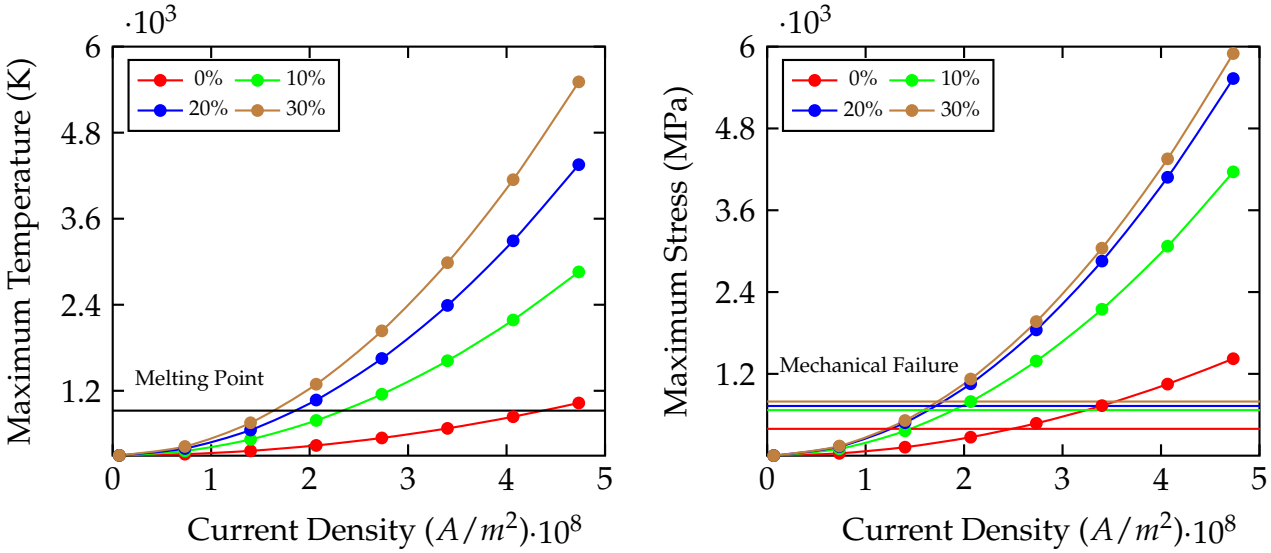

(a) Temperature Increase

(b) Stress Increase

Figure 4.3: Maximum Temperature and Von-Mises stress increase with respect to current density at different fiber orientation (15% Graphite, Natural Convection)

With the increase of the current density both temperature and von-mises stress increases. This is due to the increase of the high electric density. Due to increase of graphite content electric resistivity increases. For this both temperature and von-mises stress also increases.

In figure 4.3a, we can see that the temperature increases with the increase of the graphite content. Electric resistivity increase is much significant than increase of thermal conductivity, so, the resistivity plays a vital role in increasing the heat generation. So, the temperature increases with the increase of graphite content. For a fixed graphite content, we can see an increase of temperature with the increase of current. Using the melting point of Aluminium we can determine the maximum current density for melting failure for a fixed graphite content.

Similarly, in figure 4.3b, the von-mises stress also increases with the increase of graphite content as temperature creates thermal stress. When the von mises stress for a fixed graphite percentage becomes higher than the strength the mechanical failure occurs. By this we can determine the maximum current density for mechanical failure.

4.5 Effect of Thermal Conditions

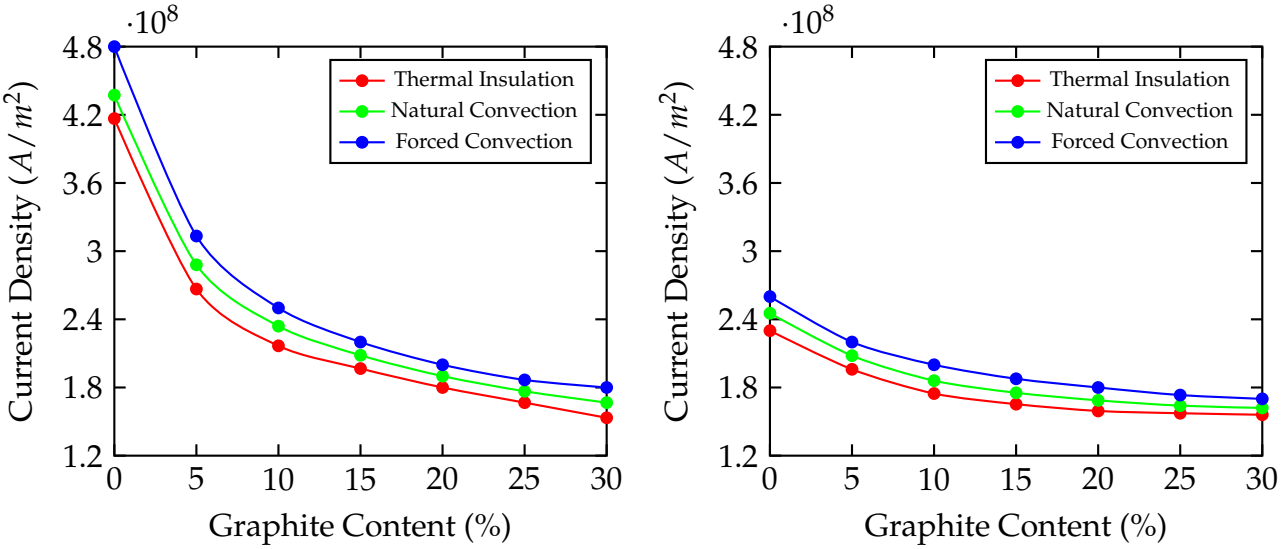

(a) Melting Point Failure

(b) Mechanical Failure

Figure 4.4: Maximum Current Density before both stress and temperature failure point for different thermal condition (5m/s air velocity, axial fiber orientation)

Thermal conditions play a vital role of decreasing the temperature and stress. As we can see in figure 4.4 that with the change of thermal condition from thermal insulation to natural convection, the maximum current carrying capacity increases slightly. But if a forced draft cooling fan with 5m/s air velocity is used the current carrying capacity increases significantly higher. This is due to the higher heat dissipation into the ambient temperature with the increase of cooling air velocity. We can also see that the mechanical failure plays an important role as it occurs before the melting failure in case of different thermal conditions.

4.6 Maximum Temperature and Von-Mises Stress

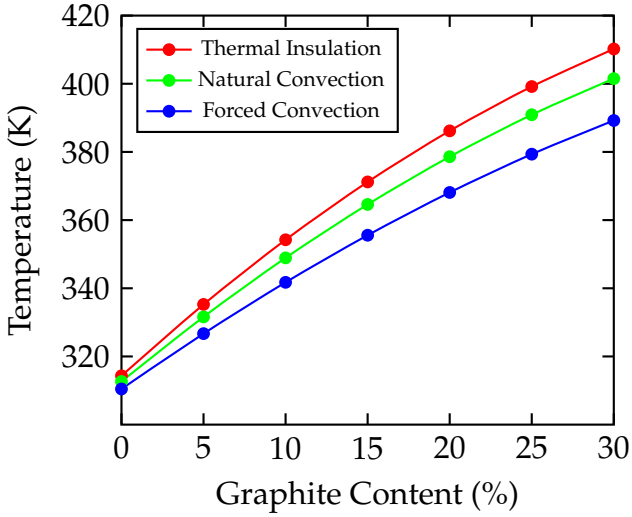

(a) Maximum Temperature (Axial)

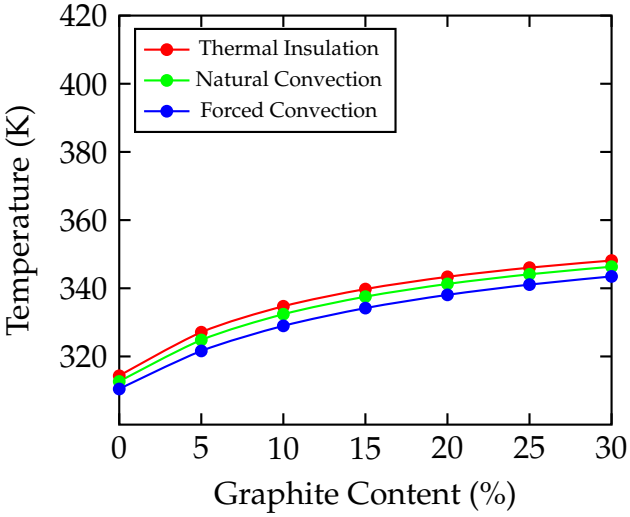

(b) Maximum Temperature (Lateral)

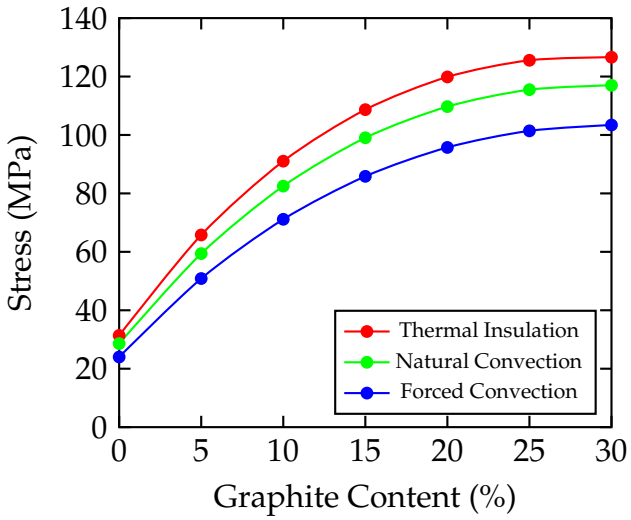

(c) Maximum Stress (Axial)

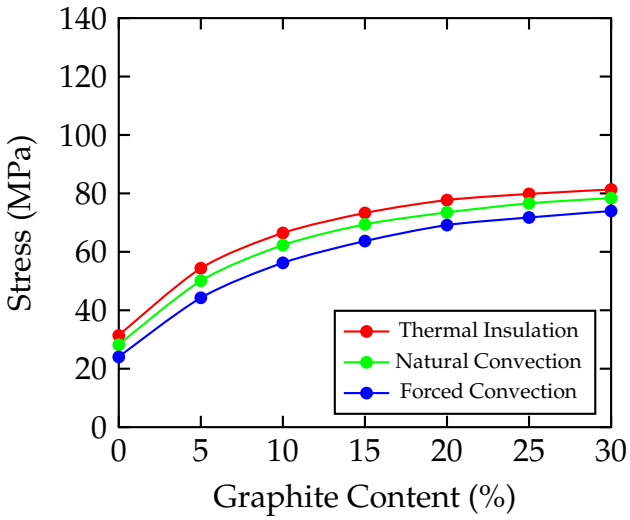

(d) Maximum Stress (Lateral)

Figure 4.5: Change of Maximum Von-Mises Stress and Temperature for different fiber orientation at different graphite content and different thermal condition (10A current, 5m/s air velocity)

The maximum temperature and von-mises stress generated at the center of the MMC line. As the failure occurs at the high temperature and stress point we have to consider the maximum temperature and stress. In figure 4.5 we have analyzed the temperature and stress generation of the MMC at axial and lateral fiber orientation.

In case of axial and lateral fiber orientation, axial fiber always gives higher temperature and stress. In figure 4.5b and 4.5d we can see that the maximum temperature and stress is lower

in the lateral fiber. In lateral fiber orientation, the fiber remains in the perpendicular of the current density. In that case the temperature and stress generation is lower than the axial fiber orientation. Also, we can observe that the temperature and von-mises stress increase at the higher graphite content becomes lower. This is due to the change of material properties. With the increase of graphite content, the elastic limit of the MMC increases.

4.7 Failure Characteristics

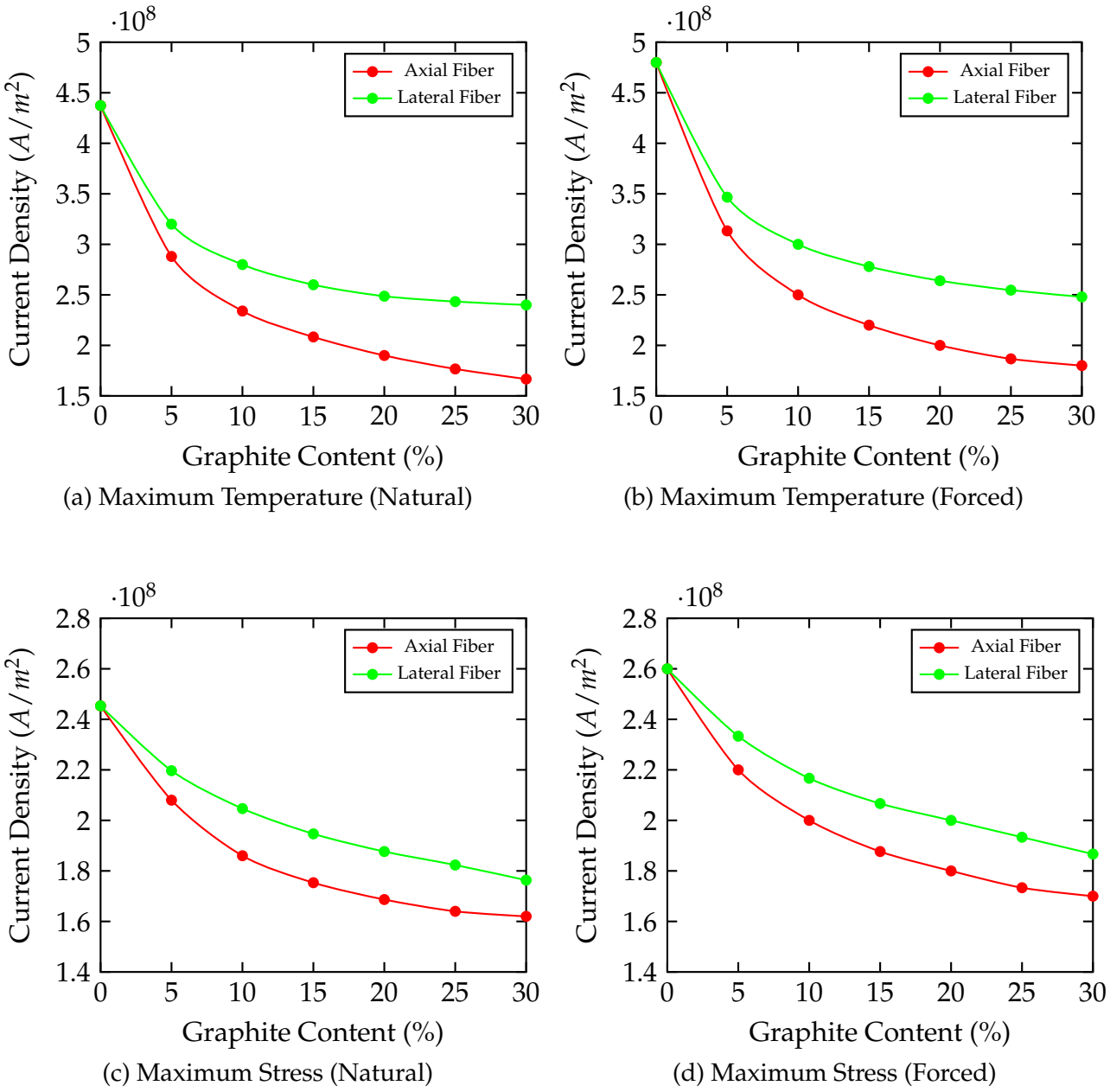

(a) Maximum Temperature (Natural)

(b) Maximum Temperature (Forced)

(c) Maximum Stress (Natural)

(d) Maximum Stress (Forced)

Figure 4.6: Change of maximum current carrying capacity for axial and lateral fiber orientation for natural and forced convection (5m/s) at different Graphite content

In figure 4.6, we have discussed about the current carrying capacity of the MMC line. At different graphite content we can see that the failure point decreases.

In axial and lateral fiber orientation current carrying capacity decreases with the increase of graphite content. This is due to the increase of temperature and von-mises stress across the MMC line. In case of temperature the current carrying capacity is relatively higher than of stress. This is due to the stress exceeds the ultimate strength before the matrix reaches the

melting point temperature. This means that the mechanical failure occurs relatively before the melting failure. The failure due to melting is considered for aluminium matrix as the melting point of aluminium is lower than graphite. In figure 4.6c and 4.6d we can see that the current capacity is lower than melting as shown in figure 4.6a and 4.6b.

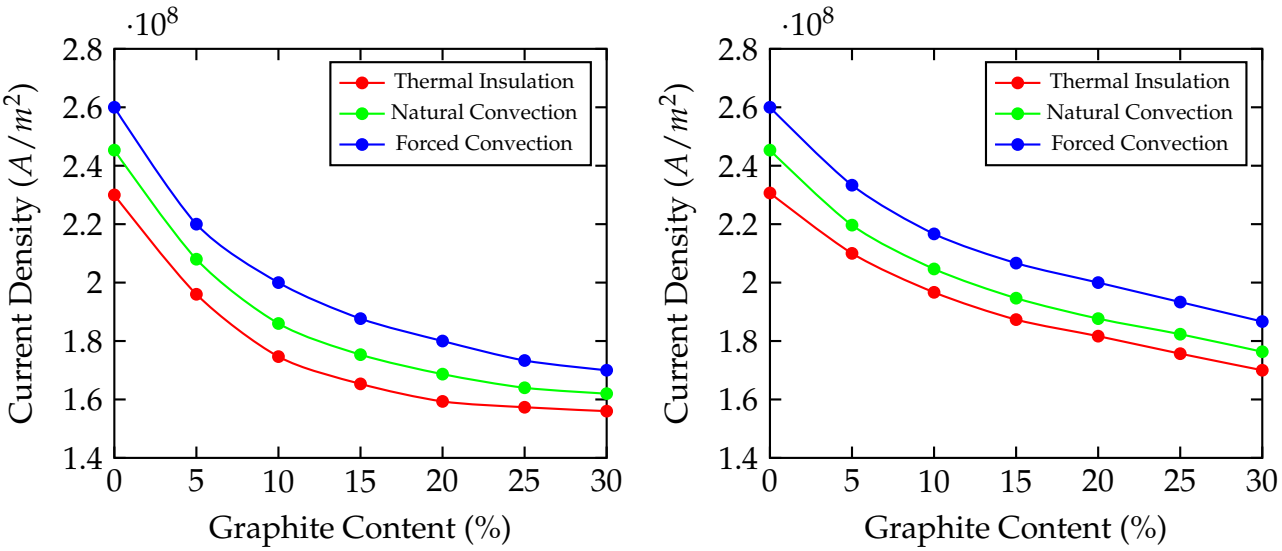

(a) Axial Fiber Direction

(b) Lateral Fiber Direction

Figure 4.7: Maximum Current Density before mechanical failure along MMC line for thermal insulation, natural and forced condition (5m/s air velocity)

In case of axial and lateral fiber orientation, we can observe the current carrying capacity in figure 4.7. In case of lateral fiber orientation shown in figure 4.7b, we can see that the current carrying capacity is relatively higher than axial fiber orientation shown in figure 4.7a. This is due to the high stress generation in the axial fiber orientation due to electric current. Also the current carrying capacity remains closer at the higher graphite content. This is due to the low change of material properties. In the higher graphite content, the elastic limit becomes higher. In that case the compressive strength of the MMC line increases.

4.8 Effect of Heat Convection

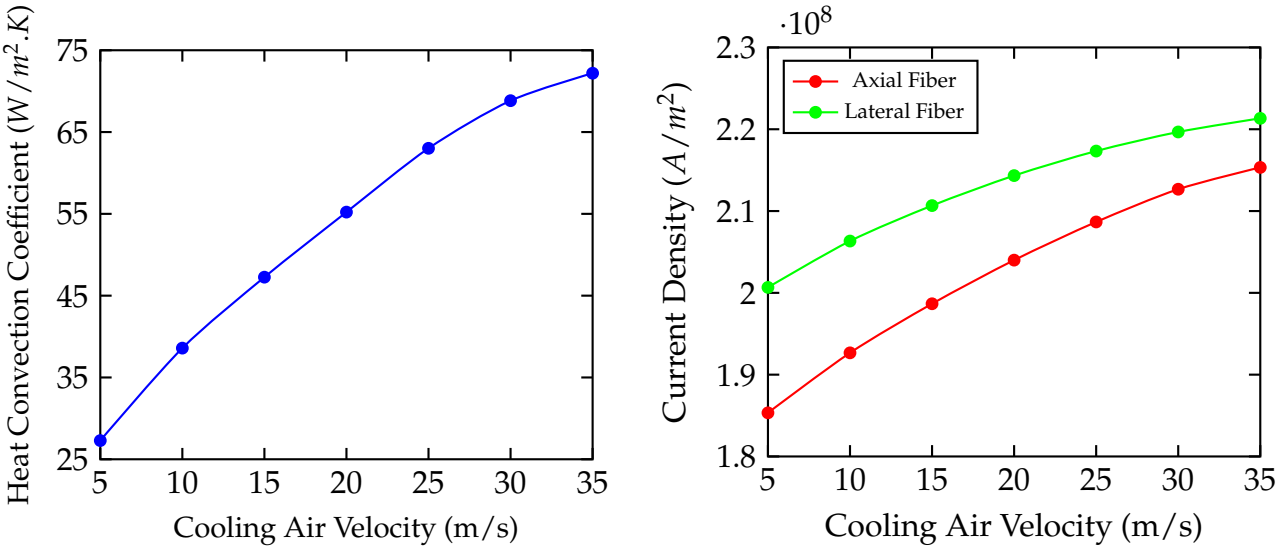

(a) Heat Convection Coefficient

(b) Mechanical Failure

Figure 4.8: Maximum current carrying capacity that can be withstand before the failure due to mechanical at different cooling air velocity (15% graphite)

The increase of cooling air velocity increases heat conduction coefficient of air to plate. So, more heat dissipates into the ambient temperature. Heat generation decreases due to the cooling air and temperature rise decreases. In case of increasing air velocity, the current carrying capacity of the MMC line increases. Discussed in previous section and as shown in figure 4.8b, the lateral fiber direction current carrying capacity is higher than axial fiber orientation.

4.9 Validation

To check the dependency of the result we have cross checked the electric potential, temperature and stress with finite element formulation as this is used in commercial simulation based software.

Table 4.1: Validation Parameters

Orientation	Parameter	Finite Difference Method	Finite Element Method	Error (%)
Al metal line	Max Temperature	314.332K	314.297K	0.011
Ambient Temperature=298.15K	Max Electric Potential	0.084V	0.083V	1.20
Current Density=$6.67 \times 10^7\ A/m^2$	Min Electric Potential	-0.084V	-0.085V	1.17
Thermal Condition= Insulation	Max Von-Mises Stress	31.382MPa	31.358MPa	0.0765
Al-Gr MMC line	Max Temperature	371.198K	371.159K	0.125
Current Density= $6.67 \times 10^7\ A/m^2$	Max Electric Potential	0.46V	0.45V	2.22
15% Gr and Axial fiber orientation	Min Electric Potential	-0.46V	-0.46V	0
Thermal Condition= Insulation	Max Von-Mises Stress	108.667MPa	108.638MPa	0.0267

4.10 Convergence Test

For different mesh size, the convergence of the result is calculated in our investigation. With the increase of the mesh, the error generated due to different order decreases.

Table 4.2: Mesh Dependency

Mesh Density	Max Temperature (K)	Error (%)	Max Stress (MPa)	Error (%)
60*40	364.599	0.00	99.019	0.00
90*60	364.596	8.22×10^{-4}	99.032	0.013
100*100	364.598	5.84×10^{-4}	99.041	9.08×10^{-3}
120*90	364.598	0.00	99.041	0.00
150*120	364.599	2.74×10^{-4}	99.043	2.011×10^{-3}

Chapter 5

Conclusion

In this presented work, we took an approach to determine the effectiveness of graphite reinforced metal matrix composites. We observed the current carrying capacity of the MMC line. We have also analyzed the effect of thermal conditions on the MMC line and the change of current carrying capacity. To solve the problem we have developed a finite difference formulation. We have developed the equations using a scalar variable ψ. Different parameters and conditions have been utilized to investigate the current carrying capacity of the graphite reinforced metal matrix composite. In our study we have observed that the temperature and von-mises stress increases with the increase of current density. The increase of graphite content also increases the temperature and stress as material becomes more elastic with that. So, the compressive strength becomes higher.

With the increase of current density the electric potential increases which in terms increases temperature. When the temperature reaches the melting point of the matrix (the matrix has lower melting point), the MMC thermally fails. With the increase of graphite content, electric resistivity increases. Therefore, at higher graphite content, temperature rise is higher. Melting failure occurs way before.

Temperature creates thermal stress across the MMC line. With the increase of current von-mises stress generation increases. Similarly with the increase of graphite content, the stress generation also increases.

We have analyzed the current carrying capacity at different thermal conditions. We can see that the capacity decreases with the increase of graphite content. This is due to high temperature and thermal stress rise. Different thermal conditions give different current carrying capacity. Forced convection dissipates more heat into surroundings so current capacity is higher at that condition.

For fiber orientation, lateral fiber orientation gives more current carrying capacity as the fiber is at the perpendicular position of current flow. So, lateral fiber orientation is more sustainable than axial in terms of electrical appliances.

In future different geometry can be applied to see the change of current carrying capacity of the metal matrix composites.

Bibliography

[1] O. Zhupanska and R. Sierakowski. "Electro-thermo-mechanical coupling in carbon fiber polymer matrix composites". In: *Acta Mechanica* 218 (2011), pp. 319–332.

[2] A. Ghorbanpour Arani et al. "Electro-thermo-mechanical behaviors of FGPM spheres using analytical method and ANSYS software". In: *Applied Mathematical Modelling* 36.1 (2012), pp. 139–157. ISSN: 0307-904X. DOI: https://doi.org/10.1016/j.apm.2011.05.031.

[3] Ali Ghorbanpour Arani et al. "Electro-thermo-mechanical response of thick-walled piezoelectric cylinder reinforced by boron-nitride nanotubes". In: *Strength of Materials* 45 (Mar. 2013). DOI: 10.1007/s11223-013-9437-2.

[4] Wikipedia contributors. *Orthotropic material — Wikipedia, The Free Encyclopedia*. https://en.wikipedia.org/w/index.php?title=Orthotropic_material&oldid=957771844. [Online; accessed 29-March-2021]. 2020.

[5] Wikipedia contributors. *Metal matrix composite — Wikipedia, The Free Encyclopedia*. https://en.wikipedia.org/w/index.php?title=Metal_matrix_composite&oldid=948475788. [Online; accessed 29-March-2021]. 2020.

[6] A.K. Kaw. *Mechanics of composite materials, second edition*. Jan. 2005, pp. 1–467.

[7] J. Kováčik, Š. Emmer, and J. Bielek. "Thermal conductivity of Cu-graphite composites". In: *International Journal of Thermal Sciences* 90 (2015), pp. 298–302. ISSN: 1290-0729. DOI: https://doi.org/10.1016/j.ijthermalsci.2014.12.017.

[8] J.K. Chen and I.S. Huang. "Thermal properties of aluminum–graphite composites by powder metallurgy". In: *Composites Part B: Engineering* 44.1 (2013), pp. 698–703. ISSN: 1359-8368. DOI: https://doi.org/10.1016/j.compositesb.2012.01.083.

[9] *Evaluating the Mechanical Properties of Carbon Fiber Reinforced Polymer Matrix Composite Materials at Room and Elevated Temperatures*. Vol. Volume 3: Design, Materials and Manufacturing, Parts A, B, and C. ASME International Mechanical Engineering Congress and Exposition. Nov. 2012, pp. 1151–1158. DOI: 10.1115/IMECE2012-85671.

[10] Wikipedia contributors. *Electric potential — Wikipedia, The Free Encyclopedia*. https://en.wikipedia.org/w/index.php?title=Electric_potential&oldid=949545468. [Online; accessed 29-March-2021]. 2020.

[11] H.S. Carslaw, J.C. Jaeger, and J.C.J. Jaeger. *Conduction of Heat in Solids*. Oxford science publications. Clarendon Press. ISBN: 9780198533689.

[12] M. Saka and H. Abé. "PATH-INDEPENDENT INTEGRALS FOR HEAT CONDUCTION ANALYSIS IN ELECTROTHERMAL CRACK PROBLEMS". In: *Journal of Thermal Stresses* 15.1 (1992), pp. 71–83. DOI: 10.1080/01495739208946121.

[13] K. Sasagawa, M. Saka, and H. Abé. "Current density and temperature distributions near the corner of angled metal line". In: *Mechanics Research Communications* 22.5 (1995), pp. 473–483. ISSN: 0093-6413. DOI: https://doi.org/10.1016/0093-6413(95)00051-R.

[14] J. A. Greenwood, J. B. P. Williamson, and Frank Philip Bowden. "Electrical conduction in solids II. Theory of temperature-dependent conductors". In: *Proceedings of the Royal Society of London. Series A. Mathematical and Physical Sciences* 246.1244 (1958), pp. 13–31. DOI: 10.1098/rspa.1958.0103.

[15] Yong Hoon Jang, J R Barber, and S Jack Hu. "Electrical conductance between conductors with dissimilar temperature-dependent material properties". In: *Journal of Physics D: Applied Physics* 31.22 (Nov. 1998), pp. 3197–3205. DOI: 10.1088/0022-3727/31/22/004. URL: https://doi.org/10.1088/0022-3727/31/22/004.

[16] P. Wang, Z.G. Tian, and X.Z. Bai. "Electrothermal stress in conductive body with collinear cracks". In: *Theoretical and Applied Fracture Mechanics* 40.2 (2003), pp. 187–195. ISSN: 0167-8442. DOI: https://doi.org/10.1016/S0167-8442(03)00045-4.

[17] M. Saka, Y.X. Sun, and S. Reaz Ahmed. "Heat conduction in a symmetric body subjected to a current flow of symmetric input and output". In: *International Journal of Thermal Sciences* 48.1 (2009), pp. 114–121. ISSN: 1290-0729. DOI: https://doi.org/10.1016/j.ijthermalsci.2008.03.005.

[18] Anik Adhikary, Sm Mahbobur Rahman, and S. Ahmed. "Nonlinear Analysis of Electrothermal Response of a conducting wire of Dissimilar Materials with Variable Thermal Conductivity". In: *ICME 2011 Proceedings* ICME 2011 (Dec. 2011), AM–012.

[19] Masumi Saka and Xu Zhao. "Analysis of the temperature field near a corner composed of dissimilar metals subjected to a current flow". In: *International Journal of Heat and Mass Transfer* 55.21 (2012), pp. 6090–6096. ISSN: 0017-9310. DOI: https://doi.org/10.1016/j.ijheatmasstransfer.2012.06.022.

[20] Abhishek Kumar Ghosh, Md. Rejaul Haque, and S. Reaz Ahmed. "Effect of a DC Field on Temperature Distribution in a Thin FGM Metal Line Subjected to Distributed Local Heating Sources". In: *Procedia Engineering* 105 (2015). The 6th BSME International Conference on Thermal Engineering, pp. 201–206. ISSN: 1877-7058. DOI: https://doi.org/10.1016/j.proeng.2015.05.056.

[21] Y.A. Çengel and A.J. Ghajar. *Heat and Mass Transfer: Fundamentals & Applications*. Asia Higher Education Engineering/Computer Science Mechanical Engineering. McGraw Hill Education. ISBN: 9789814595278.

[22] Jian-Ping Zhang et al. "Steady heat transfer analysis of orthotropic structure based on Element-Free Galerkin method". In: *International Journal of Thermal Sciences* 121 (2017), pp. 163–181. ISSN: 1290-0729. DOI: https://doi.org/10.1016/j.ijthermalsci.2017.06.024.

[23] Jianping Zhang et al. "Transient heat transfer analysis of anisotropic material by using Element-Free Galerkin method". In: *International Communications in Heat and Mass Transfer* 84 (2017), pp. 134–143. ISSN: 0735-1933. DOI: https://doi.org/10.1016/j.icheatmasstransfer.2017.04.003.

[24] Changzheng Cheng et al. "Analysis of the temperature field in anisotropic coating-structures by the boundary element method". In: *Engineering Analysis with Boundary Elements* 60 (2015). Boundary and Mesh Reduction Methods in Thermal and Nonhomogeneous Problems, pp. 115–122. ISSN: 0955-7997. DOI: https://doi.org/10.1016/j.enganabound.2015.01.010.

[25] *Theory of elasticity*. Engineering societies monographs. McGraw-Hill Education (India) Pvt Limited. ISBN: 9780070701229.

[26] H. D. Conway, L. Chow, and G. W. Morgan. "Analysis is Deep Beams." In: *Journal of Applied Mechanics, ASME* 18.2 (1951), pp. 163–173.

[27] H. D. Conway, L. Chow, and G. Winter. "Stresses in Deep Beams." In: *Transactions of theAmerican Society of Civil Engineers,ASCE* 118.1 (1953), pp. 686–702.

[28] R. E. CHAPEL and H. W. SMITH. "Finite-difference solutions for plane stresses." In: *AIAA Journal* 6.6 (1968), pp. 1156–1157. DOI: 10.2514/3.4691.

[29] A. J. Durelli and B. Ranganayakamma. "Parametric Solution of Stresses in Beams". In: *Journal of Engineering Mechanics* 115.2 (1989), pp. 401–414. DOI: 10.1061/(ASCE)0733-9399(1989)115:2(401).

[30] S.Reaz Ahmed, A.B.M. Idris, and Md.Wahhaj Uddin. "Numerical solution of both ends fixed deep beams". In: *Computers & Structures* 61.1 (1996), pp. 21–29. ISSN: 0045-7949. DOI: https://doi.org/10.1016/0045-7949(96)00029-6.

[31] S.R. Ahmed et al. "Investigation of stresses at the fixed end of deep cantilever beams". In: *Computers & Structures* 69.3 (1998), pp. 329–338. ISSN: 0045-7949. DOI: https://doi.org/10.1016/S0045-7949(98)00127-8.

[32] S. Reaz Ahmed, M. Zubaer Hossain, and M. Wahhaj Uddin. "A general mathematical formulation for finite-difference solution of mixed-boundary-value problems of anisotropic materials". In: *Computers & Structures* 83.1 (2005), pp. 35–51. ISSN: 0045-7949. DOI: https://doi.org/10.1016/j.compstruc.2004.08.007.

[33] A.M. Afsar and J. Go. "Finite element analysis of thermoelastic field in a rotating FGM circular disk". In: *Applied Mathematical Modelling* 34.11 (2010), pp. 3309–3320. ISSN: 0307-904X. DOI: https://doi.org/10.1016/j.apm.2010.02.022.

[34] ABM Idris, SR Ahmed, and W Uddin. "Analytical solution of a 2-D elastic problem with mixed boundary conditions". In: *JOURNAL-INSTITUTION OF ENGINEERS SINGAPORE* 36 (1996), pp. 11–20.

[35] M. Zubaer Hossain, S. Reaz Ahmed, and M. Wahhaj Uddin. "Generalized mathematical model for the solution of mixed-boundary-value elastic problems". In: *Applied Mathematics and Computation* 169.2 (2005), pp. 1247–1275. ISSN: 0096-3003. DOI: https://doi.org/10.1016/j.amc.2004.10.095.

[36] Malak Naji, M. Al-Nimr, and T. Darabseh. "Thermal stress investigation in unidirectional composites under the hyperbolic energy model". In: *International Journal of Solids and Structures* 44.16 (2007), pp. 5111–5121. ISSN: 0020-7683. DOI: https://doi.org/10.1016/j.ijsolstr.2006.12.021.

[37] M Didem Demirbas and M Kemal Apalak. "Thermal stress analysis of one- and two-dimensional functionally graded plates subjected to in-plane heat fluxes". In: *Proceedings of the Institution of Mechanical Engineers, Part L: Journal of Materials: Design and Applications* 233.4 (2019), pp. 546–562. DOI: 10.1177/1464420716675507.

[38] Munise Didem Demirbas. "Thermal stress analysis of functionally graded plates with temperature-dependent material properties using theory of elasticity". In: *Composites Part B: Engineering* 131 (2017), pp. 100–124. ISSN: 1359-8368. DOI: https://doi.org/10.1016/j.compositesb.2017.08.005.

[39] Yepeng Xu and Ding Zhou. "Two-dimensional thermoelastic analysis of beams with variable thickness subjected to thermo-mechanical loads". In: *Applied Mathematical Modelling* 36.12 (2012), pp. 5818–5829. ISSN: 0307-904X. DOI: https://doi.org/10.1016/j.apm.2012.01.048.

[40] Steven C. Chapra and Raymond Canale. *Numerical Methods for Engineers*. 5th ed. USA: McGraw-Hill, Inc., 2005. ISBN: 0073101567.

[41] Wikipedia contributors. *Joule heating — Wikipedia, The Free Encyclopedia*. https://en.wikipedia.org/w/index.php?title=Joule_heating&oldid=962888106. [Online; accessed 2-April-2021]. 2020.

Appendix

Metal Matrix Composites

The material property that are set,

Table A1: Metal Matrix Composite

Metal Matrix Composite	
Matrix	Aluminium
Fiber	Graphite

Dimensions

Dimensions of the metal line in different components

Table A2: Dimension of the metal line

Designation	Dimension	Unit
Length	**0.1**	m
Width	**0.015**	m
Thickness	$\mathbf{10^{-5}}$	m

Nusselt Number Correlations

All the correlations for Nusselt Number are

Table A3: Summary of the Correlation of the Forced Convection Flow Over Flat Plates

Type	Restrictions	Fluid Flow	Heat Transfer	
			Isothermal ($T_w = constant$)	Isoflux ($q_w = constant$)
Local	Laminar: $Re_x < 5 \times 10^5$; 0.6<Pr<50	$C_{f,x} = 0.059 Re_x^{-1/5}$	$Nu_x = 0.332 Re_x^{1/2} Pr^{1/3}$	$Nu_x = 0.453 Re_x^{1/2} Pr^{1/3}$
Average	Laminar: $Re_L < 5 \times 10^5$; 0.6<Pr<50	$C_f = 1.328 Re_L^{-1/2}$	$Nu_L = 0.664 Re_x^{1/2} Pr^{1/3}$	$Nu_L = 0.680 Re_L^{1/2} Pr^{1/3}$
Local	Turbulent: $5 \times 10^5 \leq Re_x \leq 10^7$;	$C_{f,x} = 0.059 Re_x^{-1/5}$	$Nu_x = 0.0296 Re_x^{4/5} Pr^{1/3}$	$Nu_x = 0.0308 Re_x^{4/5} Pr^{1/3}$
Average	Turbulent: $5 \times 10^5 \leq Re_L \leq 10^7$;	$C_f = 0.074 Re_L^{-1/5}$	$Nu_L = 0.037 Re_L^{4/5} Pr^{1/3}$	$Nu_L = 0.037 Re_L^{4/5} Pr^{1/3}$
Average	Partly Laminar & Turbulent: $5 \times 10^5 \leq Re_L \leq 10^7$; $0.6 \leq Pr \leq 60$; $Re_{cr} = 5 \times 10^5$	$C_f = 0.074 Re_L^{-1/5} - 1742 Re_L$	$Nu_L = (0.037 Re_L^{4/5} - 871) Pr^{1/3}$	$Nu_L = \frac{0.037 Re_L^{4/5} Pr^{1/3}}{1+12.35 \times 10^6 Re_L^{-6/5}}$

Material Properties

Material Properties of Aluminium

Table A4: Properties of Aluminium

Young's Modulus	E_m	**68.9**	GPa
Poisson's Ratio	μ_m	**0.33**	
Coefficient of Thermal Expansion	α_m	$\mathbf{2.36 \times 10^{-5}}$	$^\circ C$
Shear Modulus	G_m	**26**	GPa
Ultimate Tensile Stress	$(\sigma)_{ult}$	**310**	MPa
Ultimate Shear Stress	$(\tau)_{ult}$	**138**	MPa
Thermal Conductivity	k	**205**	W/m.K
Electrical Conductivity	κ	$\mathbf{3.77 \times 10^7}$	S/m

Material Properties of Graphite

Table A5: Properties of Graphite

Young's Modulus	Axial Transverse	E_f	**230** **27.6**	GPa GPa
Poisson's Ratio	Axial Transverse	μ_f	**0.3** **0.30**	
Coefficient of Thermal Expansion	Axial Transverse	α_f	$\mathbf{1.30 \times 10^{-6}}$ $\mathbf{7.00 \times 10^{-6}}$	$^\circ C$ $^\circ C$
Shear Modulus	Axial Transverse	G_m	**22** **22**	GPa GPa
Ultimate Tensile Stress	Axial Transverse	$(\sigma)_{ult}$	**77** **2067**	MPa MPa
Ultimate Shear Strength	Axial Transverse	$(\tau)_{ult}$	**42** **42**	MPa MPa
Thermal Conductivity		k	**1600**	W/m.K
Electrical Conductivity		κ	$\mathbf{1.30 \times 10^6}$	S/m

Properties of Aluminium Graphite Metal Matrix Composite

Table A6: Mechanical, Electrical and Thermal Properties of Aluminium-Graphite Composite (Axial fiber)

Property	Direction	Symbol	Graphite Percentage							Unit
			0%	5%	10%	15%	20%	25%	30%	
Young's Modulus	Longitudinal	E_1	68.9	76.96	85.01	93.07	101.12	109.18	117.23	GPa
	Transverse	E_2	68.9	64.10	59.93	56.27	53.03	50.14	47.55	GPa
Poisson's Ratio	Major	μ_{12}	0.33	0.3285	0.327	0.3255	0.324	0.3225	0.321	
Shear Modulus	Major	G_{12}	26	25.77	25.54	25.31	25.09	24.87	24.66	GPa
Coefficient of Thermal Expansion	Longitudinal	α_1	2.36	1.99	1.69	1.44	1.23	1.05	0.894	$K \times 10^5$
	Transverse	α_2	2.36	2.38	2.37	2.34	2.30	2.25	2.19	$K \times 10^5$
Ultimate Strength	Tensile	$(\sigma_1^t)_{ult}$	310	690.48	762.93	835.38	907.83	980.27	1052.72	MPa
		$(\sigma_2^t)_{ult}$	310	397.32	413.63	418.73	418.76	416.07	411.82	MPa
	Compressive	$(\sigma_1^c)_{ult}$	280	867.73	877.33	892.63	907.89	921.22	931.84	MPa
		$(\sigma_2^c)_{ult}$	280	237.45	202.26	175.68	154.26	136.45	121.33	MPa
	Shear	$(\tau_{12})_{ult}$	138	133.2	128.4	123.6	118.8	114	109.2	MPa
Thermal Conductivity	Longitudinal	k_1	205	274.75	344.5	414.25	484	553.75	623.5	W/m.K
	Transverse	k_2	205	214.34	224.58	235.84	248.29	262.14	277.61	W/m.K
Electrical Resistivity	Longitudinal	ρ_1	0.265	0.637	1.01	1.38	1.75	2.12	2.49	$\mu\Omega.cm$
	Transverse	ρ_2	0.265	0.279	0.294	0.310	0.329	0.349	0.373	$\mu\Omega.cm$
Melting Point		T_{max}	923	923	923	923	923	923	923	K

Table A7: Mechanical, Electrical and Thermal Properties of Aluminium-Graphite Composite (Lateral fiber)

Property	Direction	Symbol	Graphite Percentage							Unit
			0%	5%	10%	15%	20%	25%	30%	
Young's Modulus	Longitudinal	E_1	68.9	64.10	59.93	56.27	53.03	50.14	47.55	GPa
	Transverse	E_2	68.9	76.96	85.01	93.07	101.12	109.18	117.23	GPa
Poisson's Ratio	Major	μ_{12}	0.33	0.3285	0.327	0.3255	0.324	0.3225	0.321	
Shear Modulus	Major	G_{12}	26	25.77	25.54	25.31	25.09	24.87	24.66	GPa
Coefficient of Thermal Expansion	Longitudinal	α_1	2.36	2.38	2.37	2.34	2.30	2.25	2.19	$K \times 10^5$
	Transverse	α_2	2.36	1.99	1.69	1.44	1.23	1.05	0.894	$K \times 10^5$
Ultimate Strength	Tensile	$(\sigma_1^t)_{ult}$	310	397.32	413.63	418.73	418.76	416.07	411.82	MPa
		$(\sigma_2^t)_{ult}$	310	690.48	762.93	835.38	907.83	980.27	1052.72	MPa
	Compressive	$(\sigma_1^c)_{ult}$	280	237.45	202.26	175.68	154.26	136.45	121.33	MPa
		$(\sigma_2^c)_{ult}$	280	867.73	877.33	892.63	907.89	921.22	931.84	MPa
	Shear	$(\tau_{12})_{ult}$	138	133.2	128.4	123.6	118.8	114	109.2	MPa
Thermal Conductivity	Longitudinal	k_1	205	214.34	224.58	235.84	248.29	262.14	277.61	W/m.K
	Transverse	k_2	205	274.75	344.5	414.25	484	553.75	623.5	W/m.K
Electrical Resistivity	Longitudinal	ρ_1	0.265	0.279	0.294	0.310	0.329	0.349	0.373	$\mu\Omega.cm$
	Transverse	ρ_2	0.265	0.637	1.01	1.38	1.75	2.12	2.49	$\mu\Omega.cm$
Melting Point		T_{max}	923	923	923	923	923	923	923	K

Electrical Interconnect Failure due to Joule Heating

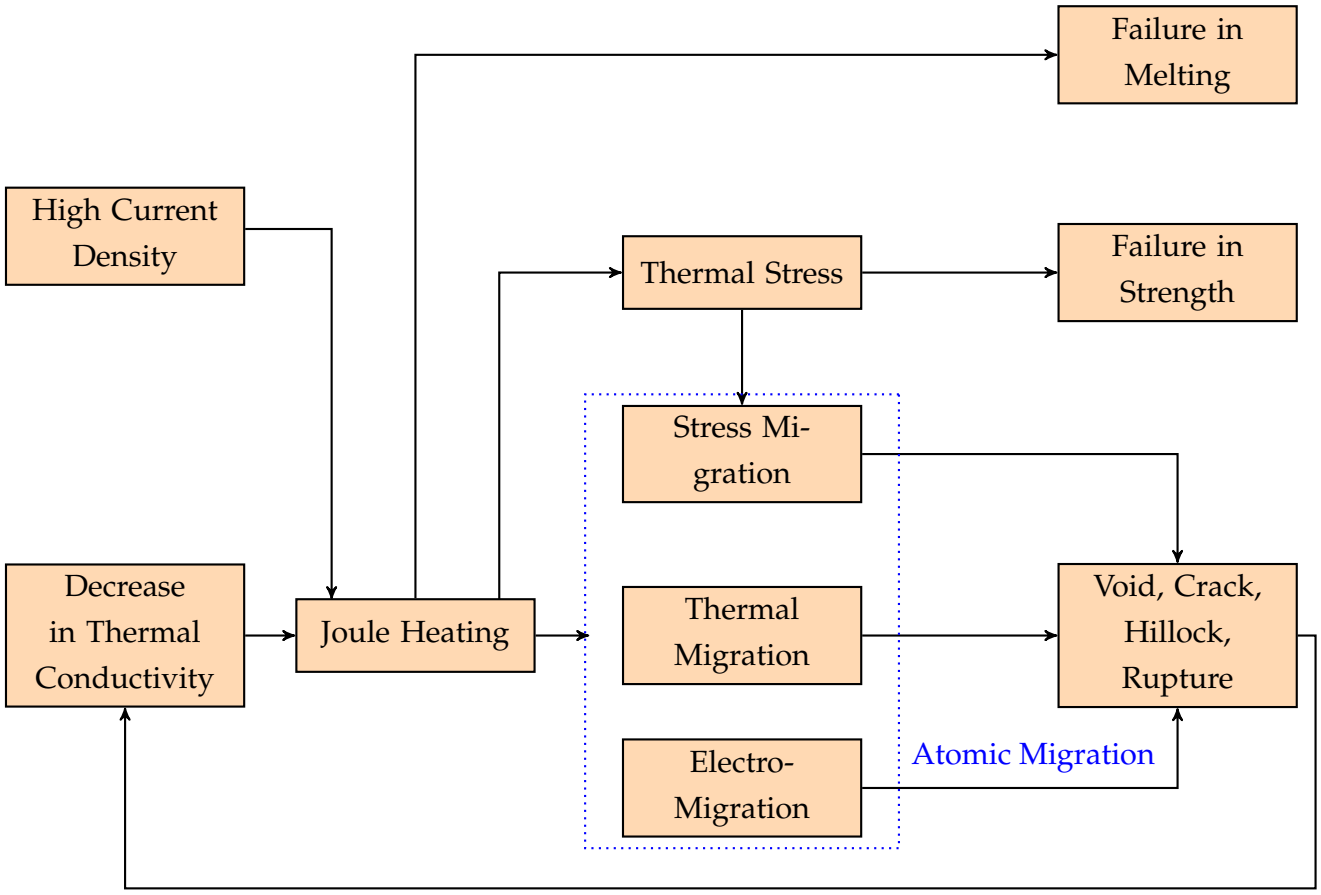

Schematic Illustration of Our Objective

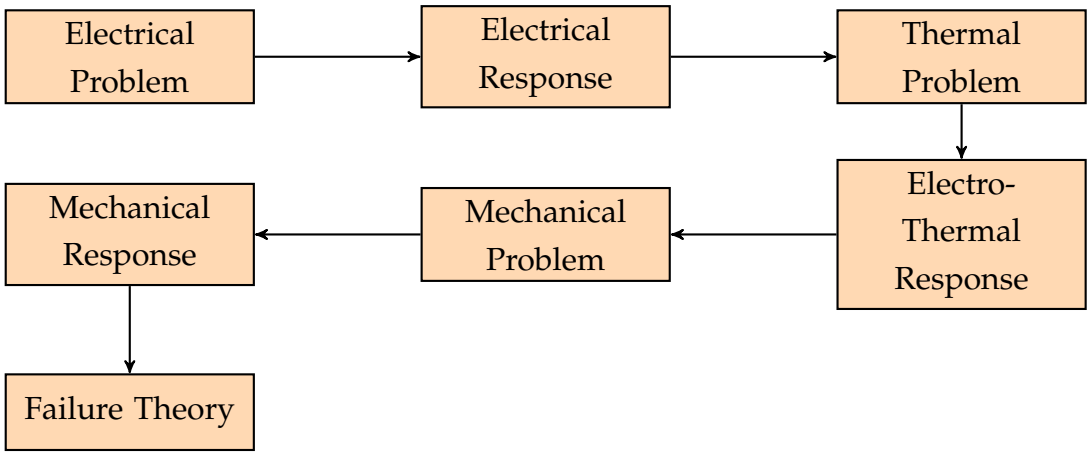

Electrical Problem Flow Chart

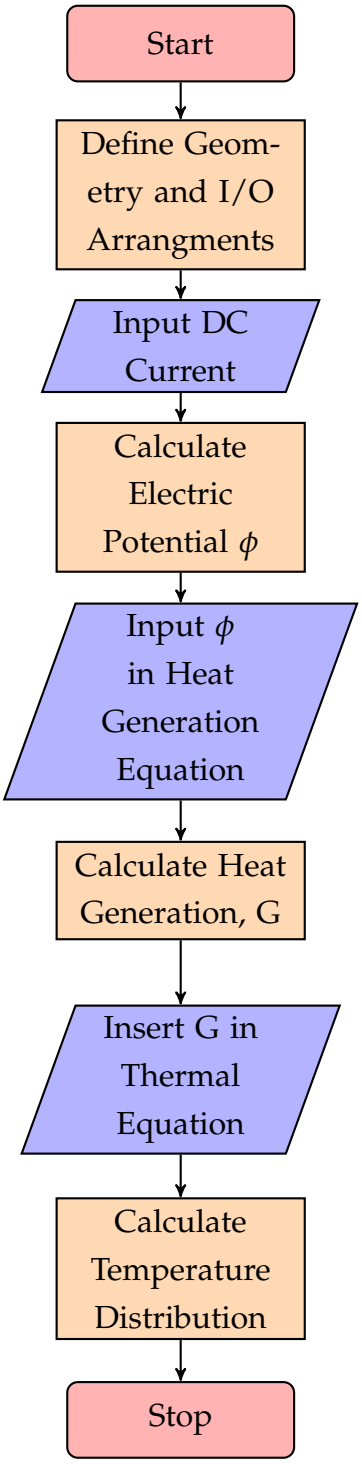

Thermal Problem Flow Chart

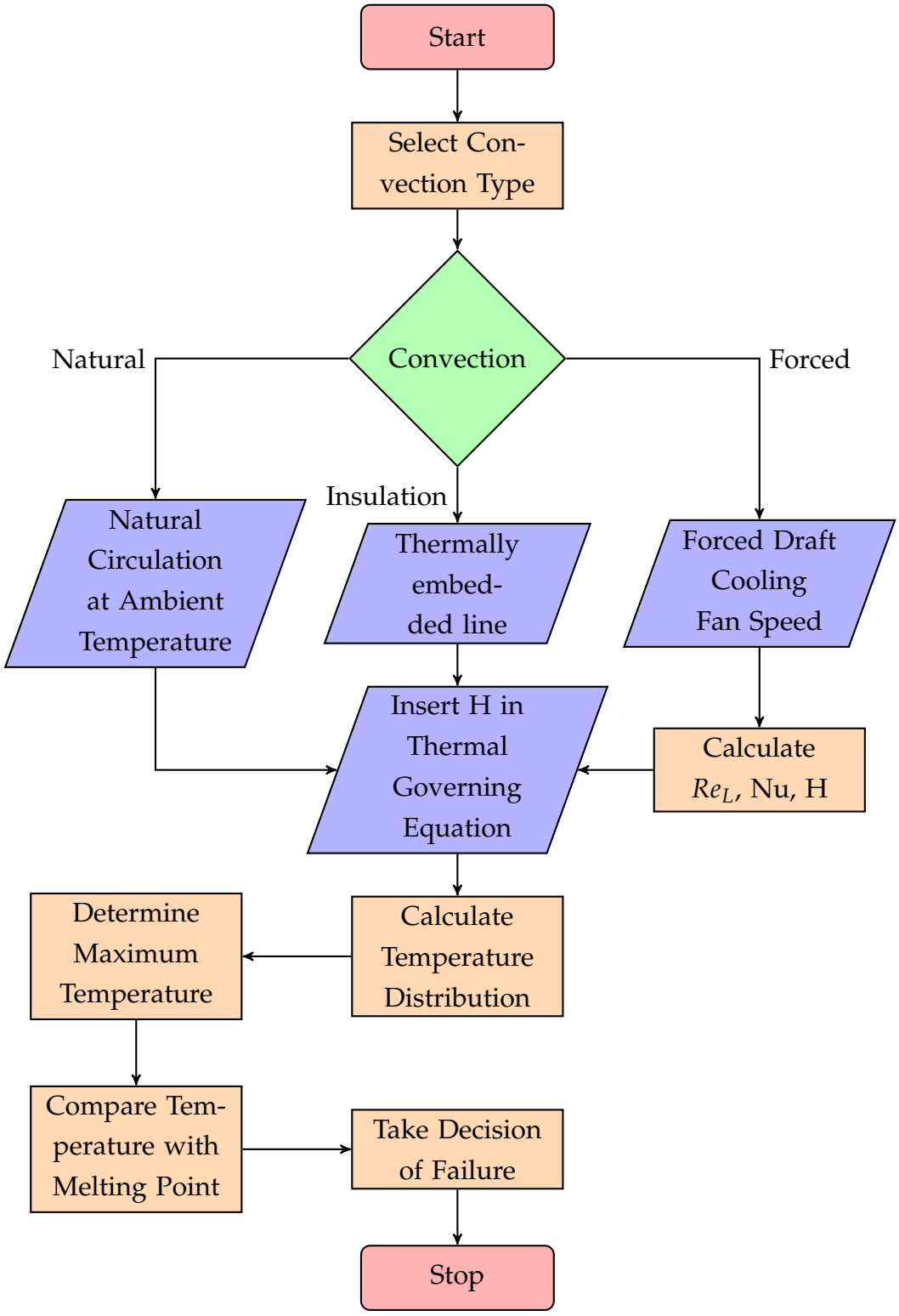

Stress Problem Flow Chart

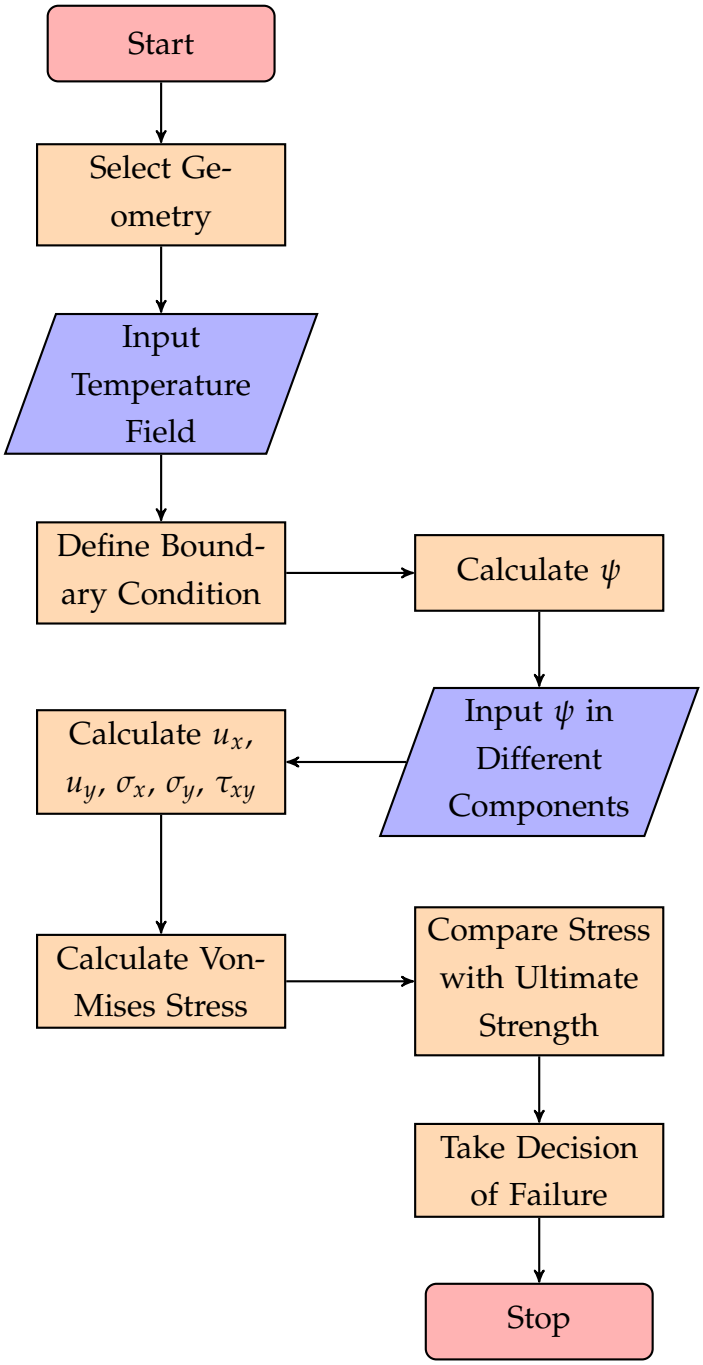

Failure Characteristics Flow Chart